ADD422508

BDX-613-1583 (Rev.)

DYNAMIC RESPONSE OF RIGID POLYURETHANE FOAM

PDO 6984191, Topical Report

R. A. Daniel, Project Leader

Project Team:
J. R. Fender
R. D. Jump
L. F. Thorne

Published September 1976

PLASTEC 35877

PL-25777

Prepared for the United States Energy
Research and Development Administration
Under Contract Number E(29-1)-613 USERDA

Bendix Kansas City Division

DISCLAIMER NOTICE

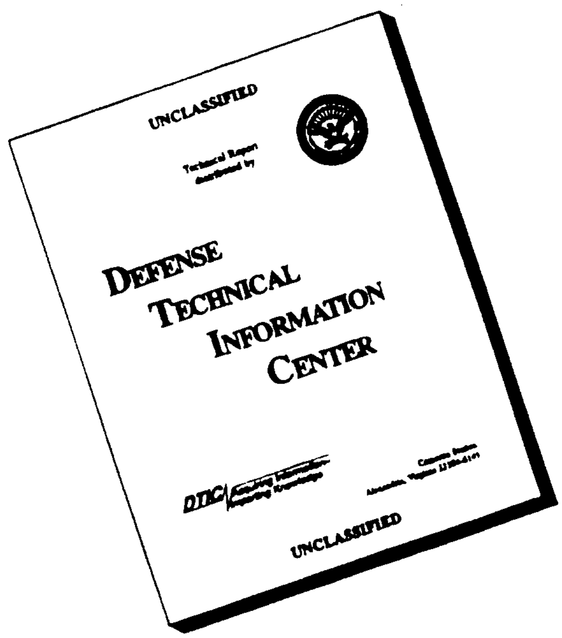

THIS DOCUMENT IS BEST QUALITY AVAILABLE. THE COPY FURNISHED TO DTIC CONTAINED A SIGNIFICANT NUMBER OF PAGES WHICH DO NOT REPRODUCE LEGIBLY.

NOTICE

Printed in the United States of America

Available From the National Technical Information Service, U.S. Department of Commerce, 5285 Port Royal Road, Springfield, Virginia 22161.

Price: Microfiche \$2.25
Paper Copy \$5.00

BDX-613-1583 (Rev.)
Distribution Category UC-38

DYNAMIC RESPONSE OF RIGID POLYURETHANE FOAM

Published September 1976

Project Leader:
R. A. Daniel
Department 861

Project Team:
J. R. Fender
R. D. Jump
L. F. Thorne

PDO 6984191
Topical Report

Technical Communications

Bendix Kansas City Division

DYNAMIC RESPONSE OF RIGID POLYURETHANE FOAM

BDX-613-1583 (Rev.), UNCLASSIFIED Topical Report, Published September 1976

Prepared by R. A. Daniel, D/861, under PDO 6984191

The dynamic characteristics of six rigid polyurethane foams were studied at impact velocities from 15.24 to 60.96 m/s (50 to 200 ft/sec). A test technique developed for crushing confined samples is described. The dynamic properties of materials tested are reported by both graphical and tabular methods.

THE BENDIX CORPORATION
KANSAS CITY DIVISION
P.O. BOX 1159
KANSAS CITY, MISSOURI 64141

A prime contractor for the United States Energy Research and Development Administration
Contract Number E(29-1)-613 USERDA

CONTENTS

ILLUSTRATIONS

TABLES

SUMMARY

Development of components for future applications is dependent on complete and precise data on the response of materials to various environments. The energy absorption of polyurethane foam material had previously been investigated at velocities below 6 m/s (20 ft/sec) and above several thousand meters/second (feet/second). However, very little work had been performed in the velocity range applicable to future designs. The purpose of this project was to develop the techniques to evaluate polyurethane foam response to impact velocities in the range of 15.24 to 91.44 m/s (50 to 300 ft/sec) and to report these data in a format usable for present and future design activities.

During the initial phase of this work, a technique for testing dynamic response from 15.24 to 60.96 m/s (50 to 200 ft/sec) was established, and two techniques were proposed for reporting these data. This work was documented in BDX-613-1059 (Rev.), August 1975.

The second phase of this project involved testing rigid polyurethane foam samples 63.5 mm (2.5 inches) in diameter and 101.6 mm (4 inches) long. The samples were placed inside a steel tube to prevent lateral expansion and were crushed in the longitudinal direction of impact velocities of 15.24, 30.48, 45.72, and 60.96 m/s (50, 100, 150, and 200 ft/sec). The materials selected for testing were CPR 1024 and 1040 (CPR Division of the UpJohn Company), BC 1200 series (Expanded Rubber Company), BKC Thermalthane 4003, BKC Rigifoam 6003, and BKC 44302 (Bendix Corporation Kansas City Division). Samples were prepared from billets with nominal densities of 160, 320, and 480 kg/m^3 (10, 20, and 30 lb/ft^3).

The impact tests were performed by using test weights of 5.4, 10.8, and 21.6 kg (2.45, 4.91, and 9.82 lb), corresponding to static loads of 3.4, 6.9, and 13.8 kPa (0.5, 1.0, and 2.0 psi). The output from an accelerometer attached to the test weight was recorded on magnetic tape. All values used to describe the dynamic behavior of the test samples were calculated from measurement of the impact velocity and the record of acceleration experienced by the test weight as it crushed the samples.

For each combination of foam type, sample density, and static load, graphs were plotted showing force versus sample deflection at 15.24, 30.48, 45.72, and 60.96 m/s (50, 100, 150, and 200 ft/sec. In addition, the force-deflection curve from a standard compression test is included for comparison with the dynamic data.

Test results are presented in six tables which show values for maximum test weight acceleration, maximum and final sample deflection, rebound velocity, and energy absorption efficiency.

No future work is currently planned for this project. Additional studies, if desired, will be supported by other projects.

DISCUSSION

SCOPE AND PURPOSE

Advanced product development is dependent on complete and precise data on all materials and environments. In support of this development, work was initiated to establish techniques for evaluation of foam response to impact velocities in the range of 15.24 to 91.44 m/s (50 to 300 ft/sec), and for reporting these data in a format usable to the designer specifying polyurethane foams for structural and energy absorbing media.

PRIOR WORK

Previous investigations revealed that available literature on the dynamic response of polyurethane foam discussed response at impact velocities below 6 m/s (20 ft/sec) and at several thousand ft/sec. The initial phase of this endeavor, which established the required techniques to allow testing in the range of 15.24 to 60.96 m/s (50 to 200 ft/sec) was reported in BDX-613-1059 (Rev.), *Technique for Impact Testing of Confined Rigid Foam*, August 1975.

ACTIVITY

Test Method

The basic concept used for gathering dynamic test data from foam samples is illustrated in Figure 1. All values for the terms used to describe the dynamic behavior of a test sample can be calculated from a measurement of the impact velocity and a record of the deceleration experienced by the test weight as it crushes the sample. Samples chosen for the study were 63.5 mm (2.5 inches) in diameter and 101.6 mm (4 inches) in length.

The materials selected for evaluation included those most frequently used as support materials: CPR 1024 and 1040 (CPR Division of the UpJohn Company), BC 1200 series (Expanded Rubber Company), BKC Thermalthane 4003, BKC Rigifoam 6003, and BKC 44302 (Bendix Corporation, Kansas City Division). Samples were prepared from billets with nominal densities of 160, 320, and 480 kg/m^3 (10, 20, and 30 lb/ft^3).

For each test condition, consisting of an impact load, foam type, and sample density, the impact velocity was increased in increments of 15.24 m/s (50 ft/sec) until a sample was crushed beyond critical deflection. A new sample was used for each impact. The point of critical deflection can be determined from the acceleration-time trace by a rapid rise in the acceleration level. The energy

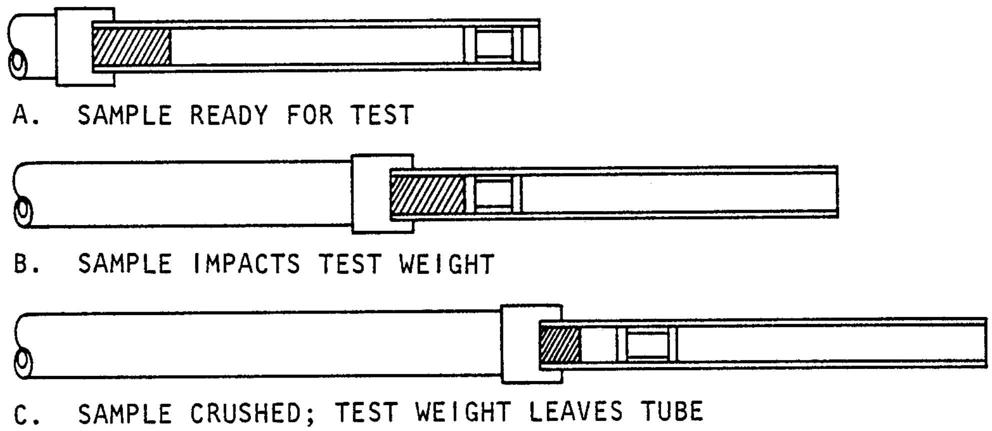

Figure 1. Basic Concept for Dynamic Testing of Foam

absorbing efficiency of the foam diminishes rapidly after critical deflection has been exceeded.

Impact testing was conducted through the use of a pneumatic mechanical shock actuator. A guide tube 1.5 meters (5 ft) long with a 76.2-mm (3-in.) inside diameter, was attached to the actuator carriage which travels on a horizontal track system. The guide tube, carriage, and actuator are shown in Figure 2. Three test weights were fabricated, weighing 5.4, 10.8, and 21.6 kg (2.45, 4.91, and 9.82 lb). Phenolic guide rings were bonded around both ends of each projectile to protect the honed inside diameter of the guide tube from damage. The accelerometer, mounted at the bottom of a recess bored into the projectile, was protected by a cover which was bolted over the recess.

The uniform compression of test samples confined in steel tubes to prevent lateral expansion was used as a simulation of the boundary conditions where polyurethane foam is typically used. The clearance between the 63.5-mm-diameter (2.5-inch) test samples and the inside diameter of the steel tube holding the samples was approximately 0.25 mm (0.010 inch). During a test, an extension of the test weight with a nominal diameter of 62.99 mm (2.480 inches) entered the specimen tube approximately 6.35 mm (0.25 inch) before it contacted and began to crush the sample. Foam samples for testing were machined from billets to minimize density variation.

To perform a test, the sample tube was positioned to the rear of the guide tube and secured in place with setscrews. The foam sample was then inserted into the sample tube. Figure 3 shows the sample in place, ready for testing. The actuator firing pressure and the gap that must be set between the sample and the

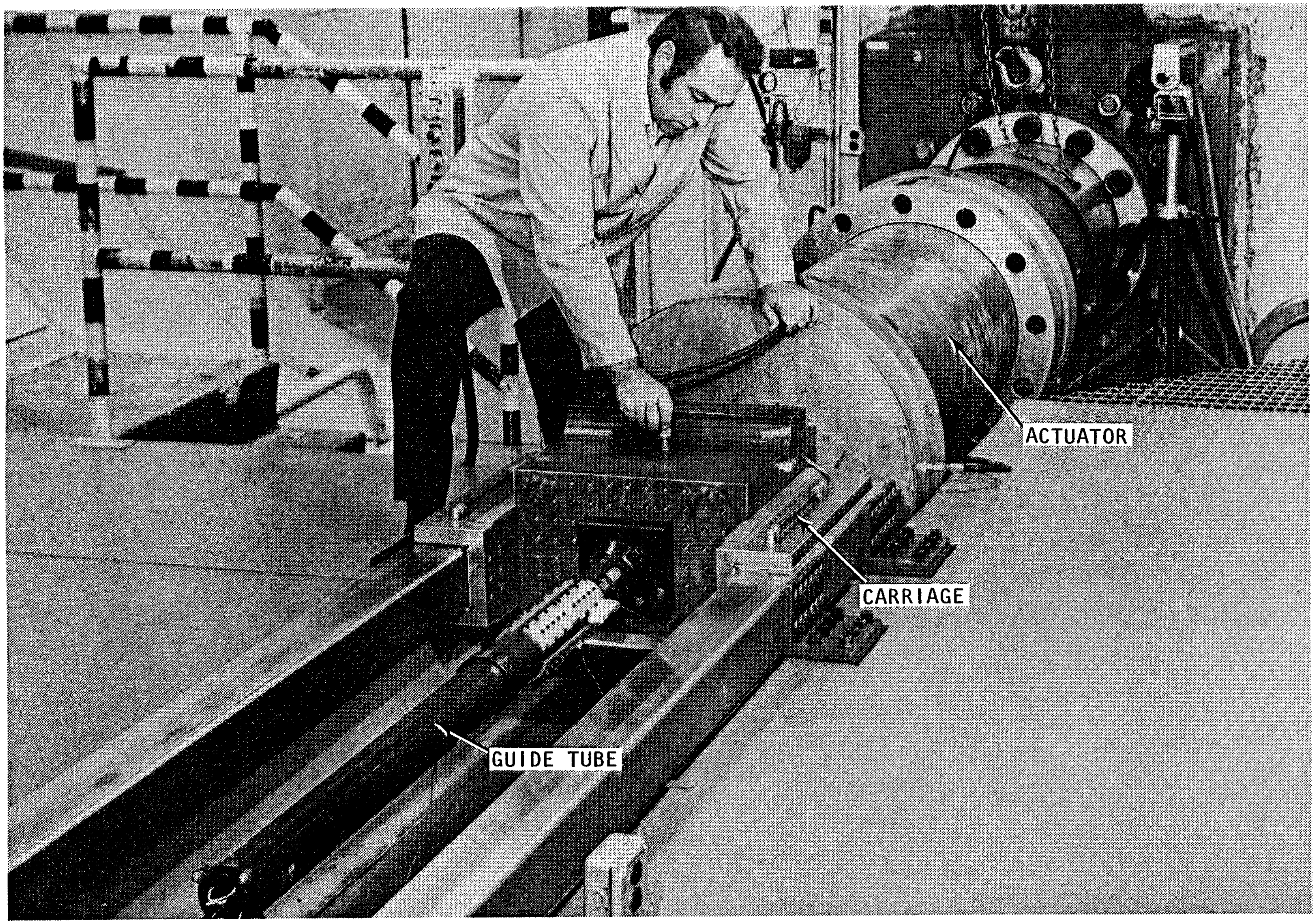

Figure 2. Test Weight Guide Tube Attached to Carriage

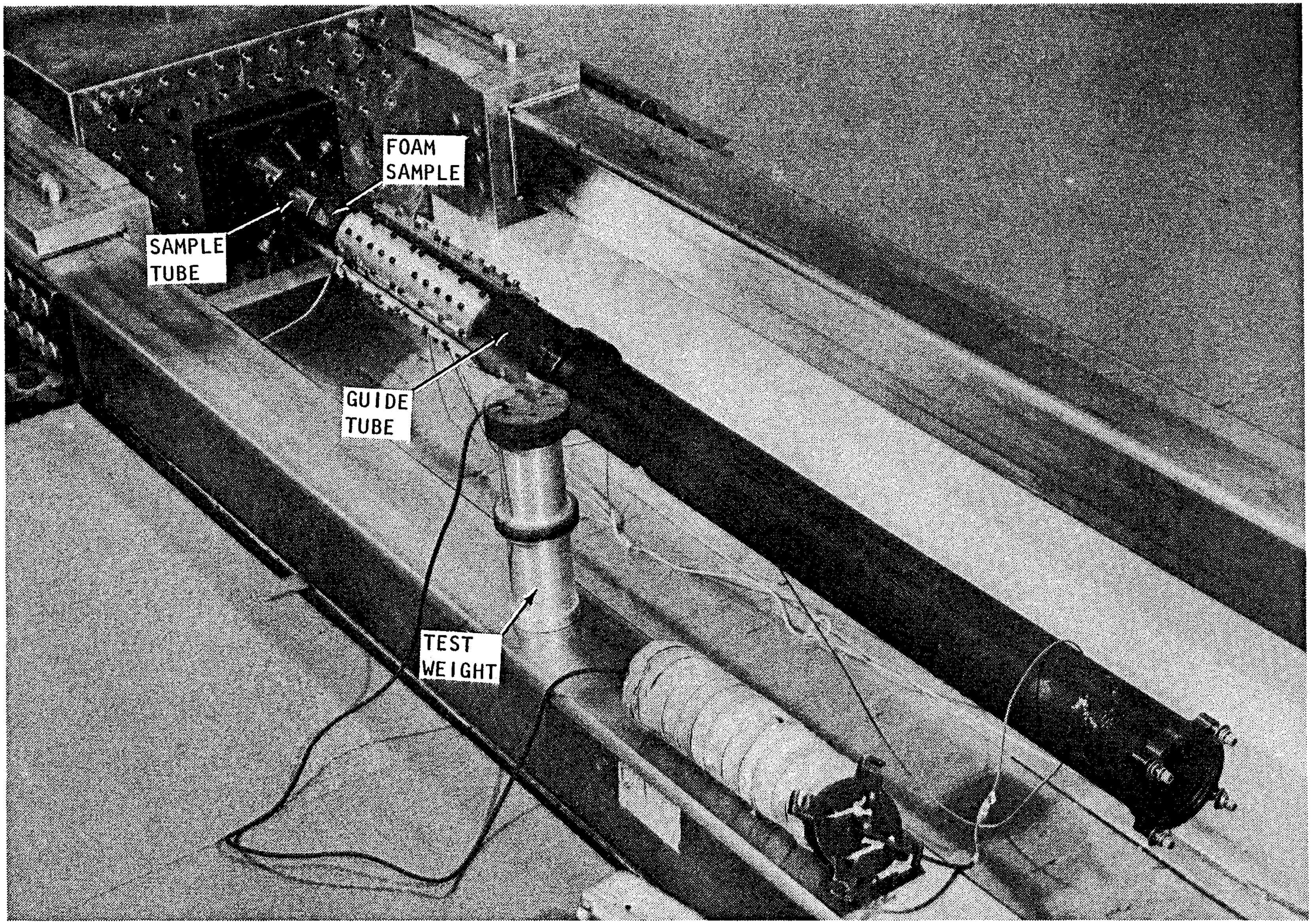

Figure 3. Test Weight With Sample Prepared for Test

test weight were selected from actuator performance data. The initial gap coincides with the distance over which the carriage and the guide tube accelerate before reaching impact velocity, which varied from 508 mm at 15.2 m/s (20 inches at 50 ft/sec) to 914 mm at 61.0 m/s (36 inches at 200 ft/sec). Impact of the sample into the test weight occurred just before the carriage separated from the actuator thrust column.

Following impact with the sample, the test weight experienced a post-crush rebound velocity that varied from a few feet per second to 40 ft/sec (12 m/s). Ensolite rubber tied to the guide tube end cap cushioned the impact of the projectile when it reached the end of the tube. A braking system built into the carriage arrested its motion within 15.2 m (50 feet).

Instrumentation

Velocity Measurement

Magnetic sensors used to measure impact velocity were installed through the wall of the guide tube. Travel time of the test weight was measured between four sensors spaced 25.4 mm (1 inch) apart. A 1.59-mm-thick (1/16 inch) steel ring, fastened to the test weight, caused a voltage output from each sensor during the motion of the guide tube prior to impact. The voltage pulses, along with 1-millisecond time marks, were recorded on magnetic tape at 3.048 m/s (120 inches/second). These were later played back at a speed of 47.62 mm/s (1-7/8 inches/second) onto an oscillograph record from which impact velocity calculations were made. Typical signals from an oscillograph record with a velocity calculation are shown in Figure 4. The calculation was generally within 5 percent of the desired test velocity. The total range of uncertainty in a calculated value for impact velocity is 3 percent.

A Kistler Model 805A accelerometer, with a 100,000-g capability and a 60 kHz resonant frequency, was selected for the tests. The block diagram in Figure 5 illustrates the instrumentation system employed to measure the acceleration of the test weight. The acceleration trace as well as the magnetic-pickup outputs and the 1-millisecond time marks were recorded on magnetic tape at a speed of 3.048 m/s (120 inches/second). Data records were obtained by playing the data back at 47.62 m/s (1-7/8 inches/second) into a Honeywell oscillograph. Typical data recorded from an impact test are shown in Figure 6. After reviewing the data, acceleration traces to be digitized were selected and scaled for playback into a Biomation Model 810 transient recorder at 3.048 m/s (120 inches/second). The transient recorder converted the data into digital form and stored it in an internal memory system. The digital data then were punched on paper tape in standard ASCII code.

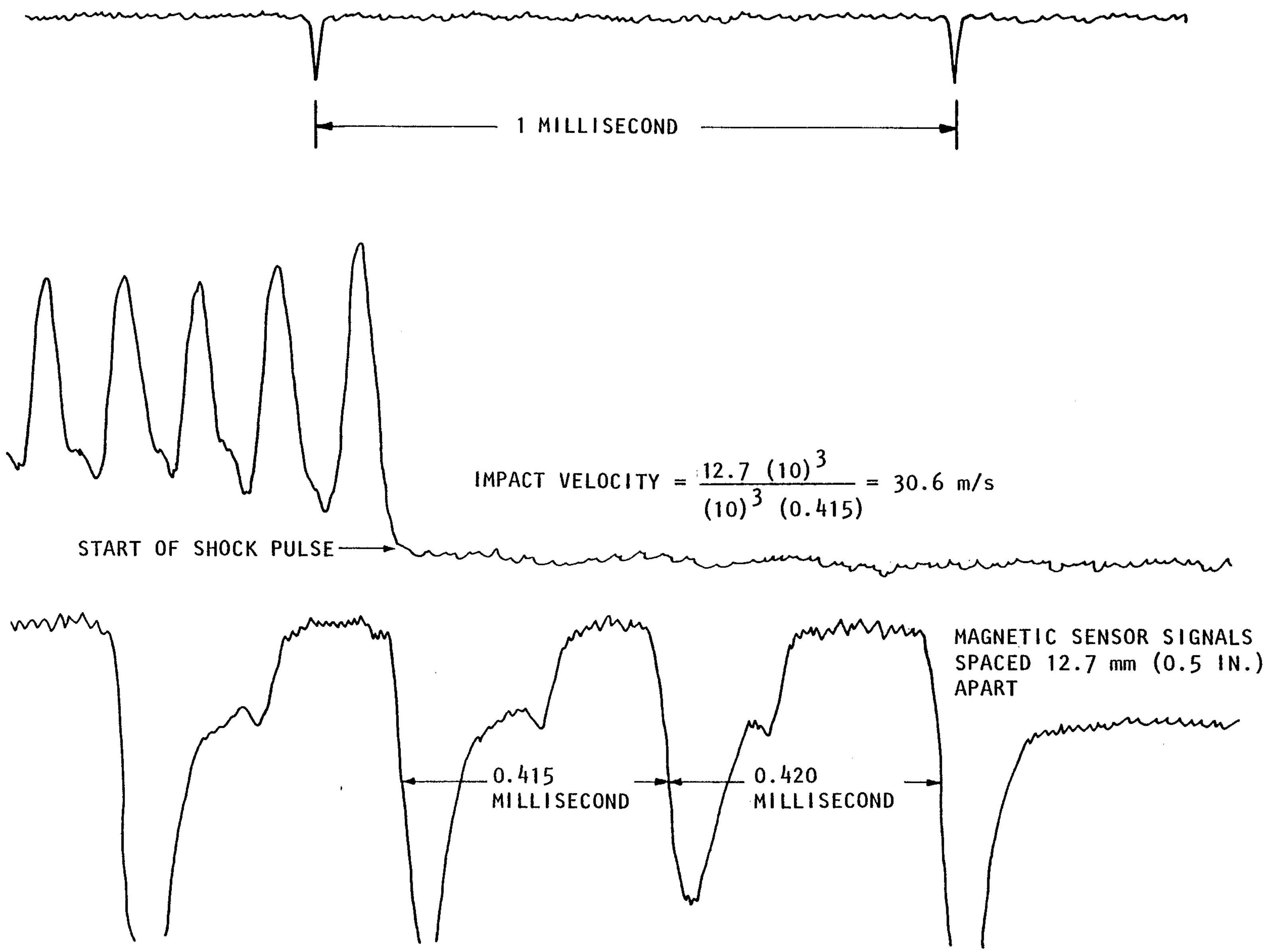

Figure 4. Velocity Calculation From Typical Output of Magnetic Sensors (Tracing)

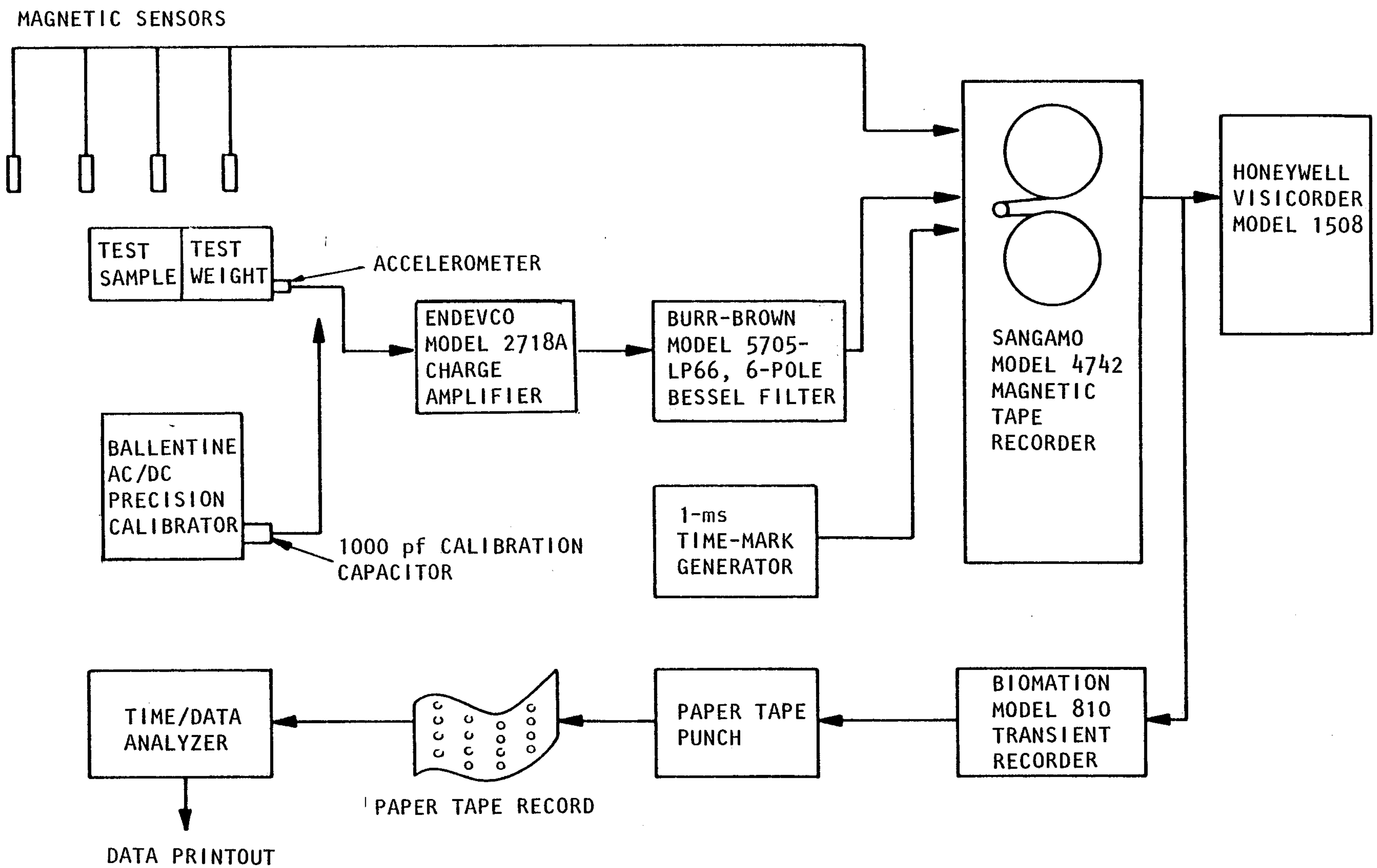

Figure 5. Block Diagram of Instrumentation System

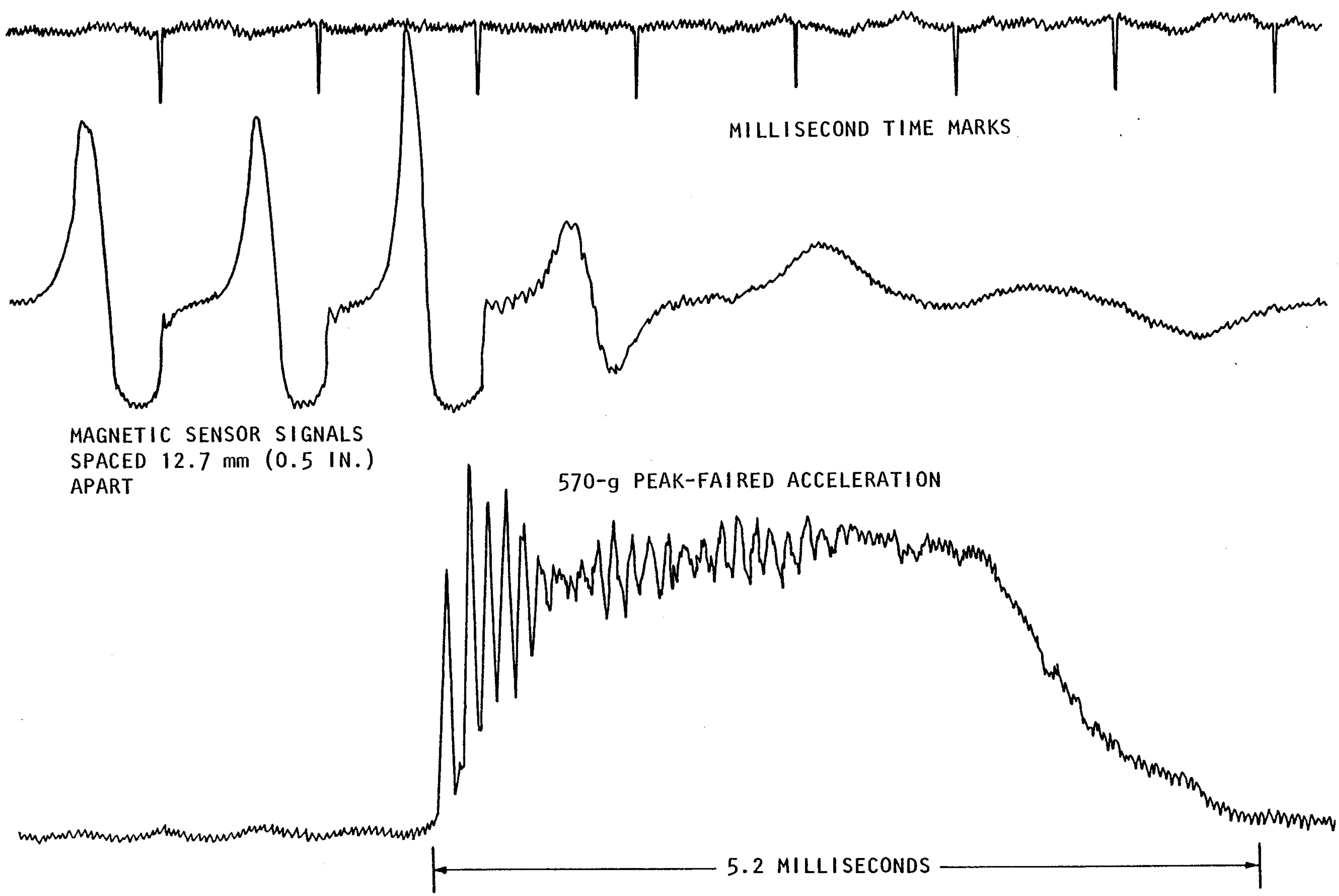

Figure 6. Typical Oscillograph Record of Impact Test (Tracing)

Data Reduction

The paper tape recorder of a test was entered into a time-data, time-series analyzer. The acceleration record was faired by first using a three-point smoothing algorithm. The program routine selected the baseline and limits of integration. The above information was displayed, giving the operator an opportunity to correct any unsatisfactory parameters before continuing. The program routine then determined velocity, sample deflection, and dynamic force versus time along with values for percent rebound, and energy absorbing efficiencies.

Energy-Absorption Efficiency

Energy-absorption efficiency is defined as the ratio of the energy absorbed per unit volume by the test material to the energy absorbed by an ideal material. An ideal energy-absorbing material is one which deflects at a constant stress, thus providing a constant deceleration for 100 percent of its thickness. The kinetic energy absorbed by a material bears the following relationship to the energy absorbed by an ideal material.

$$MV_i^2/2 = Md_m h, \qquad (1)$$

where

M = mass of impacting object,

V_i = impact velocity,

d_m = maximum deceleration,

h = material thickness, and

Md_m = maximum decelerating force.

By definition, the energy-aborbing efficiency (K) exhibited by a test material can be represented by the following equation:

$$K = V_i^2/2\ hd_m, \qquad (2)$$

where, for an ideal material,

$K = 1$.

The conclusion, therefore, can be reached that when V_i is low, the impact energy will probably be small in relation to the stiffness of the foam. There will be little compression; and K

will, therefore, be low. If V_i is too high, the impact energy will be large in relation to the stiffness of the foam; the critical strain will be exceeded (which will rapidly increase d_m); and K again will be low. At some intermediate value of V_i, K will exhibit a maximum. Values for energy-absorbing efficiency (K) are reported in Appendix A for each impact condition. The specific energy at each impact condition is provided in Table 1.

Data Presentation

When crushed, rigid polyurethane foam samples generally experience some degree of recovery (rebound). This post-impact recovery of the material is referred to as restituted strain. The rebound velocity of the test weight expressed as a percentage of the impact velocity, and the deflection of the test weight, before and after rebound, were determined for each impact condition. The numerical data for these conditions are provided in Appendix A.

Appendix B provides a graphical presentation of acceleration versus displacement for each test condition. In addition, a static compressive strength plot is superimposed on each set of dynamic plots to allow simultaneous evaluation of static and dynamic response. Samples for static testing were prepared in a manner identical to the dynamic testing samples and were crushed at a rate of 0.42 mm/s (1 inch/minute), using conventional load-deflection measuring equipment.

To allow effective use of the data in this report, a study was made to evaluate the effect of input errors on the accuracy of a typical test. A square wave best represents the acceleration time-trace obtained during the crush of a foam sample. Input errors were substituted into equations developed from the motion-time equations for a square wave pulse to indicate the total range of uncertainty for a typical impact test. It can be generally concluded that the accuracy of the output data is within ±10.5 percent. This information is detailed in Table 2.

ACCOMPLISHMENTS

Test techniques and the required equipment have been developed for use in evaluating structural support materials. These techniques have been used to evaluate six commonly used polyurethane foam systems, and the subsequent data have been published for reference.

FUTURE WORK

All planned activities have been completed. Additional studies may be performed by other endeavors as the need arises.

Table 1. Energy Related to Test Weights and Impact Velocities

Test Weight (kg) (lb)	Equivalent Static Load (kPa) (lb/in.^{2})	Impact Velocity (m/s) (ft/sec)	Impact Energy (Joules) (ft-lb)	Specific Energy (J/m^3 x 10^5) (ft-lb/in.^{3})
1.11 (2.45)	3.4 (0.5)	15.24 (50)	129.2 (95.3)	4.01 (4.85)
		30.48 (100)	516.8 (381.2)	16.06 (19.41)
		45.72 (150)	1162.9 (857.7)	36.13 (43.67)
		60.96 (200)	2067.4 (1524.8)	64.24 (77.64)
2.23 (4.91)	6.9 (1.0)	15.24 (50)	258.4 (190.6)	8.03 (9.70)
		30.48 (100)	1035.0 (763.4)	32.10 (38.80)
		45.72 (150)	2325.8 (1715.4)	72.23 (87.30)
		60.96 (200)	4134.7 (3049.6)	128.49 (155.30)
4.46 (9.82)	13.8 (2.0)	15.24 (50)	516.8 (381.2)	16.06 (19.41)
		30.48 (100)	2067.4 (1524.8)	64.24 (77.64)
		45.72 (150)	4651.7 (3430.9)	144.53 (174.69)
		60.96 (200)	8269.7 (6099.4)	256.95 (310.56)

Table 2. Effect of Input-Parameter Errors Upon Accuracy of Output Data

Input Data Uncertainty (Percent)		Output Data Uncertainty (Percent)				
				Maximum Displacement		
		Dynamic Force	Rebound	0 Rebound	0.1 Rebound	0.3 Rebound
Pulse Amplitude		±8.7	±8.7	± 8.7	±7.2	±5.2
Accelerometer	±6.0					
Calibrator	±1.0					
Digital Recorder	±0.7					
Choice of Baseline	±1.0					
Pulse Time		0	±0.28	± 0.50	±0.41	±0.30
Digital Recorder	±0.03					
Resolution	±0.25					
Impact Velocity		0	±0.43	± 0.86	±0.71	±0.51
Travel Distance	±0.10					
Travel Time	±0.30					
Tape Recorder	±0.03					
Displacement		0	0	± 0.4	±0.4	±0.4
Integration Start	±0.4					
Total Output Data Uncertainty		±8.7	±9.4	±10.5	±8.7	±6.4

Appendix A

IMPACT DATA TABLES

Table A-1. Impact Data for CPR 1024

Sample Density (kg/m^3) (lb/ft^3)	Impact Load (pa) ($lb/in.^2$)	Impact Velocity (m/s) (ft/sec)	Maximum Accel (g)	Maximum Deflection (mm) (in.)	Final Deflection (mm) (in.)	Rebound Velocity (Percent)	K*
160 (10)	3447 (0.5)	15.24 (50)	982	12.45 (0.49)	10.41 (0.41)	26.7	0.125
		30.48 (100)	1282	26.67 (1.05)	24.89 (0.98)	12.1	0.375
		45.72 (150)	**				
		60.96 (200)					
	6895 (1.0)	15.24 (50)	510	18.80 (0.74)	16.51 (0.65)	15.5	0.227
		30.48 (100)	**				
		45.72 (150)					
		60.96 (200)					
	13789 (2.0)	15.24 (50)	313	27.69 (1.09)	25.91 (1.02)	6.9	0.400
		30.48 (100)	**				
		45.72 (150)					
		60.96 (200)					
320 (20)	3447 (0.5)	15.24 (50)	2800	4.06 (0.16)	3.30 (0.13)	37.2	0.041
		30.48 (100)	3438	9.91 (0.39)	6.86 (0.27)	29.3	0.133
		45.72 (150)	3583	19.81 (0.78)	19.05 (0.75)	7.3	0.278
		60.96 (200)	5240	24.38 (0.96)	23.88 (0.94)	0.3	0.350
	6895 (1.0)	15.24 (50)	1850	6.10 (0.24)	3.81 (0.15)	44.7	0.064
		30.48 (100)	2031	25.40 (0.76)	16.26 (0.64)	22.2	0.226
		45.72 (150)	2264	34.80 (1.37)	34.29 (1.35)	5.7	0.456
		60.96 (200)	**				
	13789 (2.0)	15.24 (50)	869	11.18 (0.44)	8.13 (0.32)	27.7	0.135
		30.48 (100)	1270	26.92 (1.06)	23.37 (0.92)	20.5	0.370
		45.72 (150)	**				
		60.96 (200)					

*K = Energy Absorption Efficiency
**Critical Strain Exceeded

Table A-2. Impact Data for CPR 1040

Sample Density (kg/m^3) (lb/ft^3)	Impact Load (pa) (lb/in.^{2})	Impact Velocity (m/s) (ft/sec)	Maximum Accel (g)	Maximum Deflection (mm) (in.)	Final Deflection (mm) (in.)	Rebound Velocity (Percent)	K*
160 (10)	3447 (0.5)	15.24 (50)	680	14.22 (0.56)	14.22 (0.56)	0	0.139
		30.48 (100)	1372	22.10 (0.87)	19.56 (0.77)	15.2	0.326
		45.72 (150)	**				
		60.96 (200)					
	6895 (1.0)	15.24 (50)	684	16.51 (0.65)	12.45 (0.49)	22.5	0.182
		30.48 (100)	1062	39.62 (1.56)	38.35 (1.51)	4.7	0.476
		45.72 (150)	**				
		60.96 (200)					
	13789 (2.0)	15.24 (50)	368	23.14 (0.91)	21.34 (0.84)	11.3	0.327
		30.48 (100)	**				
		45.72 (150)					
		60.96 (200)					
320 (20)	3447 (0.5)	15.24 (50)	3691	3.56 (0.14)	2.79 (0.11)	30.4	0.034
		30.48 (100)	4009	10.41 (0.41)	9.40 (0.37)	14.9	0.117
		45.72 (150)	**				
		60.96 (200)					
	6895 (1.0)	15.24 (50)	2175	6.60 (0.26)	3.81 (0.15)	55.2	0.053
		30.48 (100)	2524	15.24 (0.60)	13.46 (0.53)	16.2	0.186
		45.72 (150)	2857	26.67 (1.05)	26.67 (1.05)	0	0.374
		60.96 (200)	**				
	13789 (2.0)	15.24 (50)	1030	11.43 (0.45)	11.18 (0.44)	4.0	0.110
		30.48 (100)	1736	20.57 (0.81)	16.76 (0.66)	25.4	0.264
		45.72 (150)	**				
		60.96 (200)					

*K = Energy Absorption Efficiency
**Critical Strain Exceeded

Table A-3. Impact Data for BC 1200 Series

Sample Density (kg/m^3) (lb/ft^3)	Impact Load (pa) (lb/in.^{2})	Impact Velocity (m/s) (ft/sec)	Maximum Accel (g)	Maximum Deflection (mm) (in.)	Final Deflection (mm) (in.)	Rebound Velocity (percent)	K*
160 (10)	3447 (0.5)	15.24 (50)	1714	3.38 (0.33)	6.60 (0.26)	89.7	0.063
		30.48 (100)	1967	20.83 (0.82)	18.29 (0.72)	18.8	0.233
		45.72 (150)	2627	34.80 (1.37)	33.02 (1.30)	13.4	0.407
		60.96 (200)					
	6895 (1.0)	15.24 (50)	880	11.94 (0.47)	10.67 (0.42)	20.4	0.138
		30.48 (100)	1174	28.96 (1.14)	27.43 (1.08)	12.2	0.381
		45.72 (150)	**				
		60.96 (200)					
	13789 (2.0)	15.24 (50)	508	16.51 (0.65)	15.24 (0.60)	14.7	0.234
		30.48 (100)	**				
		45.72 (150)					
		60.96 (200)					
320 (20)	3447 (0.5)	15.24 (50)	4300	4.83 (0.19)	2.03 (0.08)	71.1	0.030
		30.48 (100)	4600	7.37 (0.29)	5.59 (0.22)	31.5	0.102
		45.72 (150)	5500	18.03 (0.71)	14.99 (0.59)	22.5	0.187
		60.96 (200)	6537	21.34 (0.84)	17.78 (0.70)	19.1	0.280
	6895 (1.0)	15.24 (50)	2287	6.86 (0.27)	5.33 (0.21)	36.9	0.053
		30.48 (100)	2891	11.43 (0.45)	8.89 (0.35)	29.7	0.155
		45.72 (150)	**				
		60.96 (200)					
	13789 (2.0)	15.24 (50)	1199	8.34 (0.34)	7.37 (0.29)	15.9	0.093
		30.48 (100)	1687	21.34 (0.84)	19.30 (0.76)	16.4	0.277
		45.72 (150)	**				
		60.96 (200)					

Table A-3 Continued. Impact Data for BC 1200 Series

Sample Density (kg/m^3) (lb/ft^3)	Impact Load (pa) ($lb/in.^2$)	Impact Velocity (m/s) (ft/sec)	Maximum Accel (g)	Maximum Deflection (mm) (in.)	Final Deflection (mm) (in.)	Rebound Velocity (Percent)	K*
480 (30)	3447 (0.5)	15.24 (50)	6600	3.05 (0.12)	1.02 (0.04)	84.1	0.017
		30.48 (100)					
		45.72 (150)	11000	8.38 (0.33)	5.59 (0.22)	43.6	0.90
		60.96 (200)					
	6895 (1.0)	15.24 (50)	4650	4.83 (0.19)	3.56 (0.14)	67.7	0.025
		30.48 (100)	6400	7.62 (0.30)	5.84 (0.23)	35.3	0.067
		45.72 (150)	6200	15.75 (0.62)	13.72 (0.54)	18.6	0.172
		60.96 (200)	8410	20.32 (0.80)	18.80 (0.74)	16.5	0.208
	13789 (2.0)	15.24 (50)	2778	4.83 (0.19)	3.56 (0.14)	36.3	0.042
		30.48 (100)	3248	15.24 (0.60	14.22 (0.56)	9.0	0.138
		45.72 (150)	4024	21.59 (0.85)	19.56 (0.77)	16.9	0.266
		60.96 (200)	**				
	3447 (0.5)	15.24 (50)					
		30.48 (100)					
		45.72 (150)					
		60.96 (200)					
	6895 (1.0)	15.24 (50)					
		30.48 (100)					
		45.72 (150)					
		60.96 (200)					
	13789 (2.0)	15.24 (50)					
		30.48 (100)					
		45.72 (150)					
		60.96 (200)					

*K = Energy Absorption Efficiency
**Critical Strain Exceeded

Table A-4. Impact Data for BKC 4003

Sample Density (kg/m^3) (lb/ft^3)	Impact Load (pa) (lb/in.^{2})	Impact Velocity (m/s) (ft/sec)	Maximum Accel (g)	Maximum Deflection (mm) (in.)	Final Deflection (mm) (in.)	Rebound Velocity (Percent)	K*
160 (10)	3447 (0.5)	15.24 (50)	842	12.70 (0.50)	11.94 (0.47)	13.8	0.144
		30.48 (100)	1195	30.23 (1.19)	25.91 (1.02)	20.7	0.388
		45.72 (150)	**				
		60.96 (200)					
	6895 (1.0)	15.24 (50)	477	19.30 (0.76)	15.75 (0.62)	23.6	0.255
		30.48 (100)	**				
		45.72 (150)					
		60.96 (200)					
	13789 (2.0)	15.24 (50)	281	22.10 (0.87)	22.10 (0.87)	11.1	0.406
		30.48 (100)	**				
		45.72 (150)					
		60.96 (200)					
320 (20)	3447 (0.5)	15.24 (50)	3117	5.84 (0.23)	2.03 (0.08)	68.2	0.039
		30.48 (100)	3378	11.18 (0.44)	7.37 (0.29)	32.7	0.136
		45.72 (150)	4144	18.03 (0.71)	15.49 (0.61)	24.6	0.249
		60.96 (200)					
	6895 (1.0)	15.24 (50)	1345	8.38 (0.33)	8.38 (0.33)	9.0	0.083
		30.48 (100)	2042	17.53 (0.69)	14.73 (0.58)	22.3	0.230
		45.72 (150)	3551	32.26 (1.27)	28.70 (1.13)	22.4	0.307
		60.96 (200)					
	13789 (2.0)	15.24 (50)	1149	8.64 (0.34)	6.86 (0.27)	24.5	0.109
		30.48 (100)	1282	26.42 (1.04)	24.13 (0.95)	15.7	0.357
		45.72 (150)	**				
		60.96 (200)					

Table A-4 Continued. Impact Data for BKC 4003

Sample Density (kg/m^3) (lb/ft^3)	Impact Load (pa) ($lb/in.^2$)	Impact Velocity (m/s) (ft/sec)	Maximum Accel (g)	Maximum Deflection (mm) (in.)	Final Deflection (mm) (in.)	Rebound Velocity (Percent)	K*
480 (30)	3447 (0.5)	15.24 (50)	5800	3.81 (0.15)	2.03 (0.08)	58.4	0.020
		30.48 (100)	9496	5.33 (0.21)	3.30 (0.18)	40.3	0.047
		45.72 (150)					
		60.96 (200)					
	6895 (1.0)	15.24 (50)	2800	5.33 (0.21)	5.08 (0.20)	11.8	0.038
		30.48 (100)					
		45.72 (150)	5547	16.51 (0.65)	15.75 (0.62)	7.1	0.186
		60.96 (200)	7255	25.40 (1.00)	23.37 (0.92)	12.7	0.253
	13789 (2.0)	15.24 (50)	2505	4.32 (0.17)	1.27 (0.05)	50.8	0.047
		30.48 (100)	3105	12.19 (0.48)	9.14 (0.36)	26.1	0.159
		45.72 (150)	3858	20.07 (0.79)	15.75 (0.62)	29.0	0.267
		60.96 (200)					
	3447 (0.5)	15.24 (50)					
		30.48 (100)					
		45.72 (150)					
		60.96 (200)					
	6895 (1.0)	15.24 (50)					
		30.48 (100)					
		45.72 (150)					
		60.96 (200)					
	13789 (2.0)	15.24 (50)					
		30.48 (100)					
		45.72 (150)					
		60.96 (200)					

*K = Energy Absorption Efficiency
**Critical Strain Exceeded

Table A-5. Impact Data for BKC 6003

Sample Density (kg/m^3) (lb/ft^3)	Impact Load (pa) ($lb/in.^2$)	Impact Velocity (m/s) (ft/sec)	Maximum Accel (g)	Maximum Deflection (mm) (in.)	Final Deflection (mm) (in.)	Rebound Velocity (Percent)	K*
160 (10)	3447 (0.5)	15.24 (50)	1020	9.91 (0.39)	8.38 (0.33)	23.2	0.115
		30.48 (100)	1351	28.70 (1.13)	24.89 (0.98)	14.2	0.356
		45.72 (150)	**				
		60.96 (200)					
	6895 (1.0)	15.24 (50)	585	16.26 (0.64)	14.22 (0.56)	16.0	0.189
		30.48 (100)	972	39.88 (1.57)	38.61 (1.52)	0	0.483
		45.72 (150)	**				
		60.96 (200)					
	13789 (2.0)	15.24 (50)	338	25.40 (1.00)	25.40 (1.00)	0	0.374
		30.48 (100)	**				
		45.72 (150)					
		60.96 (200)					
320 (20)	3447 (0.5)	15.24 (50)	3756	3.81 (0.15)	2.54 (0.10)	46.3	0.033
		30.48 (100)	4187	9.65 (0.38)	8.38 (0.33)	15.0	0.112
		45.72 (150)					
		60.96 (200)					
	6895 (1.0)	15.24 (50)	1086	8.89 (0.35)	8.89 (0.35)	0	0.103
		30.48 (100)	2676	16.51 (0.65)	13.97 (0.55)	16.6	0.178
		45.72 (150)	3754	21.34 (0.84)	10.92 (0.43)	13.6	0.275
		60.96 (200)					
	13789 (2.0)	15.24 (50)	1178	9.14 (0.36)	7.37 (0.29)	24.6	0.102
		30.48 (100)	1790	20.07 (0.79)	18.80 (0.74)	12.0	0.255
		45.72 (150)	**				
		60.96 (200)					

Table A-5 Continued. Impact Data for BKC 6003

Sample Density (kg/m^3) (lb/ft^3)	Impact Load (pa) ($lb/in.^2$)	Impact Velocity (m/s) (ft/sec)	Maximum Accel (g)	Maximum Deflection (mm) (in.)	Final Deflection (mm) (in.)	Rebound Velocity (Percent)	K*
480 (30)	3447 (0.5)	15.24 (50)	6000	2.79 (0.11)	1.02 (0.04)	48.6	0.021
		30.48 (100)	7600	5.84 (0.23)	3.81 (0.15)	50.8	0.058
		45.72 (150)	8000	10.67 (0.42)	9.40 (0.37)	22.8	0.124
		60.96 (200)					
	6895 (1.0)	15.24 (50)	3150	4.32 (0.17)	2.29 (0.09)	44.9	0.034
		30.48 (100)	4185	12.19 (0.48)	10.16 (0.40)	22.9	0.115
		45.72 (150)	5584	14.99 (0.59)	12.19 (0.48)	22.1	0.188
		60.96 (200)	6000	22.10 (0.87)	22.10 (0.87)	0	0.305
	13789 (2.0)	15.24 (50)	1865	7.62 (0.30)	5.08 (0.20)	33.9	0.066
		30.48 (100)	2879	13.72 (0.54)	6.60 (0.26)	41.3	0.171
		45.72 (150)	3447	25.40 (1.00)	16.00 (0.63)	24.4	0.305
		60.96 (200)	**				
	3447 (0.5)	15.24 (50)					
		30.48 (100)					
		45.72 (150)					
		60.96 (200)					
	6895 (1.0)	15.24 (50)					
		30.48 (100)					
		45.72 (150)					
		60.96 (200)					
	13789 (2.0)	15.24 (50)					
		30.48 (100)					
		45.72 (150)					
		60.96 (200)					

*K = Energy Absorption Efficiency
**Critical Strain Exceeded

Table A-6. Impact Data for BKC 44302

Sample Density (kg/m^3) (lb/ft^3)	Impact Load (pa) (lb/in.^{2})	Impact Velocity (m/s) (ft/sec)	Maximum Accel (g)	Maximum Deflection (mm) (in.)	Final Deflection (mm) (in.)	Rebound Velocity (Percent)	K*
160 (10)	3447 (0.5)	15.24 (50)	1178	9.40 (0.37)	7.37 (0.29)	30.9	0.100
		30.48 (100)	1466	22.86 (0.90)	20.07 (0.79)	16.0	0.321
		45.72 (150)	2109	42.67 (1.68)	42.67 (1.68)	0	0.489
		60.96 (200)					
	6895 (1.0)	15.24 (50)	612	15.49 (0.61)	12.7 (0.50)	26.2	0.185
		30.48 (100)	1113	38.86 (1.53)	38.1 (1.50)	5.4	0.432
		45.72 (150)	**				
		60.96 (200)					
	13789 (2.0)	15.24 (50)	352	23.88 (0.94)	20.07 (0.79)	19.2	0.310
		30.48 (100)	1718	53.09 (2.09)	53.09 (2.09)	0	0.273
		45.72 (150)	**				
		60.96 (200)					
320 (20)	3447 (0.5)	15.24 (50)	3900	4.32 (0.17)	2.29 (0.09)	51.3	0.031
		30.48 (100)	4083	11.43 (0.45)	9.40 (0.37)	24.4	0.115
		45.72 (150)	4605	18.03 (0.71)	17.27 (0.68)	4.5	0.220
		60.96 (200)	5808	23.88 (0.94)	20.57 (0.81)	14.0	0.316
	6895 (1.0)	15.24 (50)	2010	5.59 (0.22)	3.30 (0.13)	39.5	0.056
		30.48 (100)	2655	18.29 (0.72)	16.26 (0.64)	15.3	0.190
		45.72 (150)	3038	27.18 (1.07)	26.42 (1.04)	0	0.339
		60.96 (200)	5705	37.34 (1.47)	32.26 (1.27)	4.18	0.321
	13789 (2.0)	15.24 (50)	1033	11.43 (0.45)	9.65 (0.38)	21.8	0.113
		30.48 (100)	1688	23.88 (0.94)	20.32 (0.80)	18.1	0.271
		45.72 (150)	**				
		60.96 (200)					

Table A-6 Continued. Impact Data for BKC 44302

Sample Density (kg/m^3) (lb/ft^3)	Impact Load (pa) ($lb/in.^2$)	Impact Velocity (m/s) (ft/sec)	Maximum Accel (g)	Maximum Deflection (mm) (in.)	Final Deflection (mm) (in.)	Rebound Velocity (Percent)	K*
480 (30)	3447 (0.5)	15.24 (50)	5310	3.30 (0.13)	2.29 (0.09)	34.0	0.022
		30.48 (100)	10730	5.08 (0.20)	2.29 (0.09)	57.1	0.047
		45.72 (150)	10800	9.91 (0.39)	8.64 (0.34)	19.4	0.095
		60.96 (200)					
	6895 (1.0)	15.24 (50)	4477	4.32 (0.17)	1.78 (0.07)	80.8	0.024
		30.48 (100)					
		45.72 (150)					
		60.96 (200)	7931	19.56 (0.77)	19.05 (0.75)	0.5	0.231
	13789 (2.0)	15.24 (50)	2624	3.56 (0.14)	0.76 (0.03)	59.8	0.041
		30.48 (100)	3527	12.45 (0.49)	8.38 (0.33)	38.2	0.135
		45.72 (150)					
		60.96 (200)	5578	29.72 (1.17)	28.19 (1.11)	10.6	0.329
	3447 (1.5)	15.24 (50)					
		30.48 (100)					
		45.72 (150)					
		60.96 (200)					
	6895 (1.0)	15.24 (50)					
		30.48 (100)					
		45.72 (150)					
		60.96 (200)					
	13789 (2.0)	15.24 (50)					
		30.48 (100)					
		45.72 (150)					
		60.96 (200)					

*K = Energy Absorption Efficiency
**Critical Strain Exceeded

Appendix B

ACCELERATION VERSUS DISPLACEMENT GRAPHS

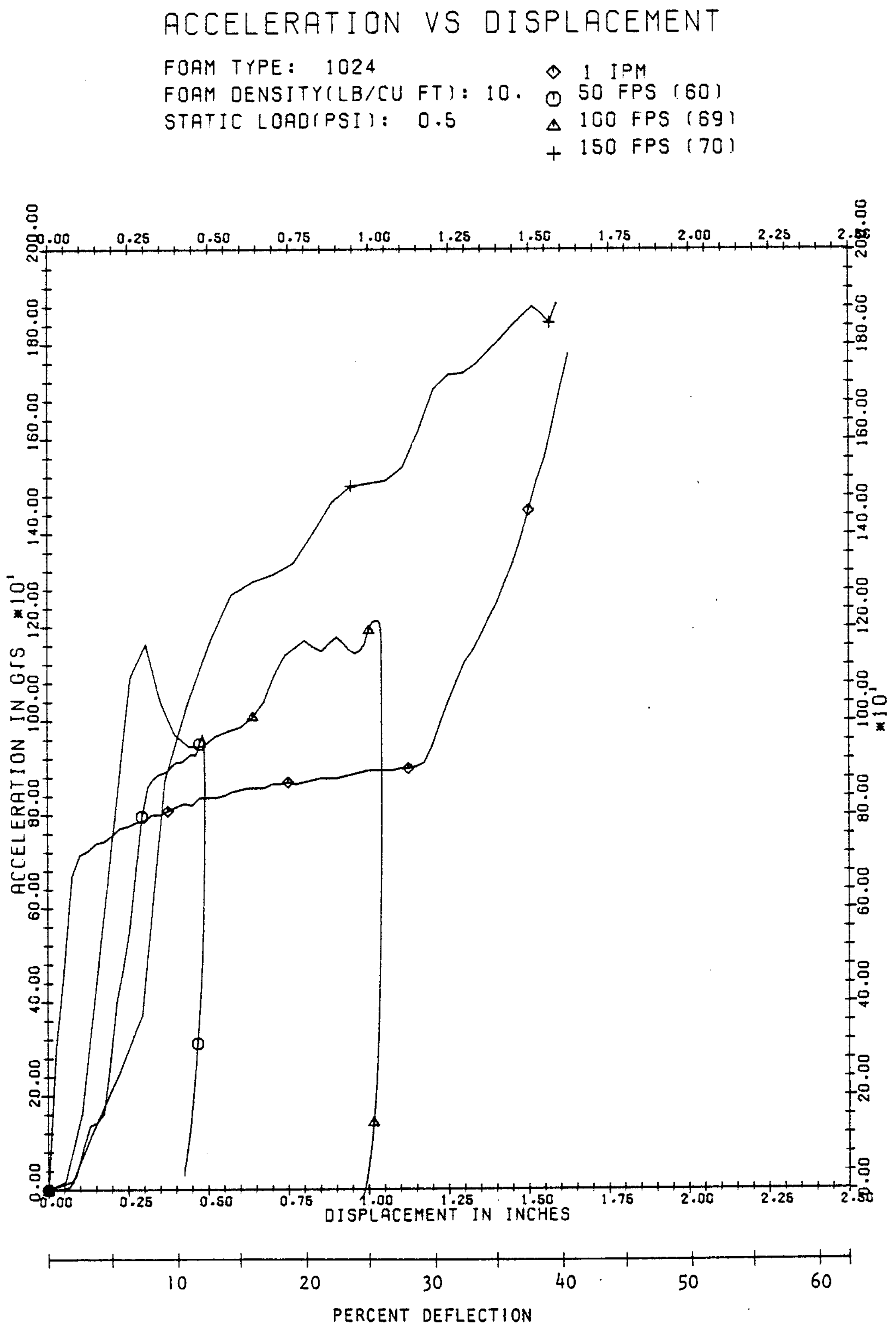

Figure B-1. CPR 1024, 10 LB/FT^3, 0.5 PSI

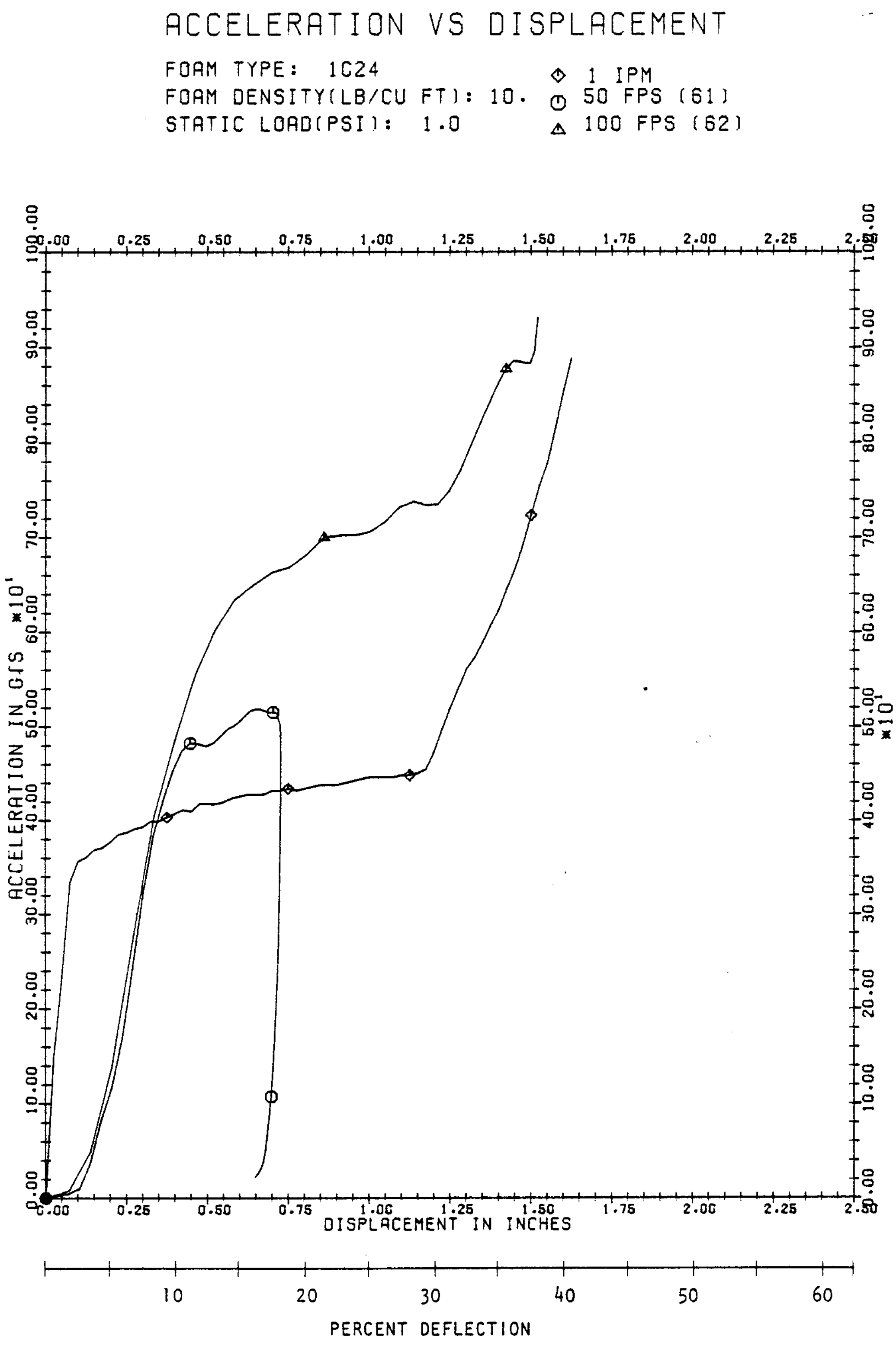

Figure B-2. CPR 1024, 10 LB/FT^3, 1.0 PSI

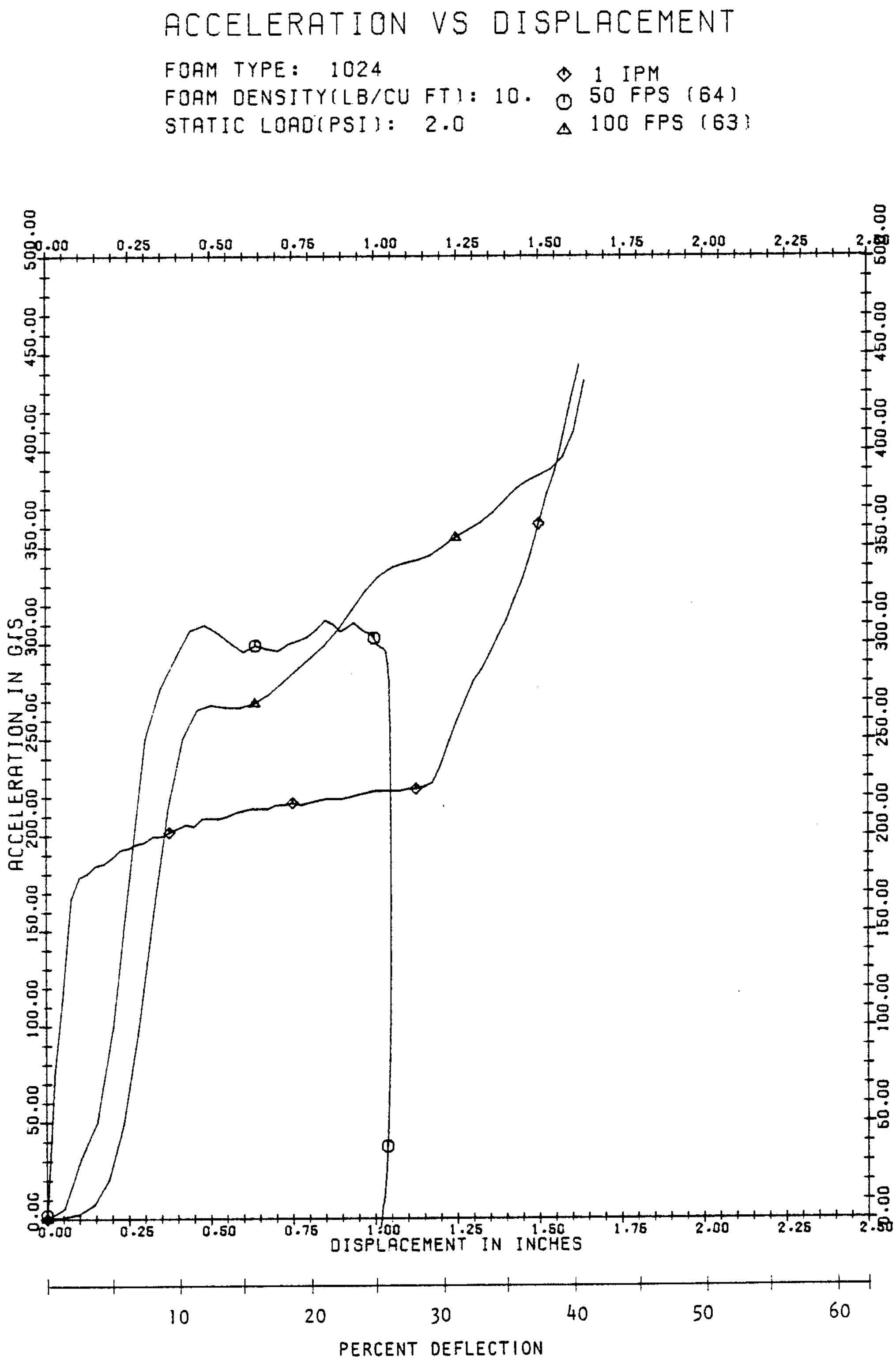

Figure B-3. CPR 1024, 10 LB/FT^3, 2.0 PSI

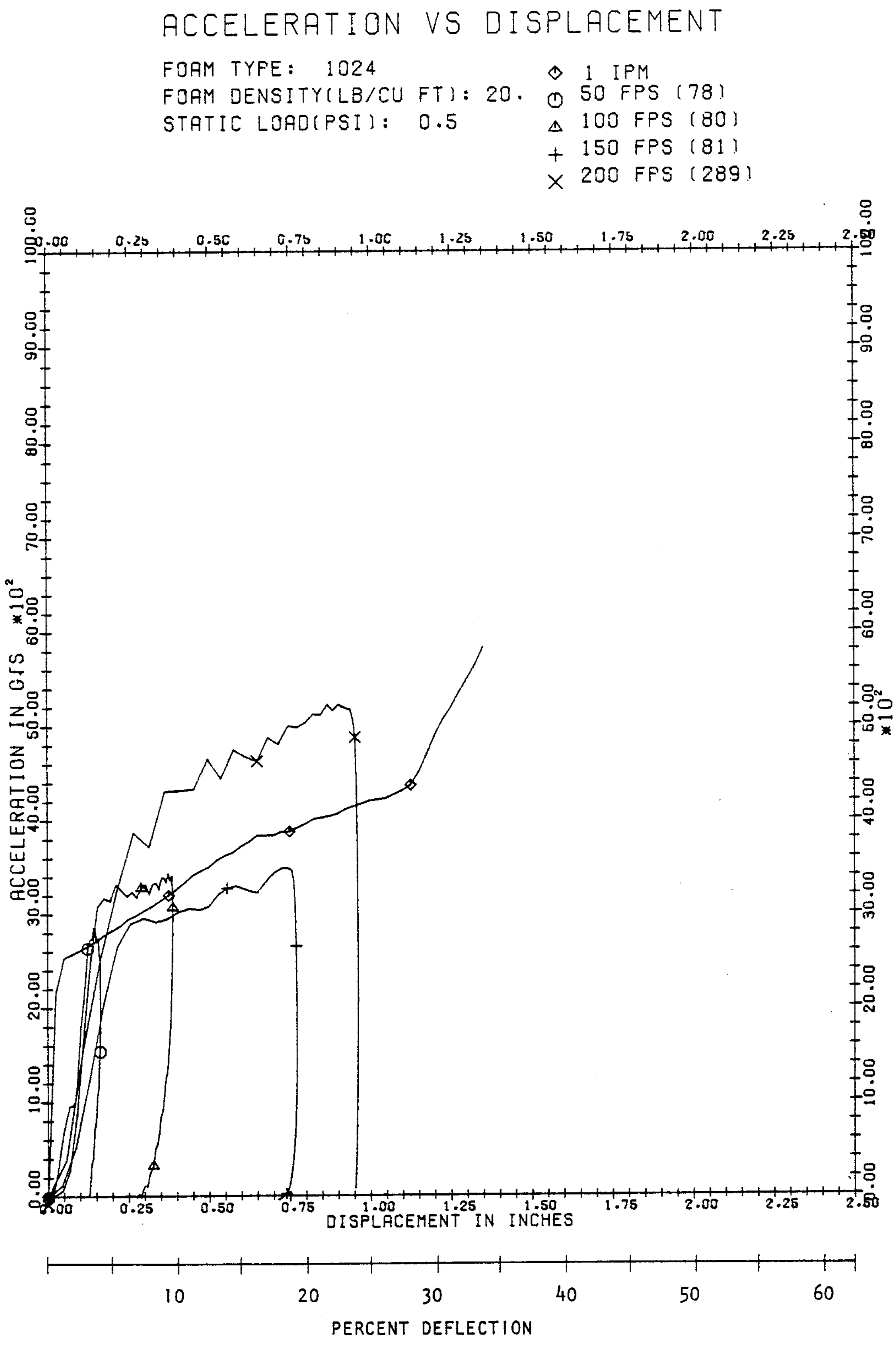

Figure B-4. CPR 1024, 20 LB/FT^3, 0.5 PSI

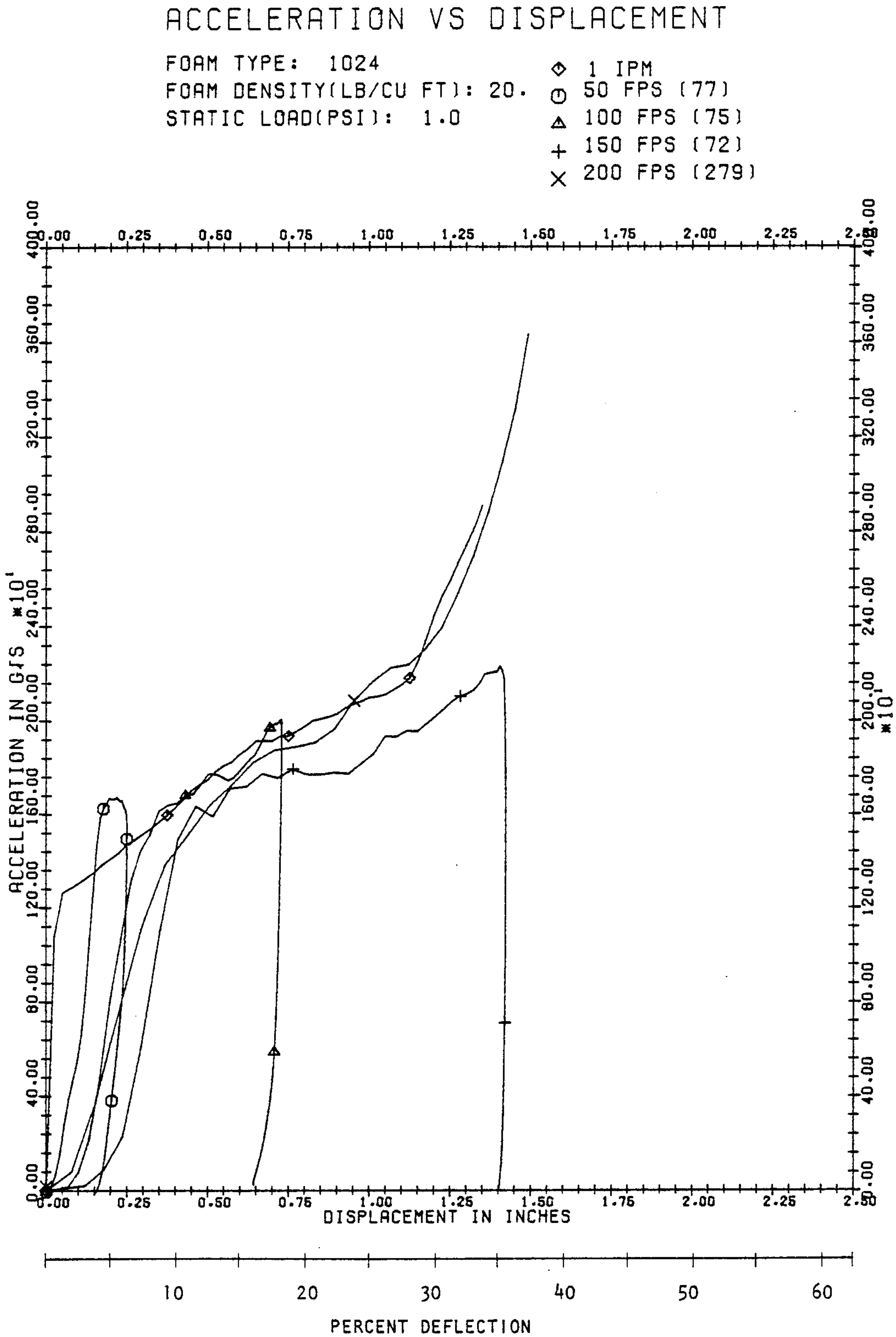

Figure B-5. CPR 1024, 20 LB/FT^3, 1.0 PSI

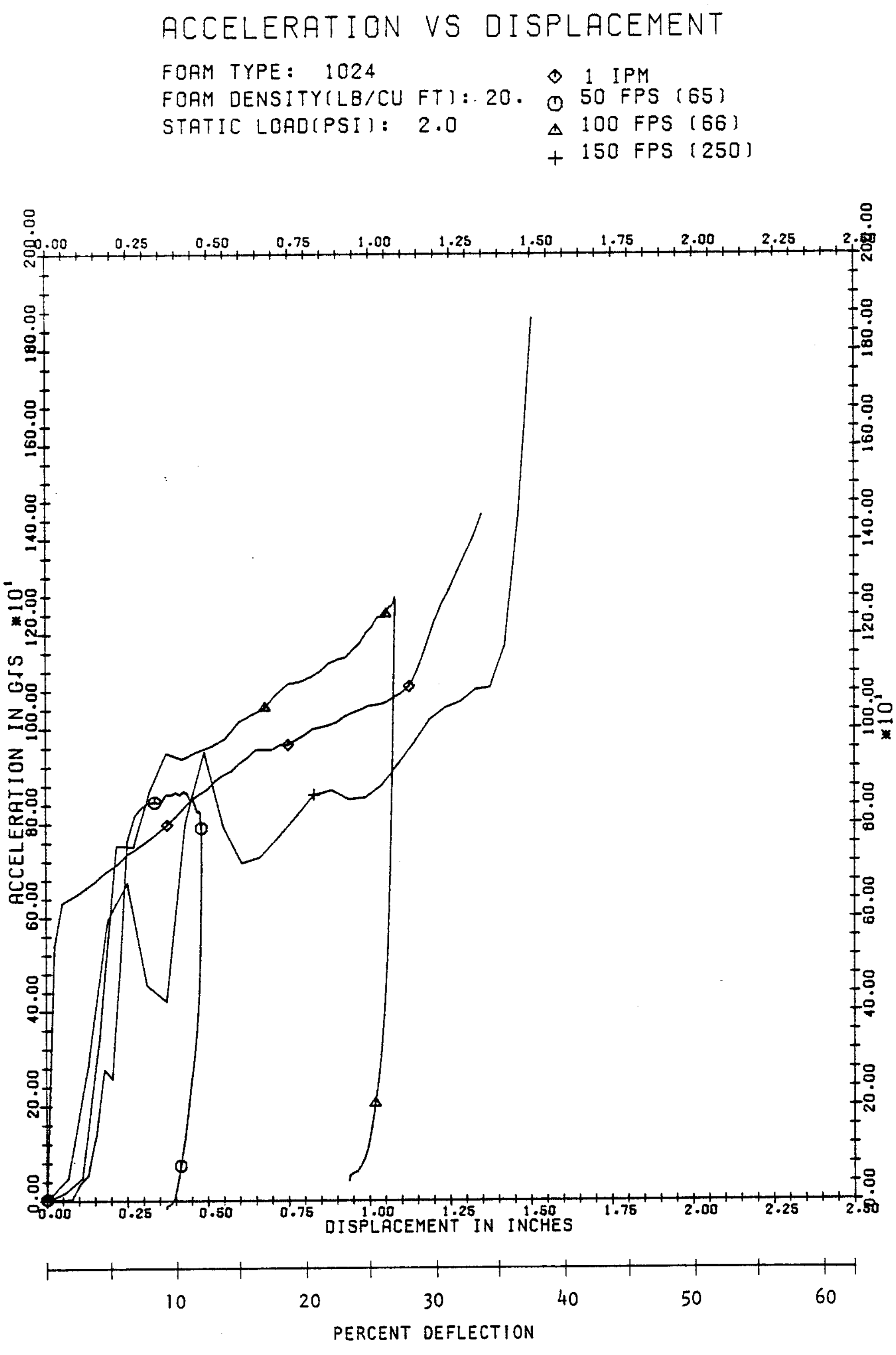

Figure B-6. CPR 1024, 20 LB/FT^3, 2.0 PSI

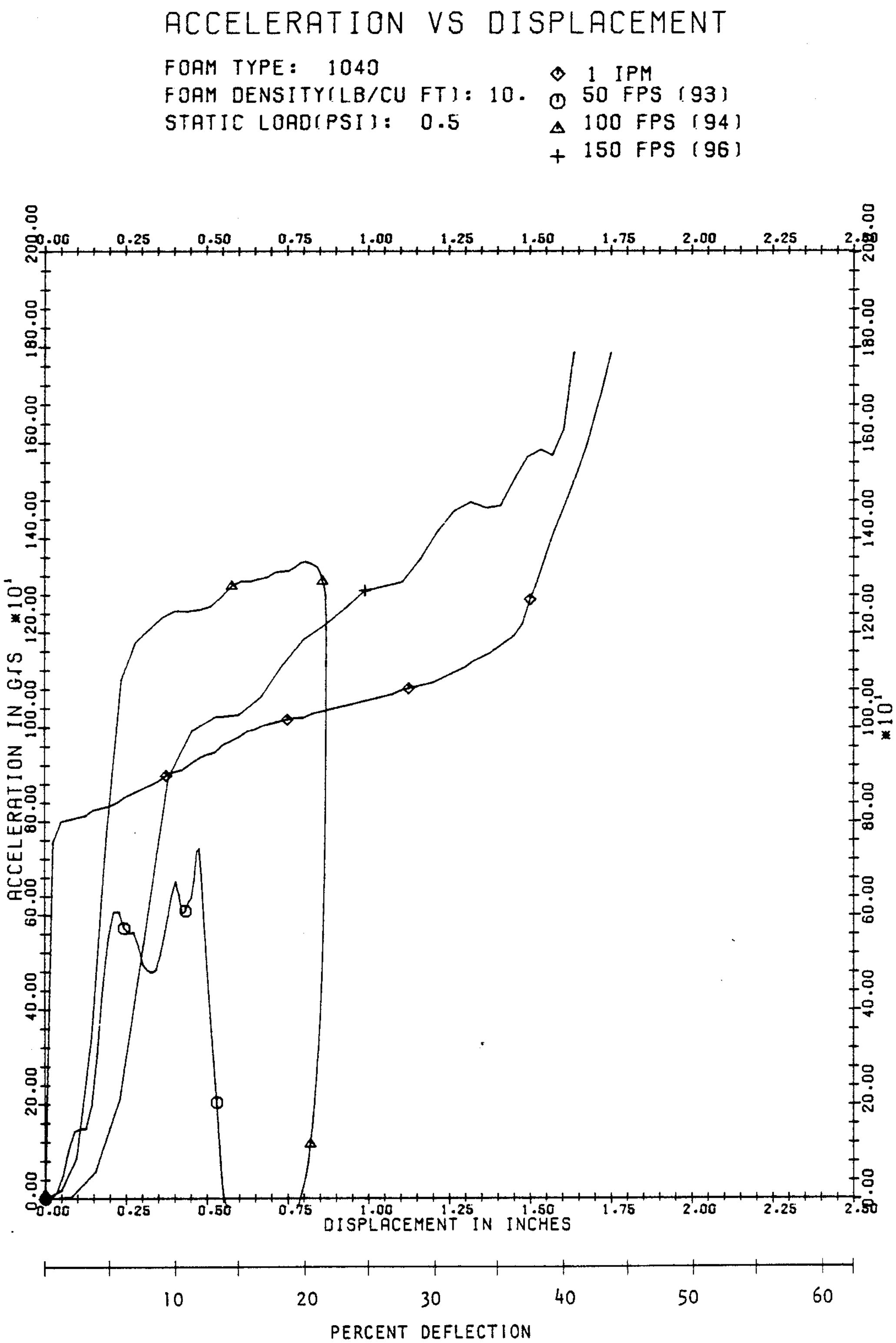

Figure B-7. CPR 1040, 10 LB/FT^3, 0.5 PSI

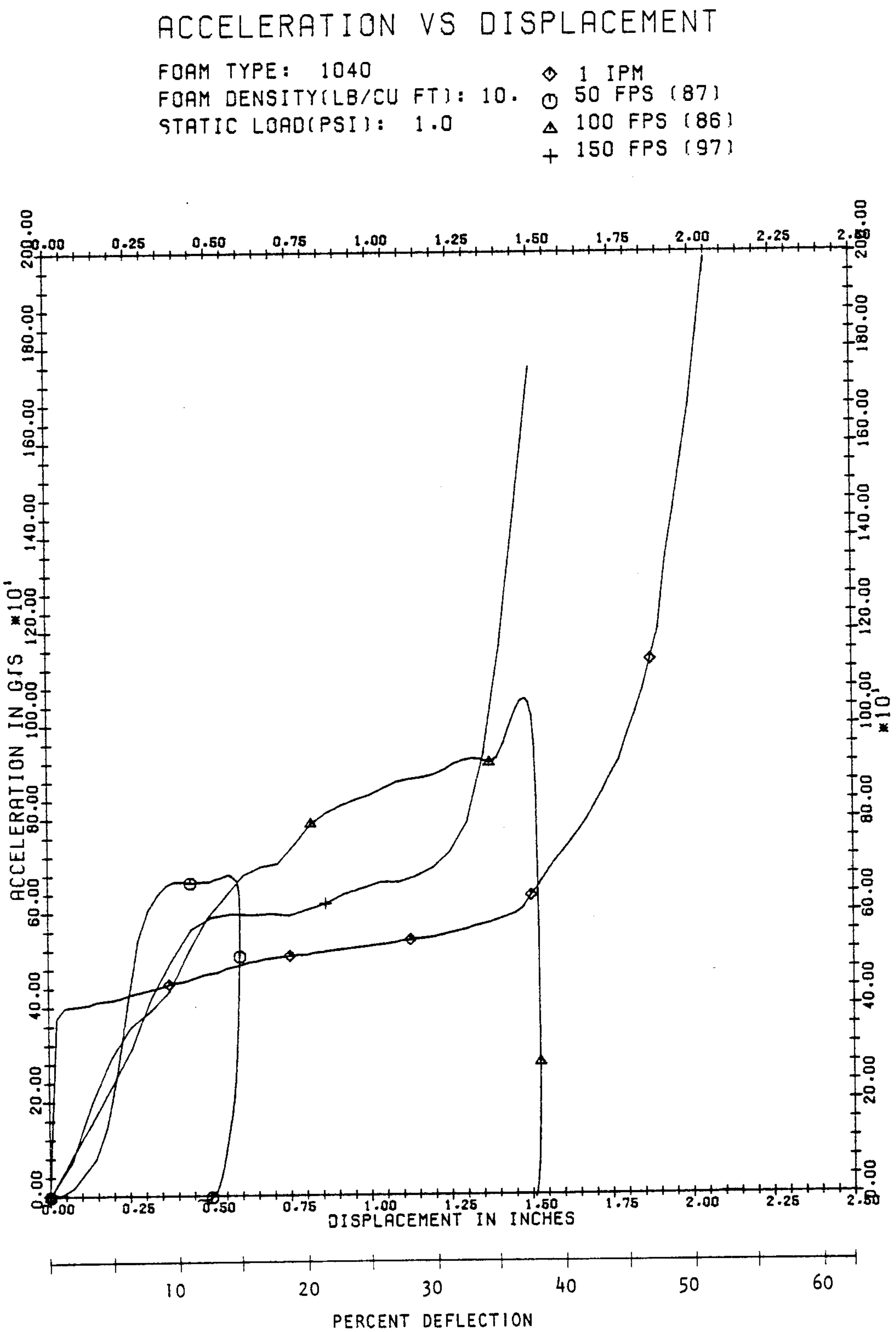

Figure B-8. CPR 1040, 10 LB/FT^3, 1.0 PSI

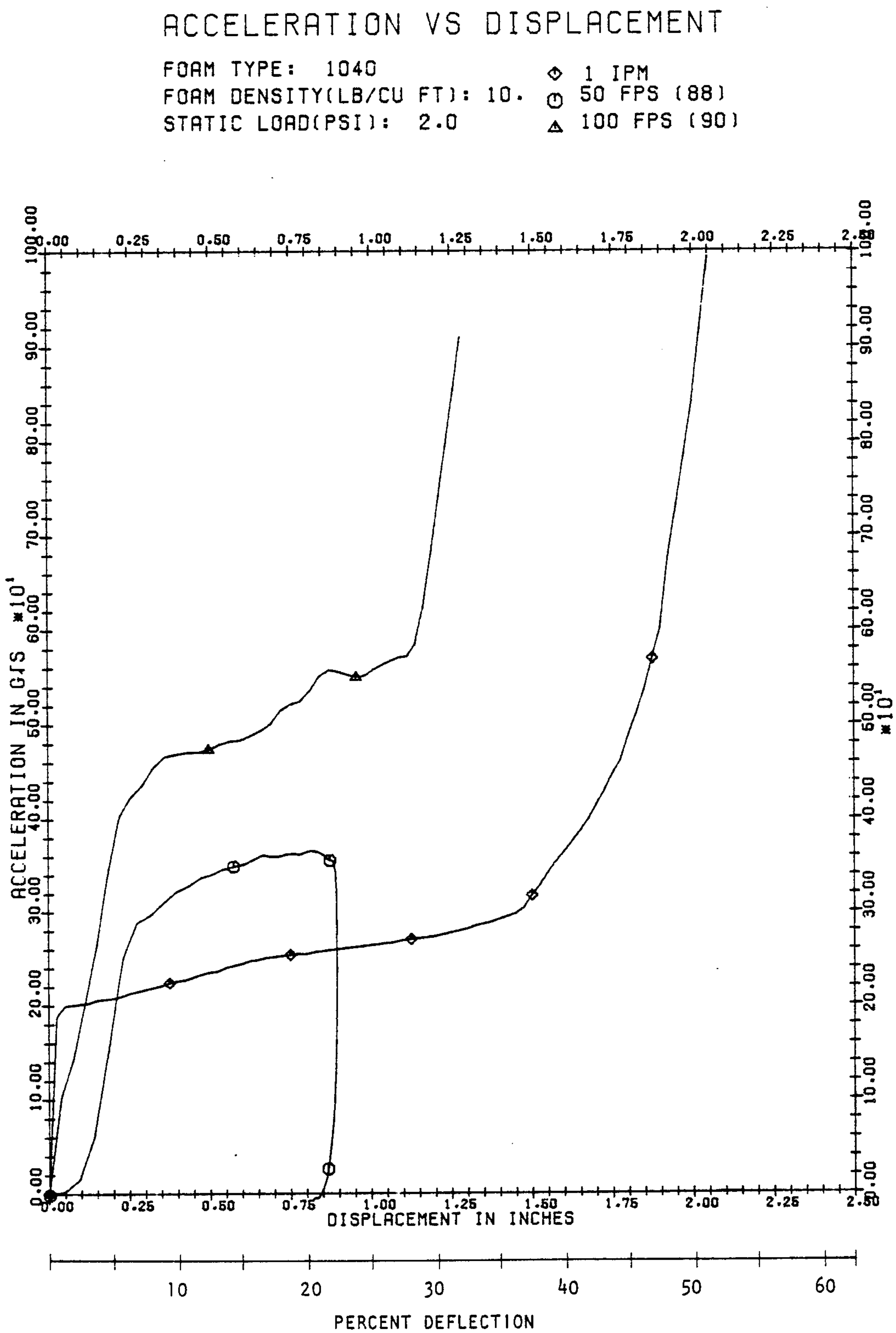

Figure B-9. CPR 1040, 10 LB/FT^3, 2.0 PSI

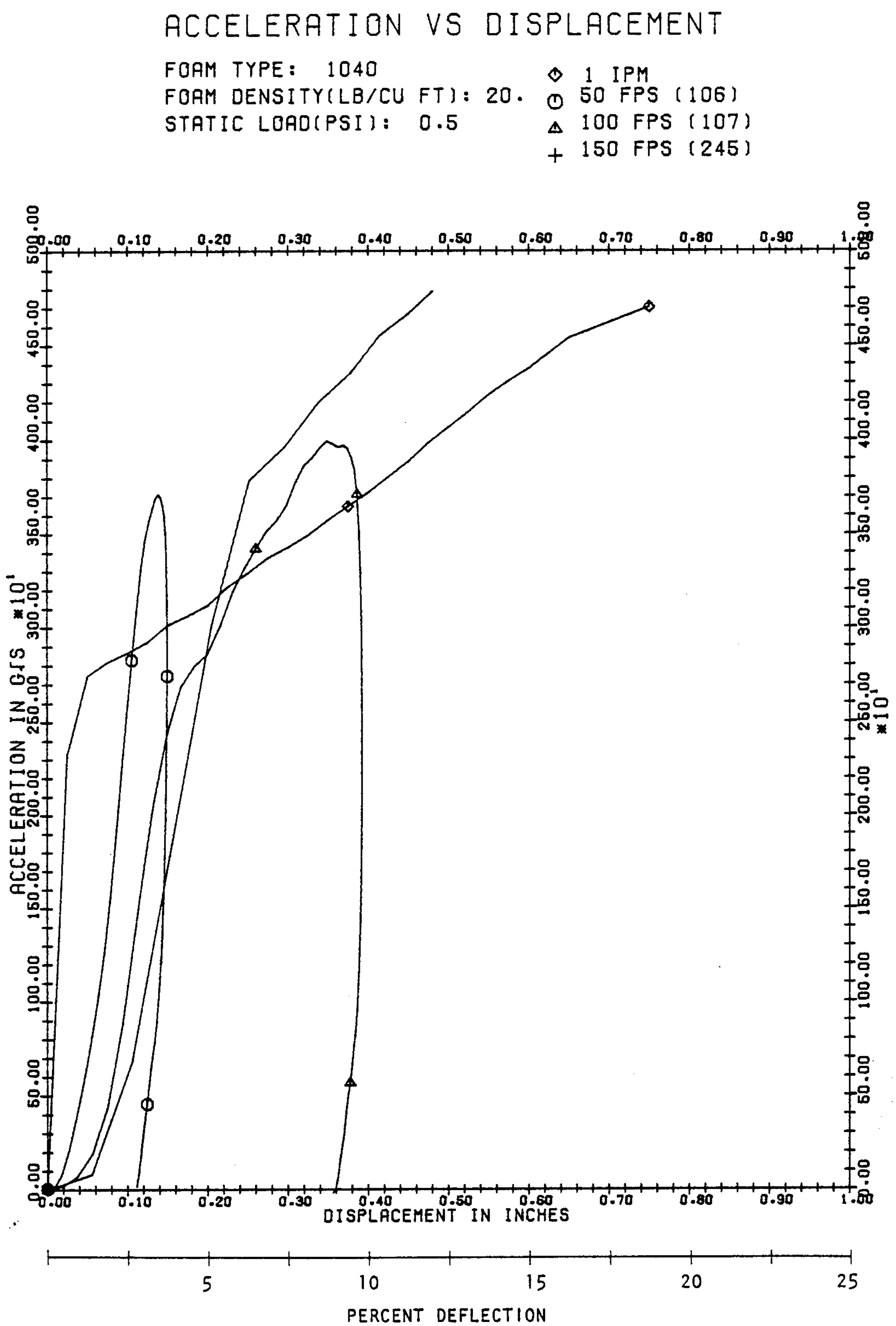

Figure B-10. CPR 1040, 20 LB/FT^3, 0.5 PSI

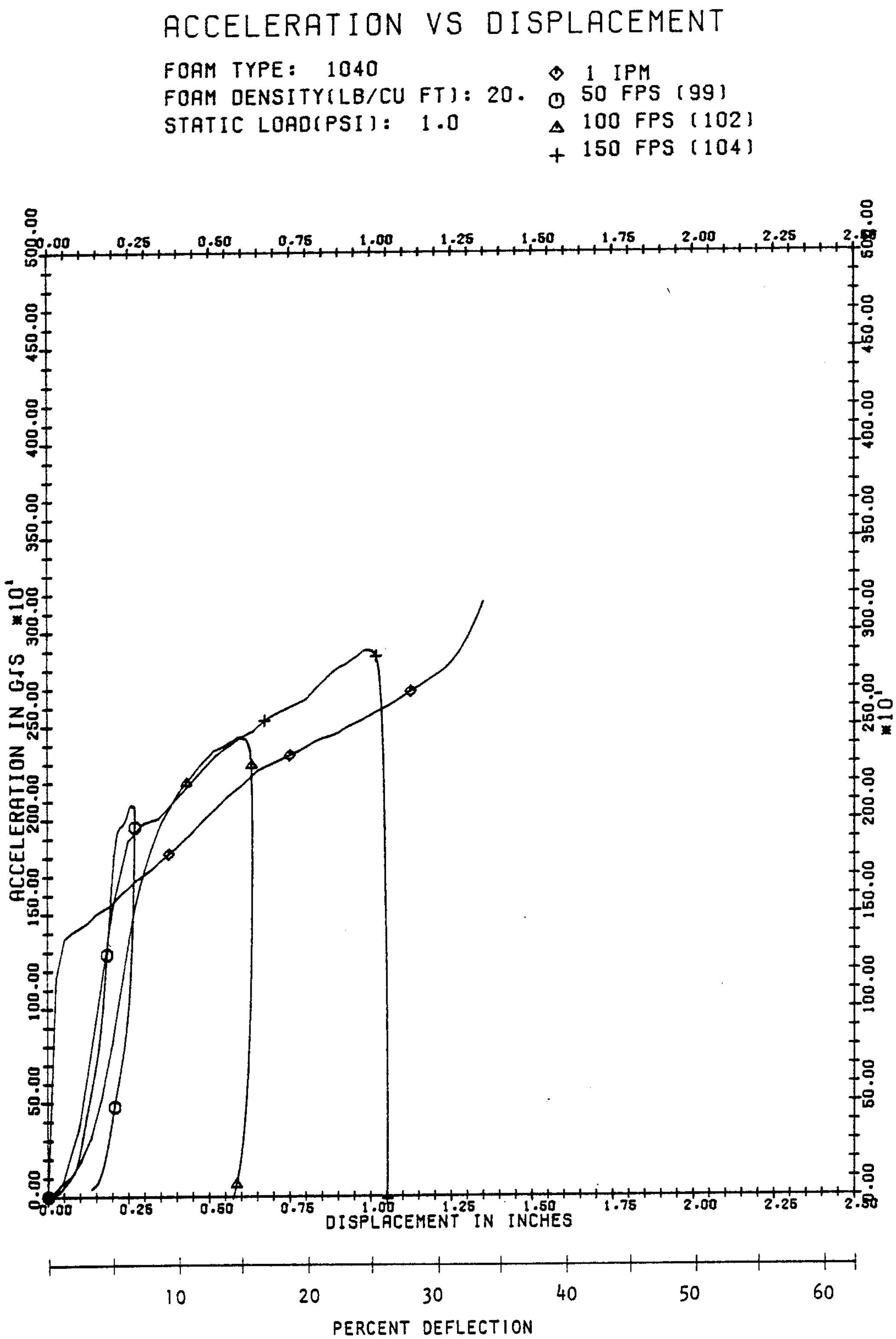

Figure B-11. CPR 1040, 20 LB/FT^3, 1.0 PSI

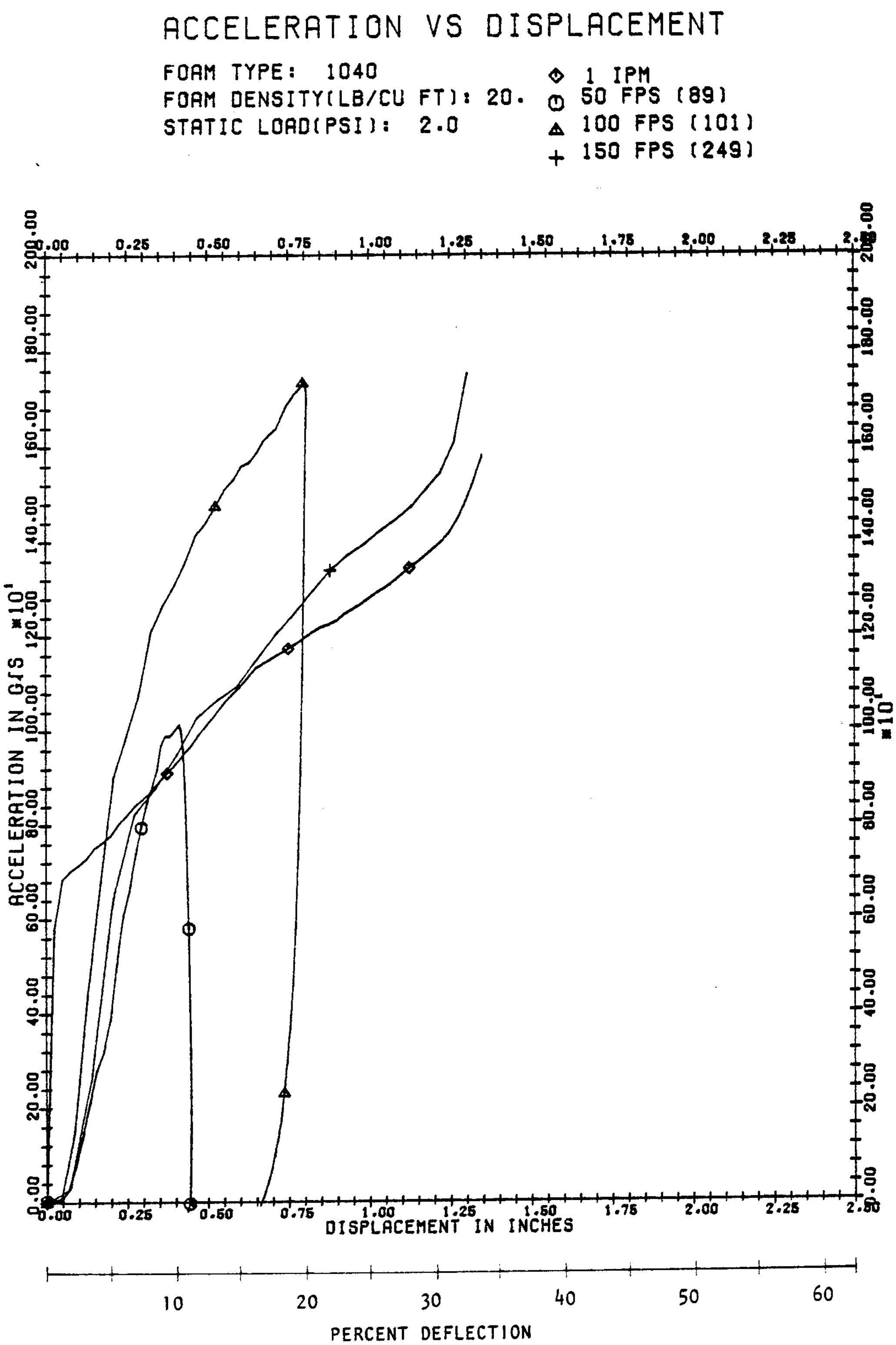

Figure B-12. CPR 1040, 20 LB/FT^3, 2.0 PSI

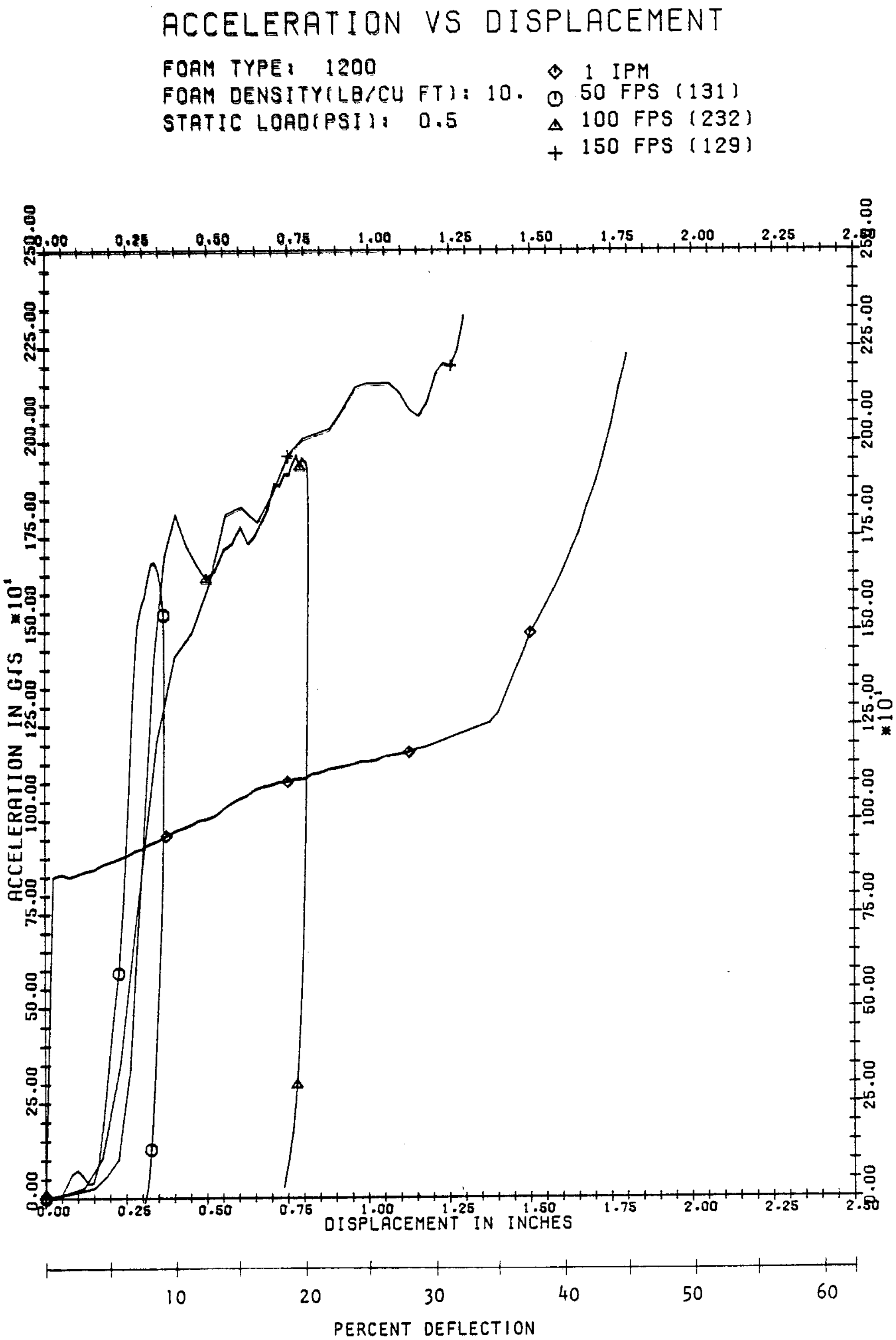

Figure B-13. BC 1200, 10 LB/FT^3, 0.5 PSI

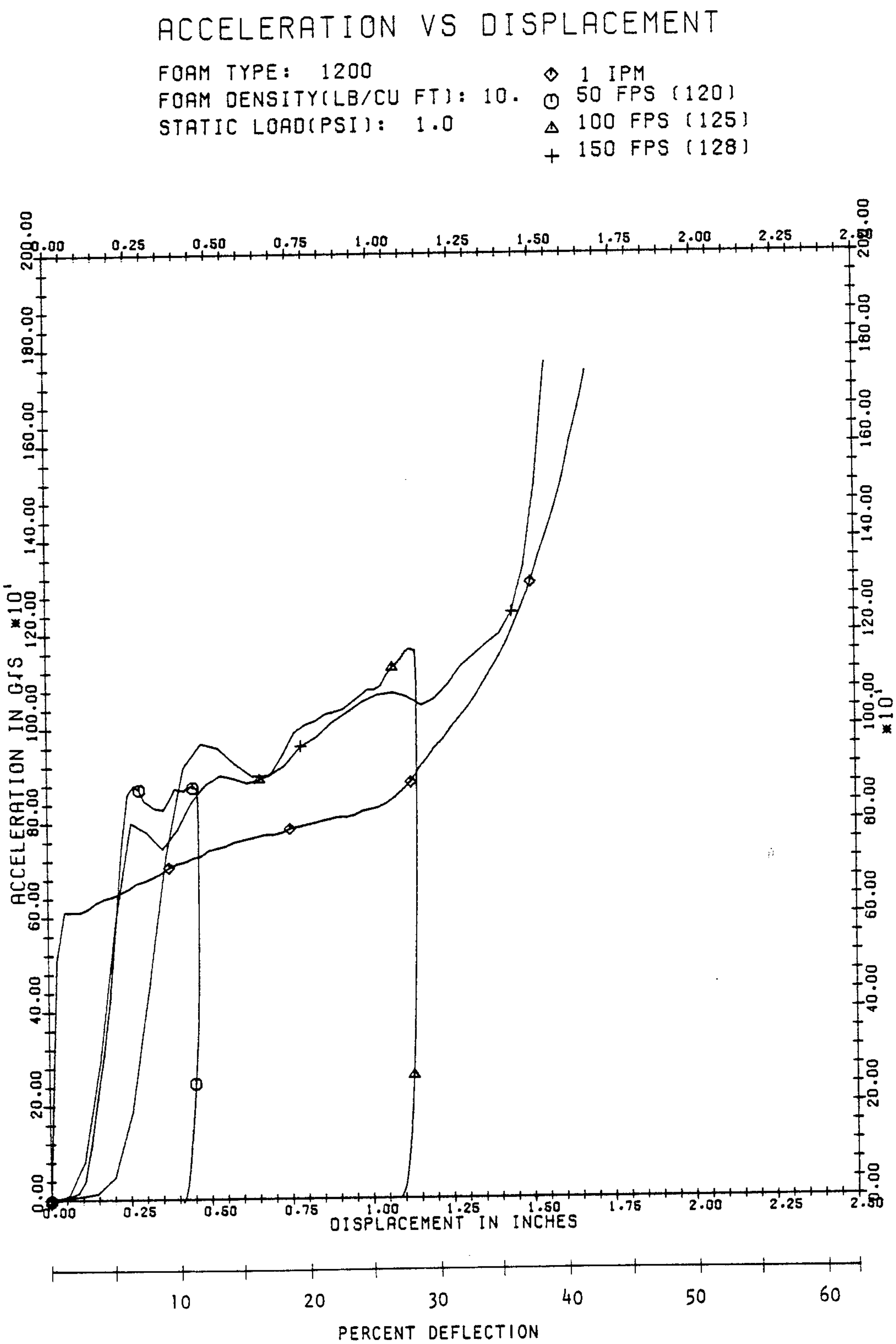

Figure B-14. BC 1200, 10 LB/FT^3, 1.0 PSI

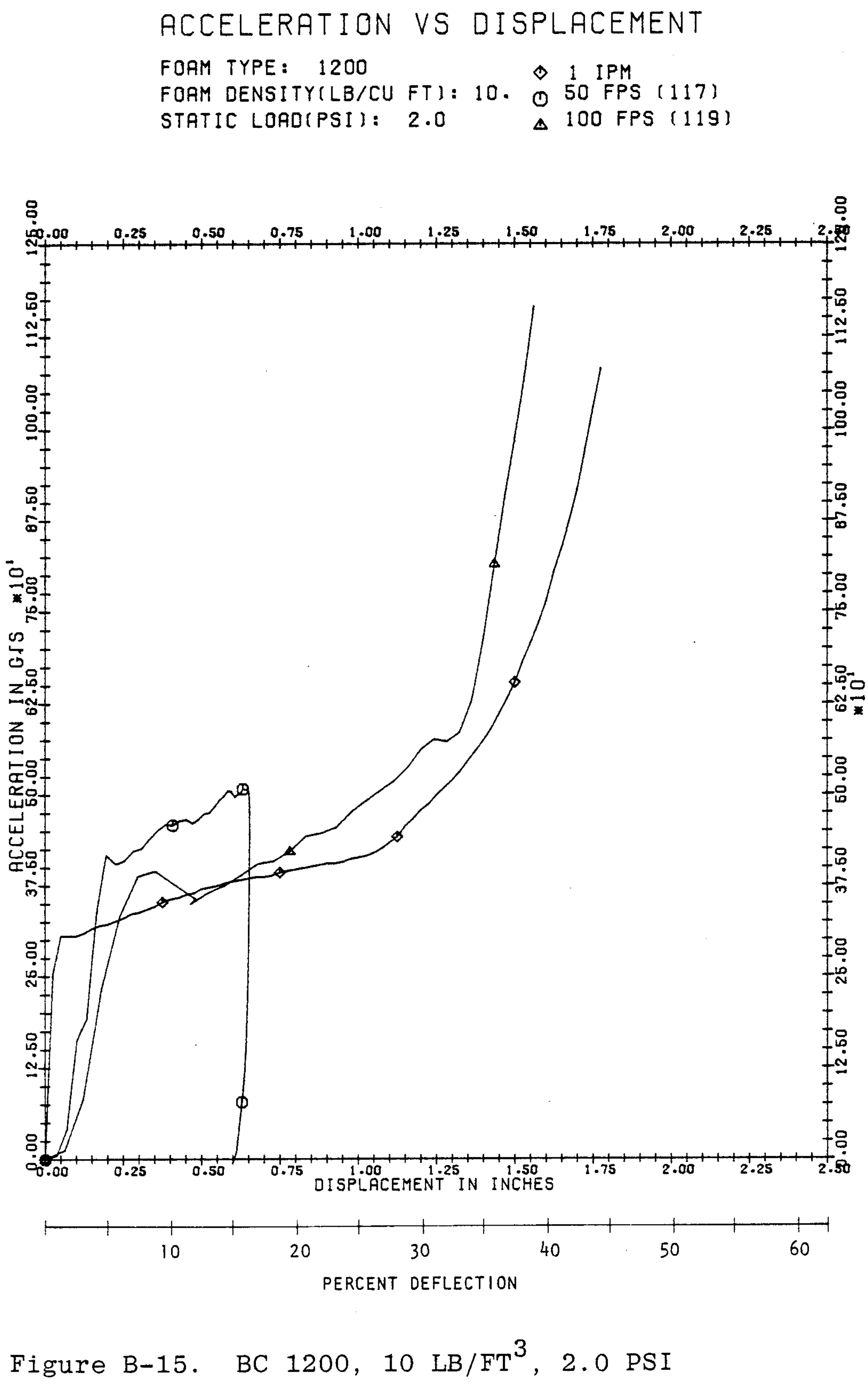

Figure B-15. BC 1200, 10 LB/FT^3, 2.0 PSI

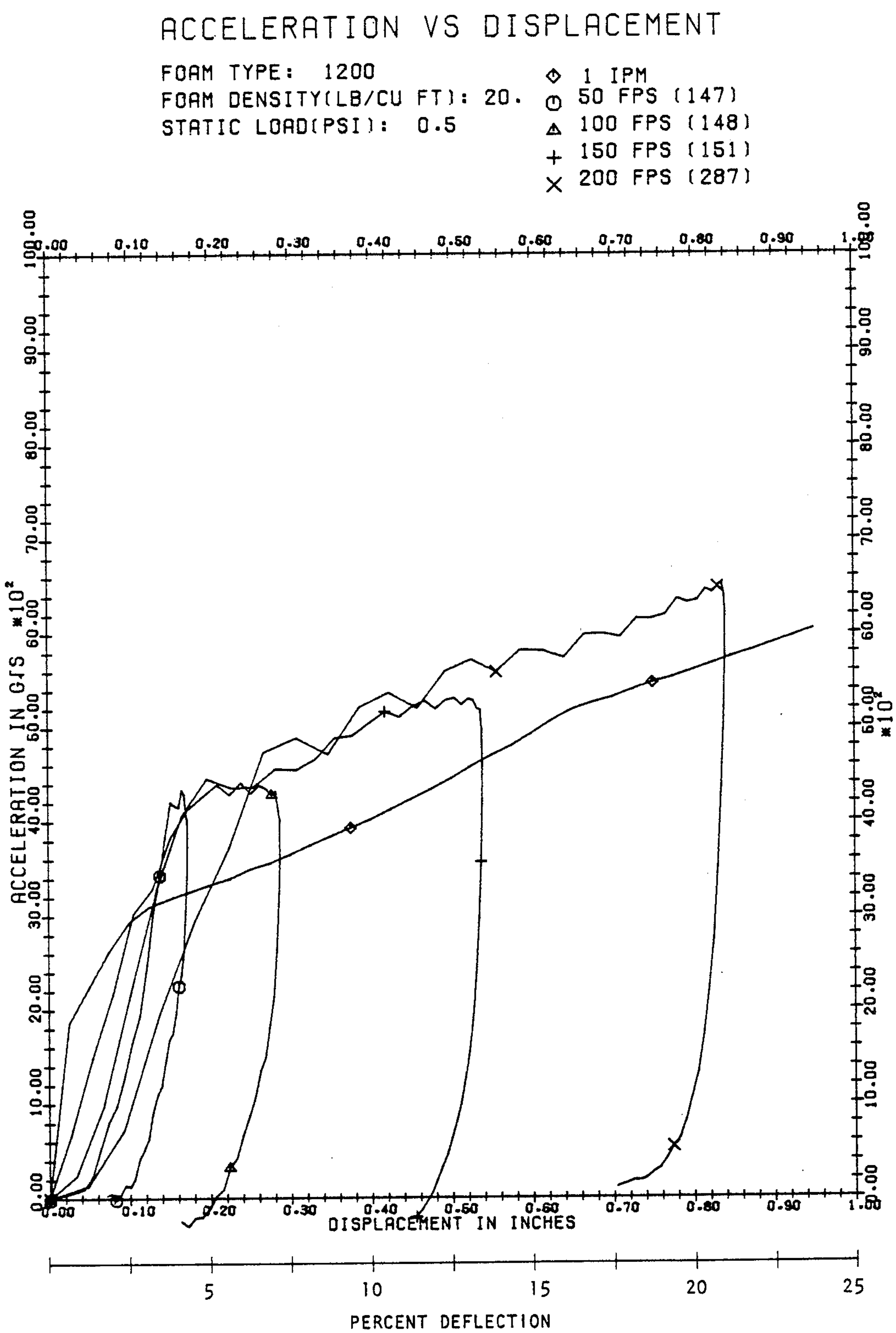

Figure B-16. BC 1200, 20 LB/FT^3, 0.5 PSI

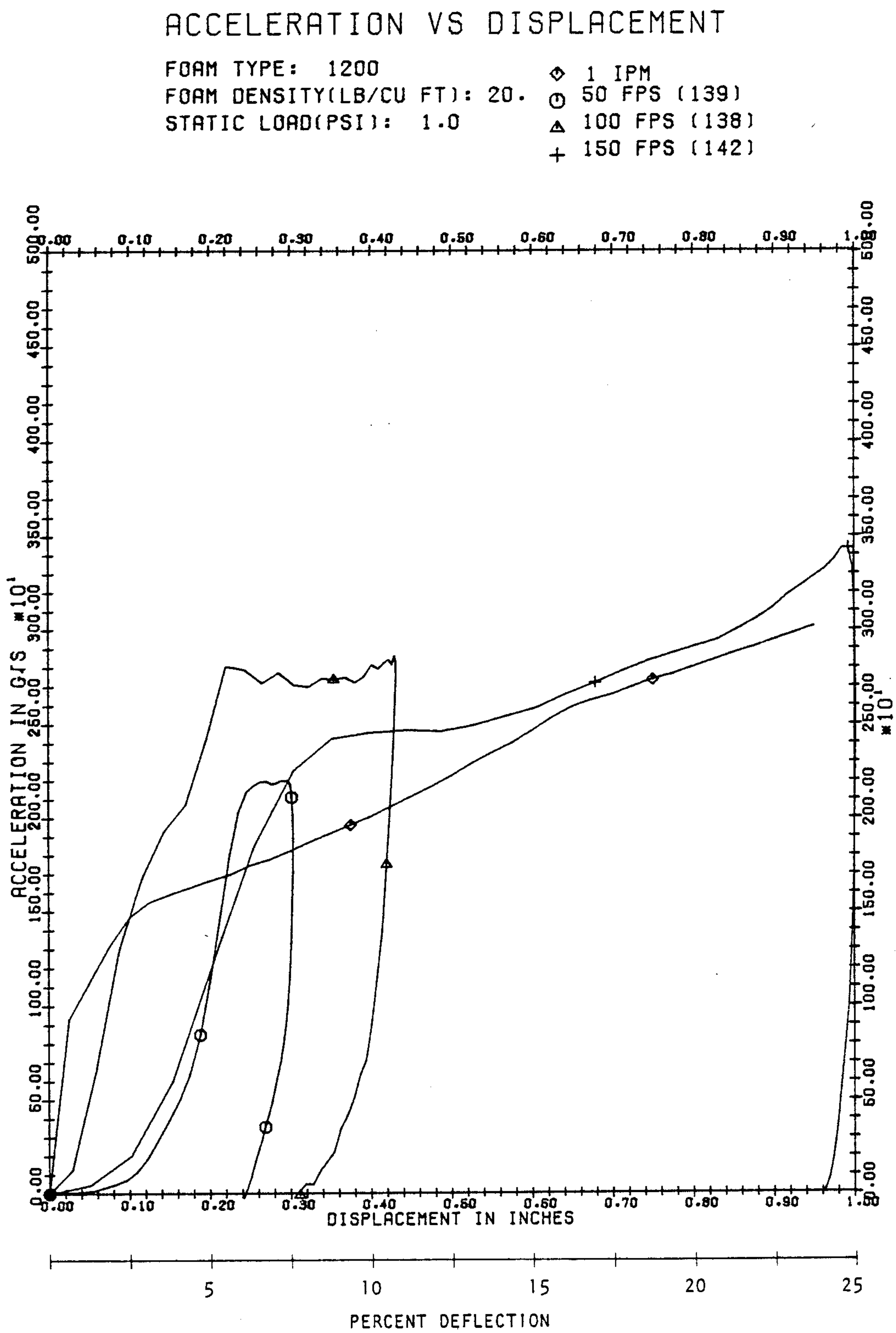

Figure B-17. BC 1200, 20 LB/FT^3, 1.0 PSI

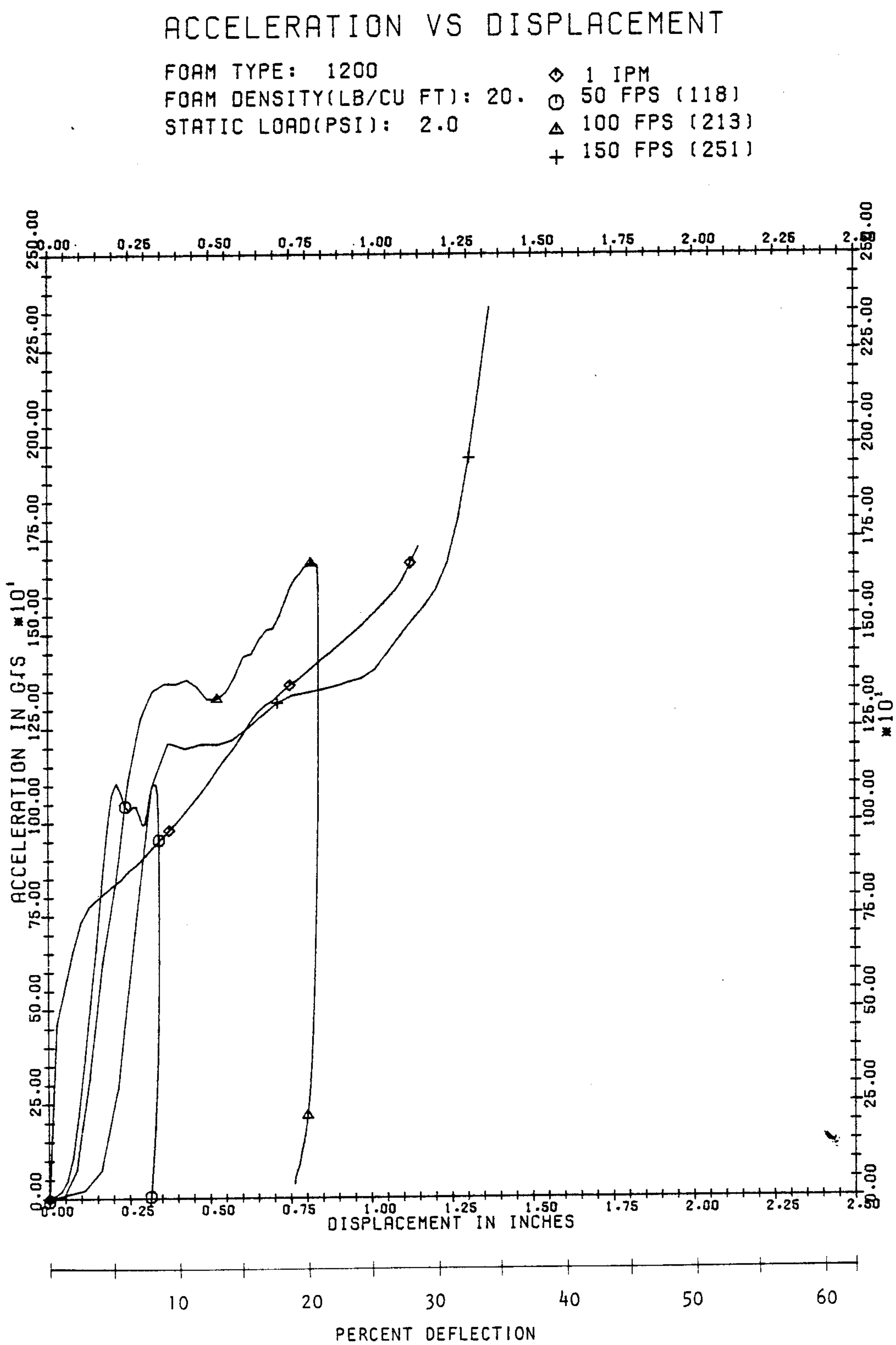

Figure B-18. BC 1200, 20 LB/FT^3, 2.0 PSI

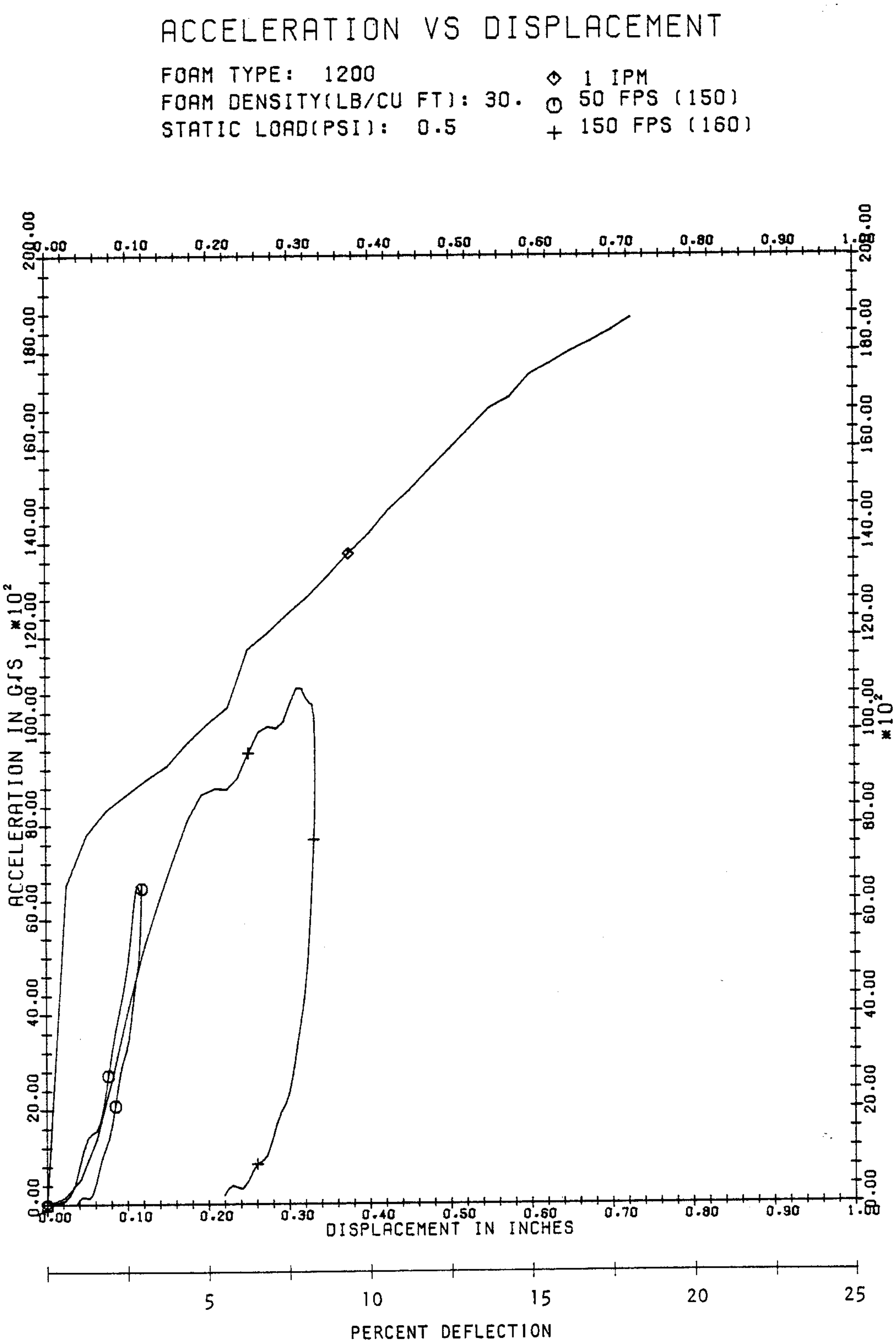

Figure B-19. BC 1200, 30 LB/FT^3, 0.5 PSI

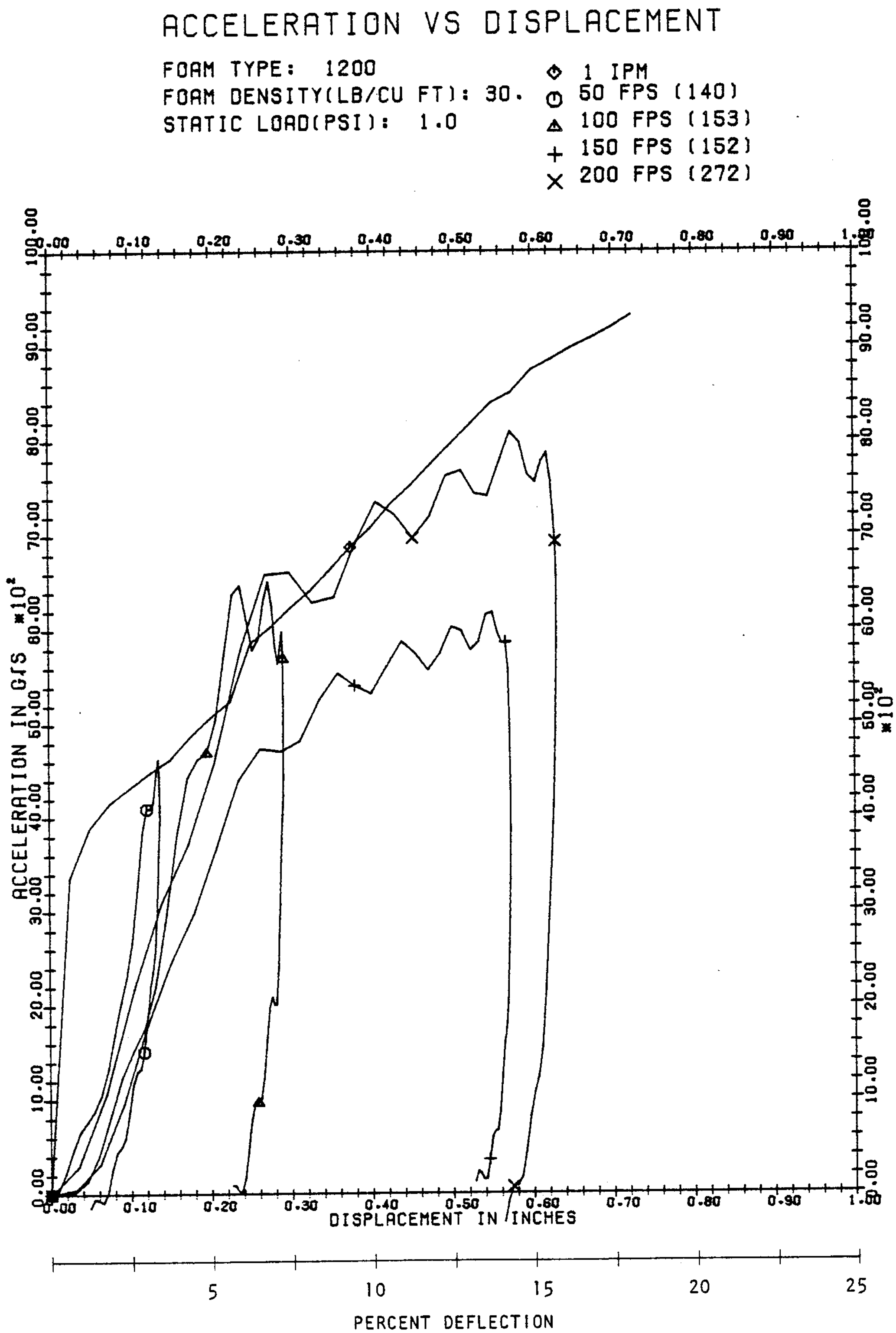

Figure B-20. BC 1200, 30 LB/FT^3, 1.0 PSI

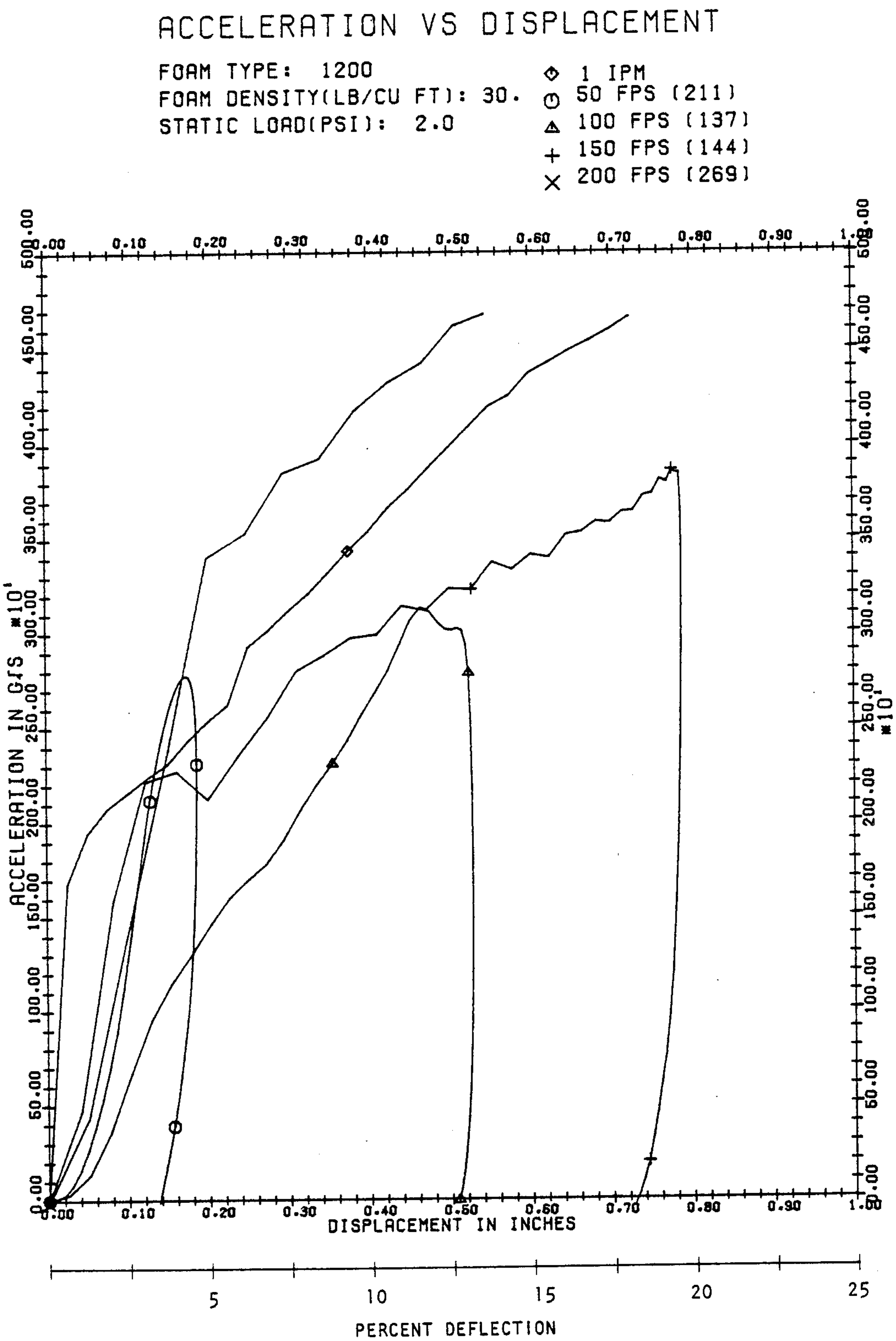

Figure B-21. BC 1200, 30 LB/FT^3, 2.0 PSI

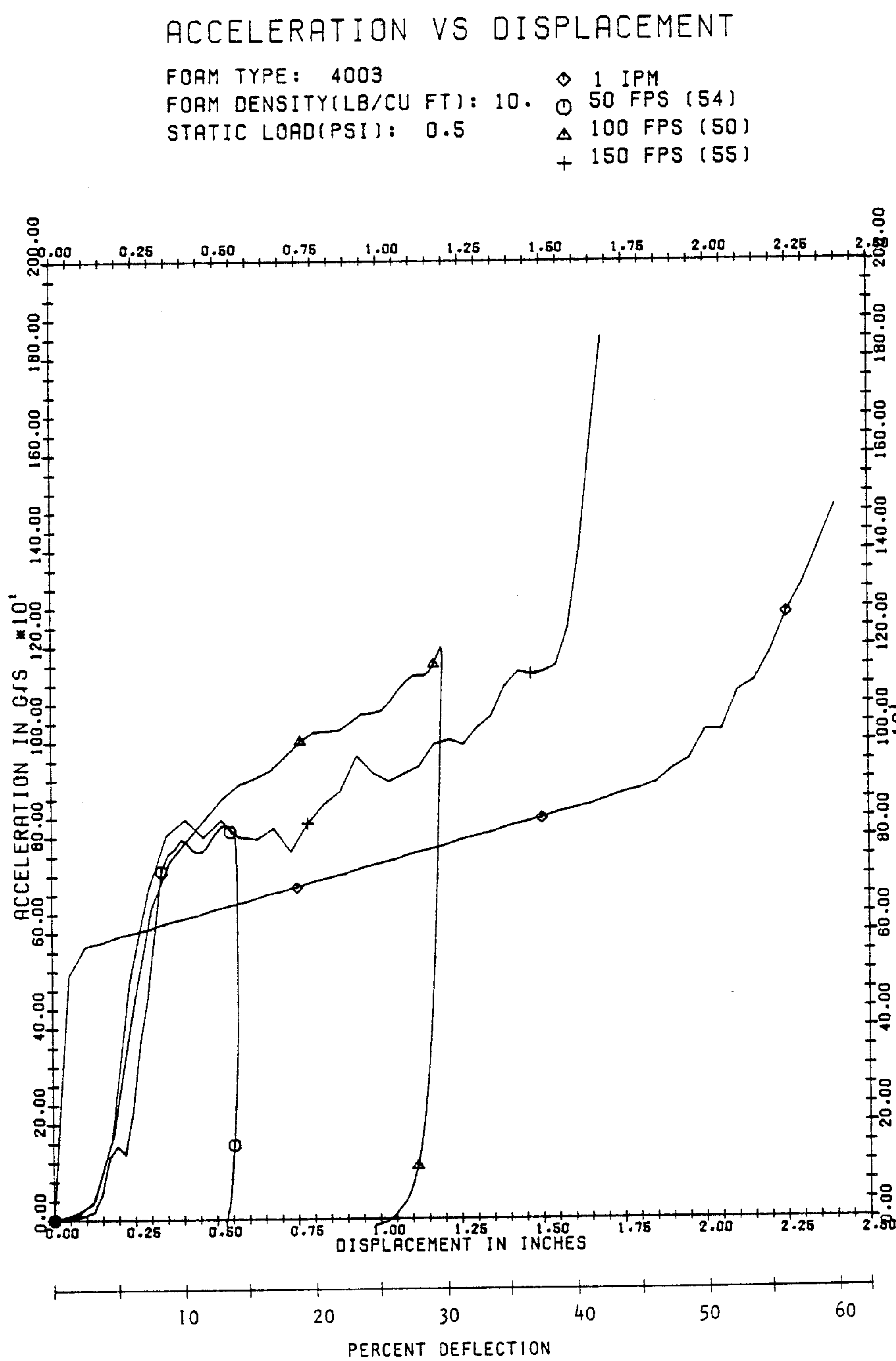

Figure B-22. BX 4003, 10 LB/FT^3, 0.5 PSI

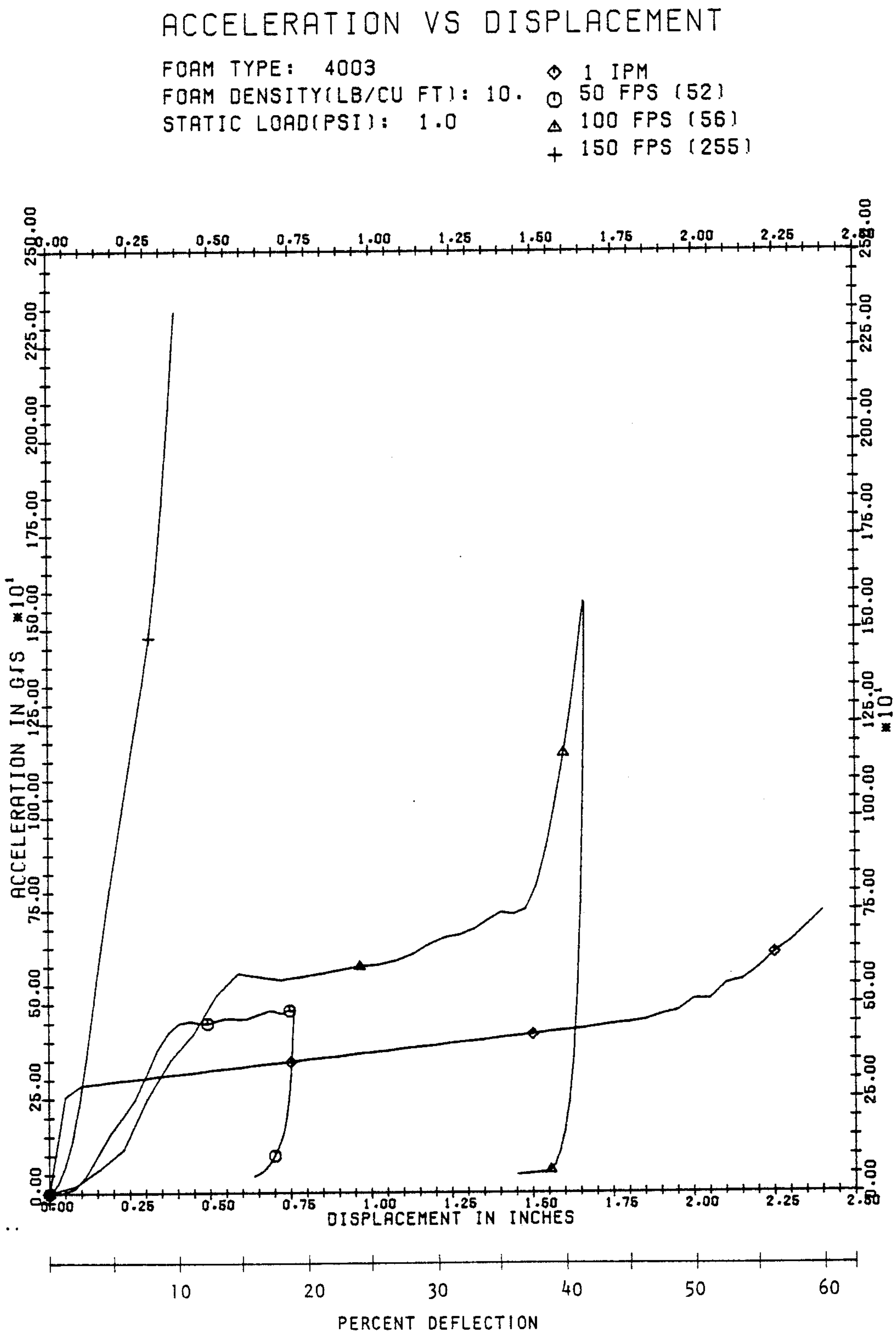

Figure B-23. BX 4003, 10 LB/FT^3, 1.0 PSI

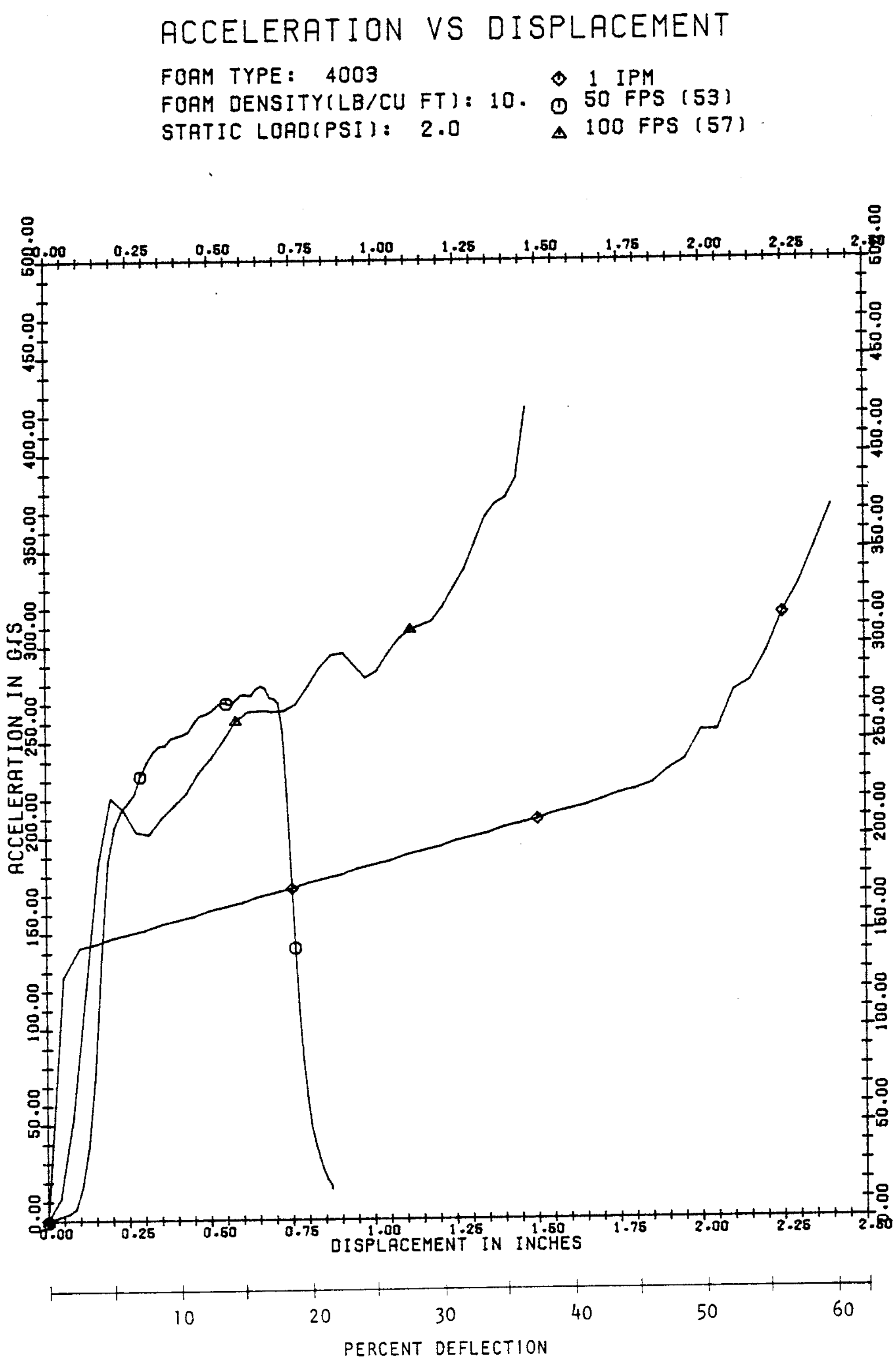

Figure B-24. BX 4003, 10 LB/FT^3, 2.0 PSI

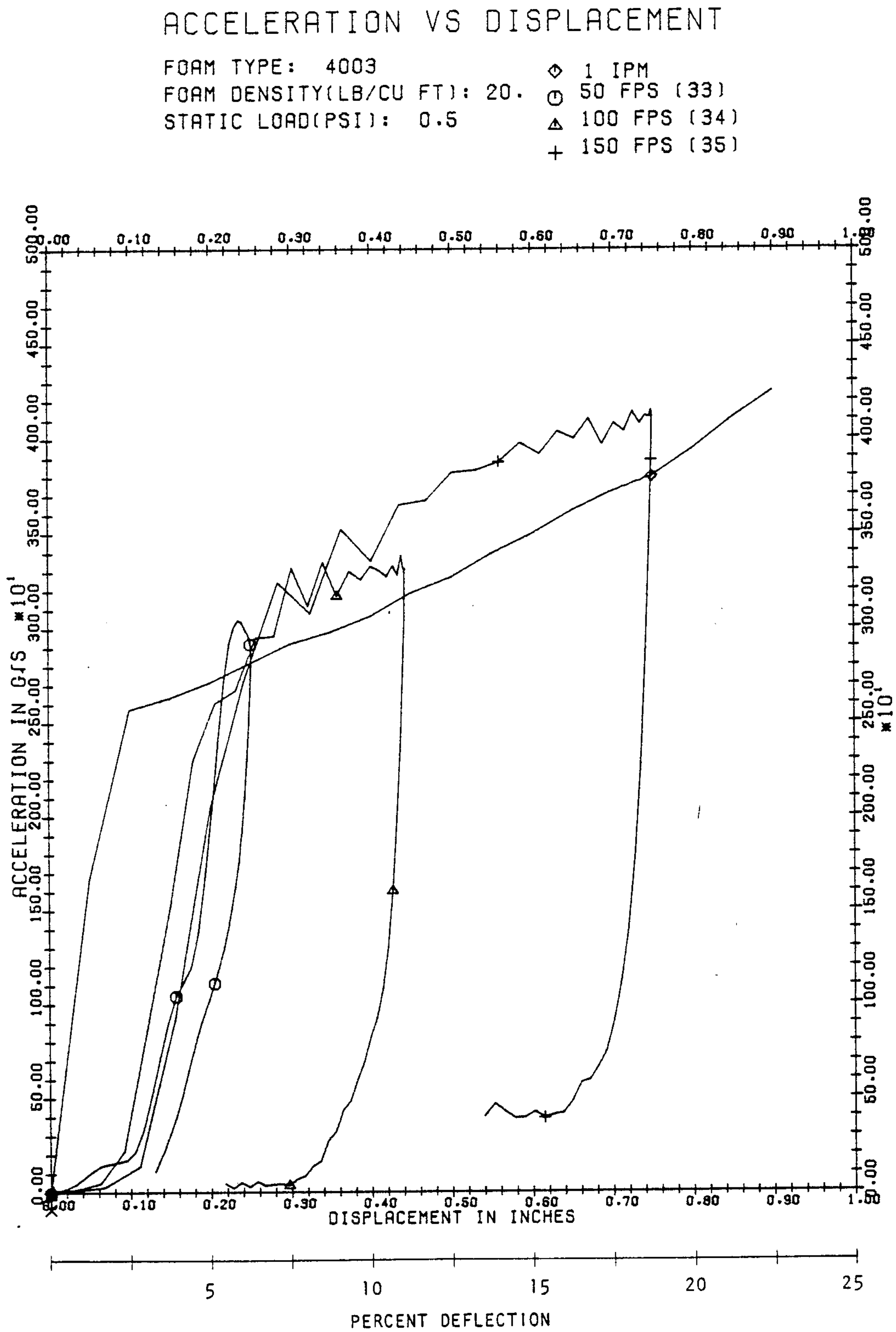

Figure B-25. BX 4003, 20 LB/FT^3, 0.5 PSI

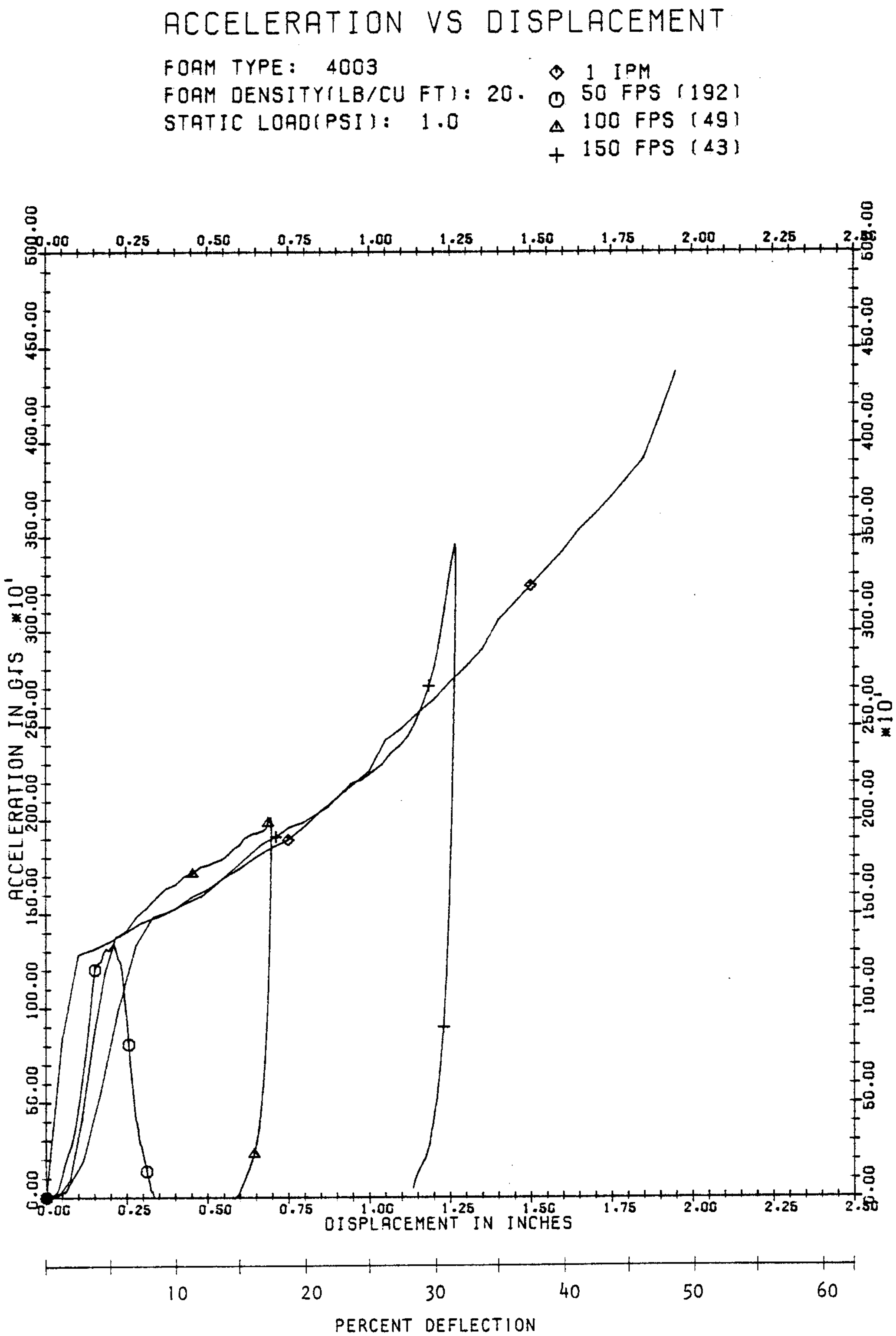

Figure B-26. BX 4003, 20 LB/FT^3, 1.0 PSI

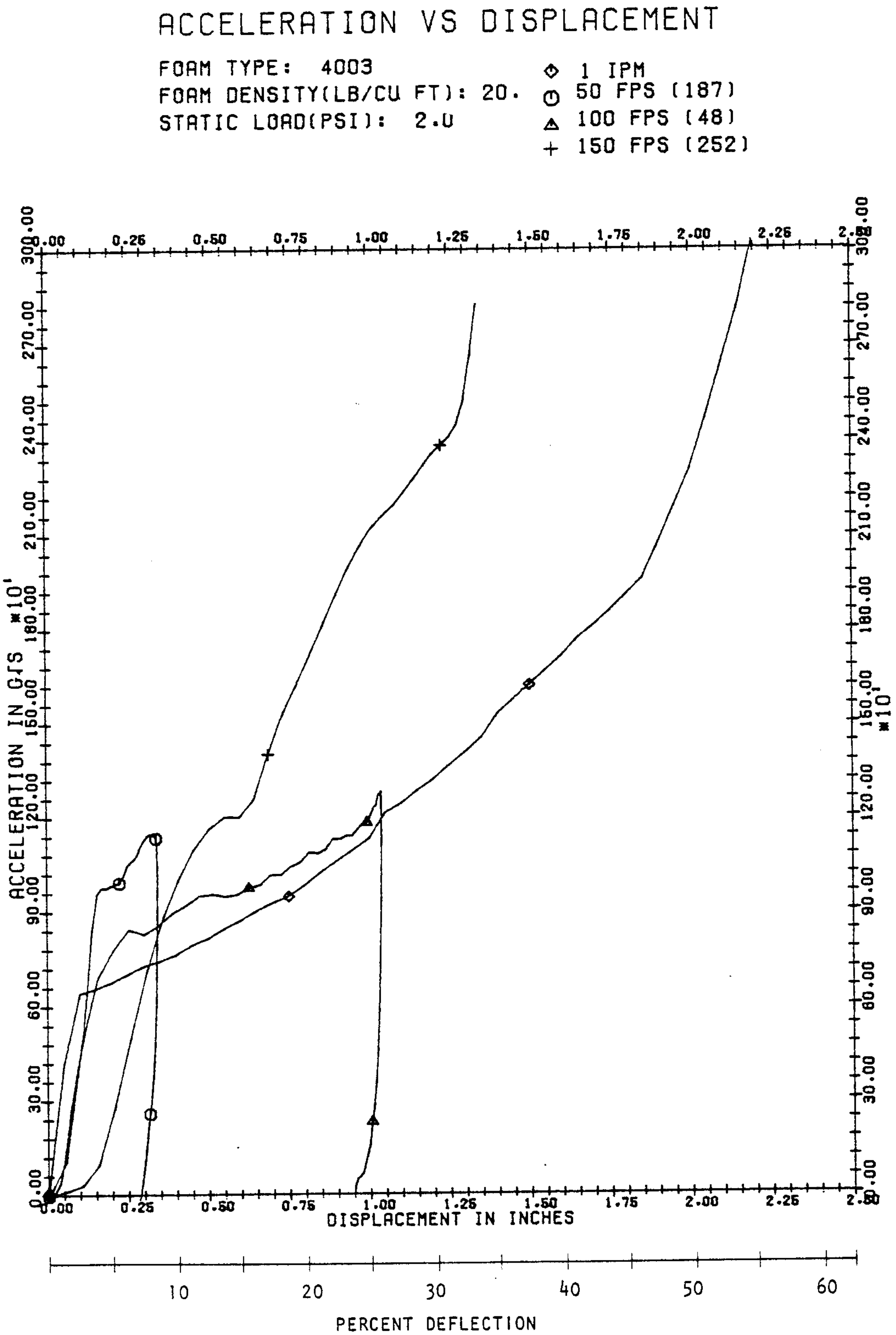

Figure B-27. BX 4003, 20 LB/FT^3, 2.0 PSI

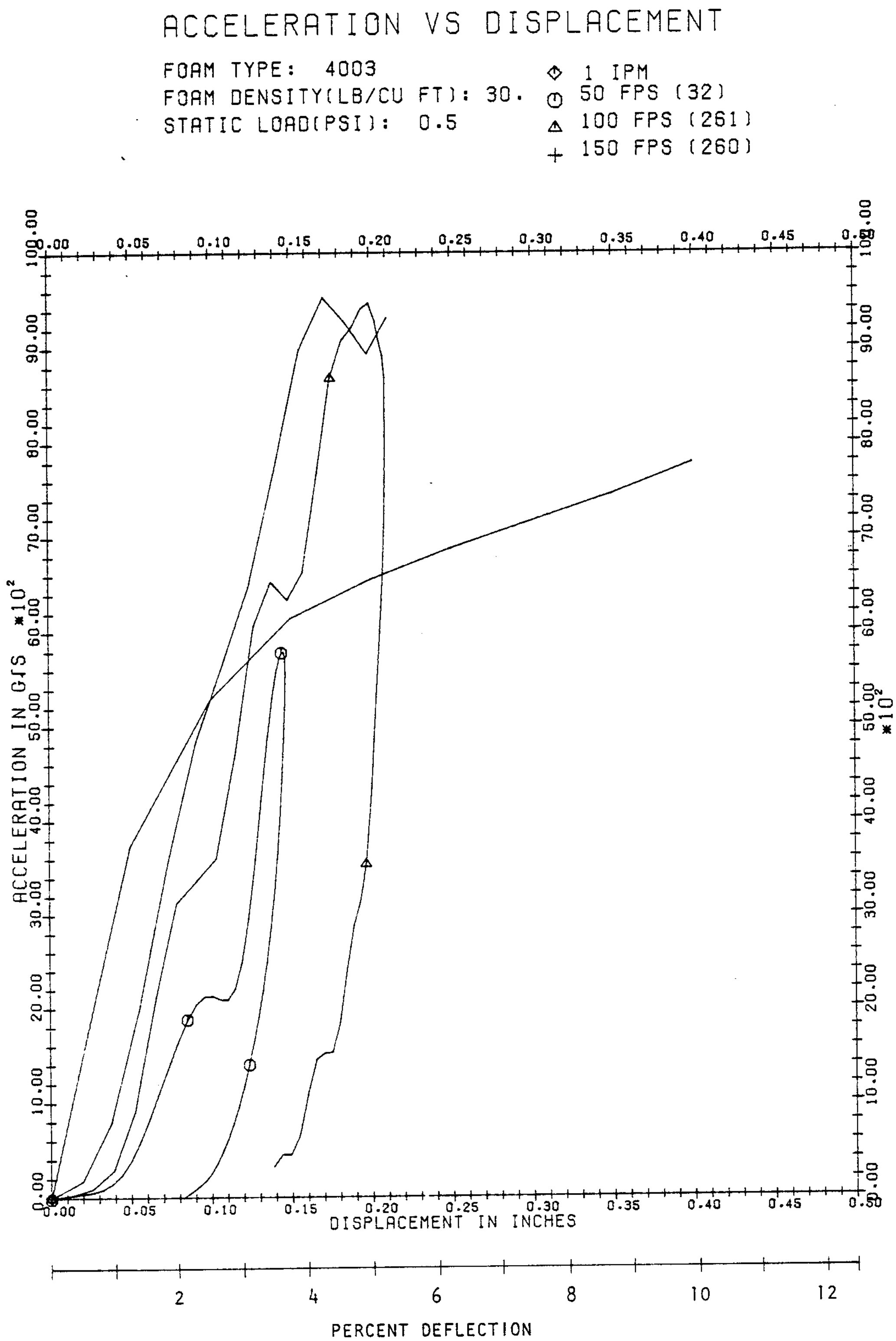

Figure B-28. BX 4003, 30 LB/FT^3, 0.5 PSI

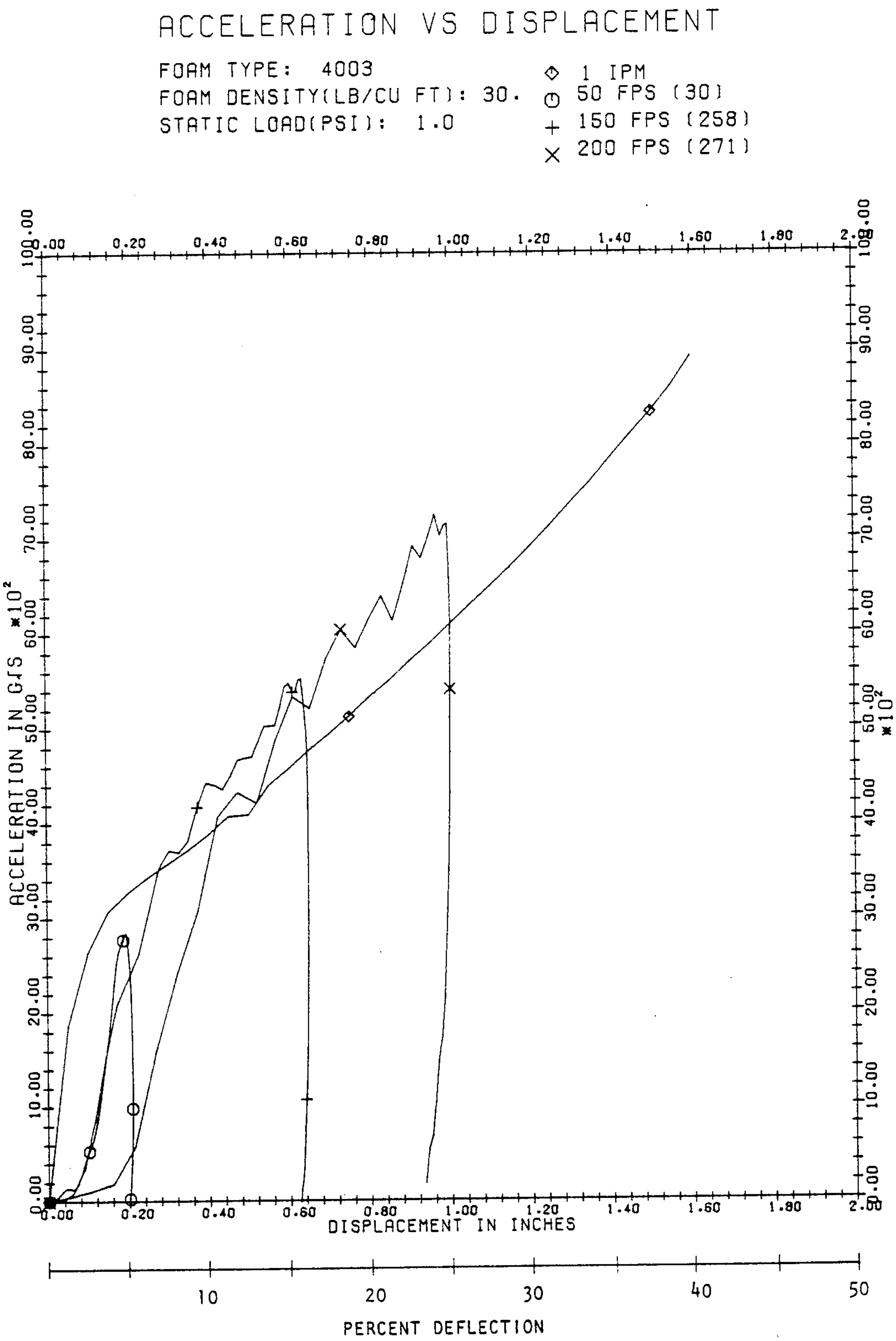

Figure B-29. BX 4003, 30 LB/FT^3, 1.0 PSI

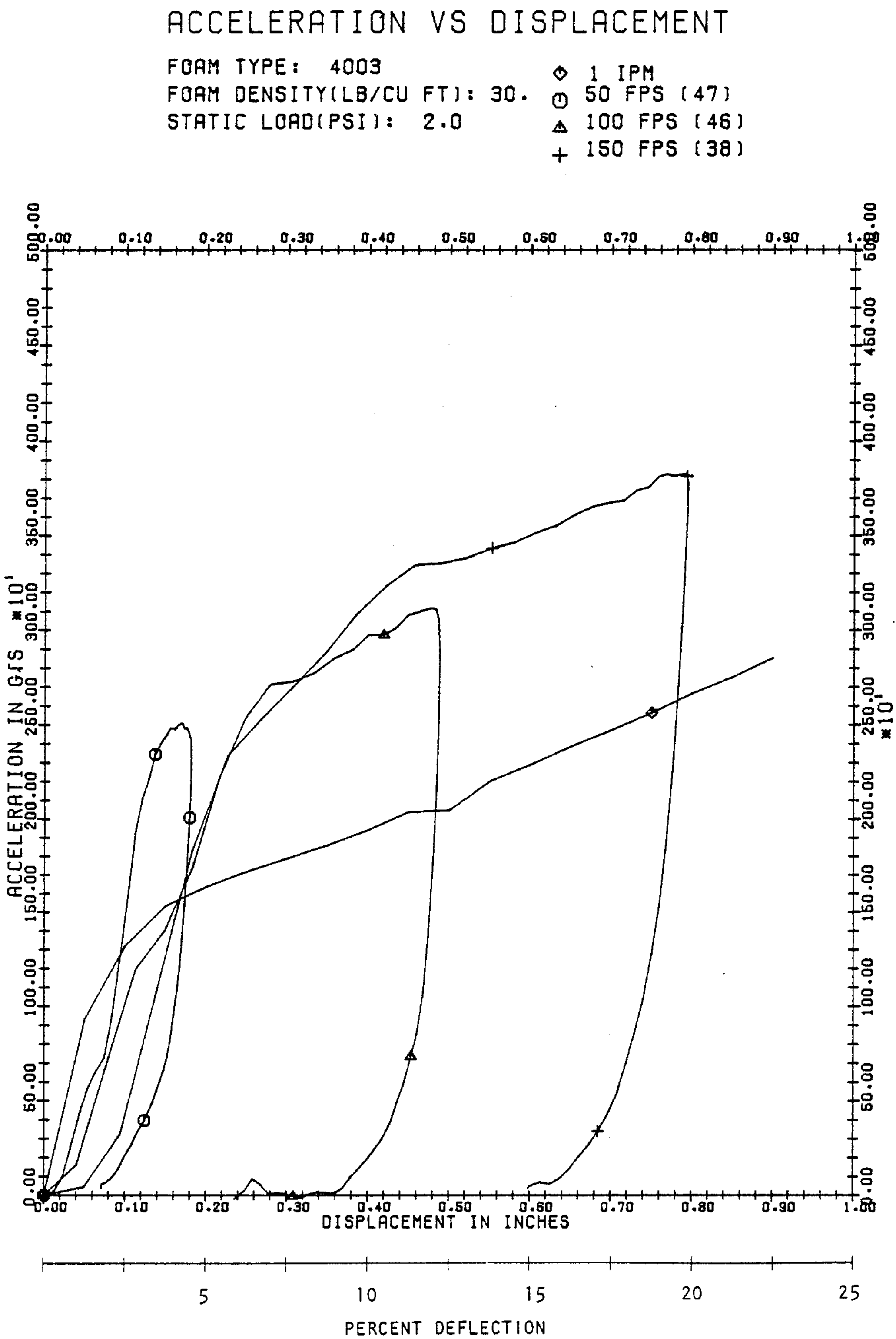

Figure B-30. BX 4003, 30 LB/FT^3, 2.0 PSI

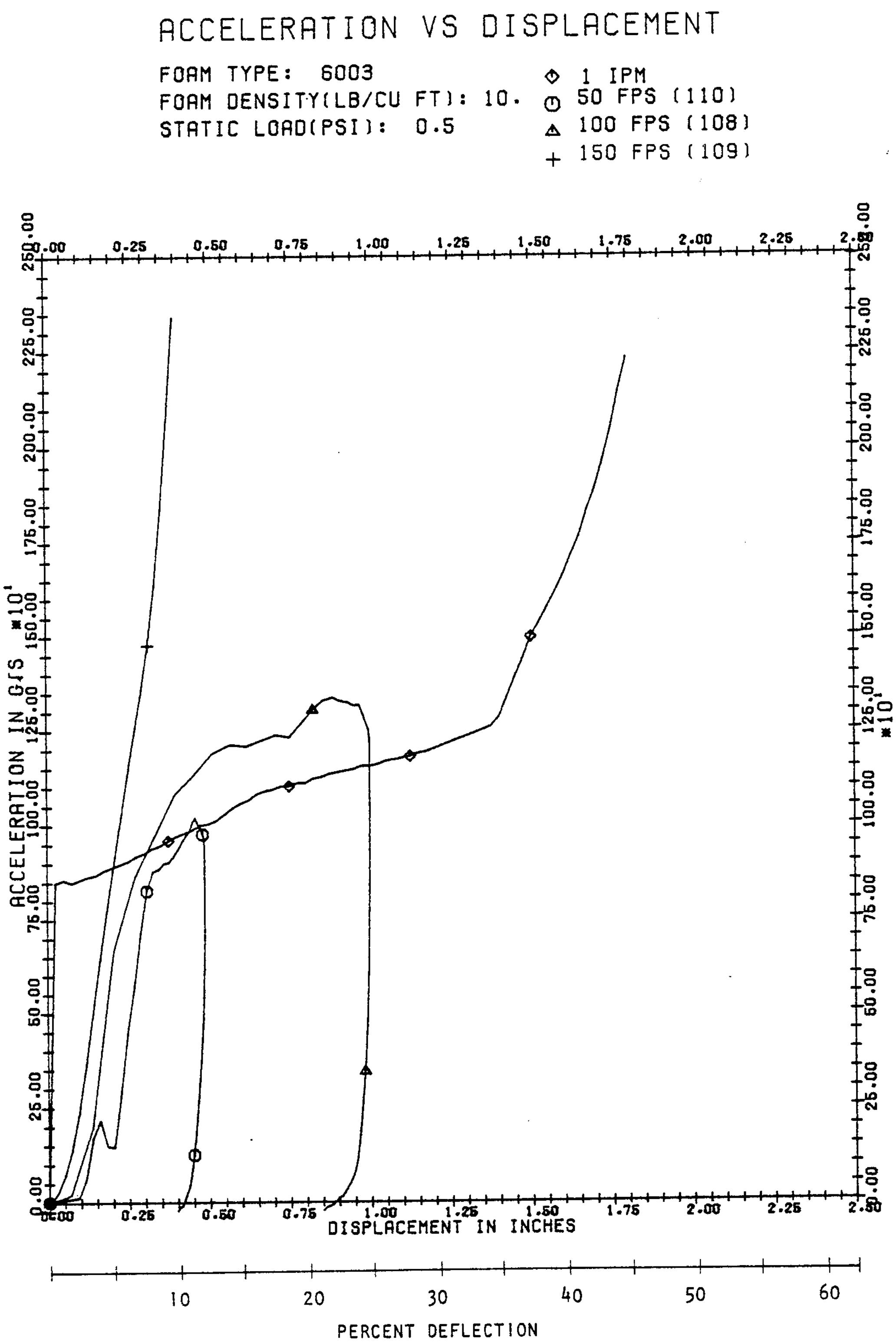

Figure B-31. BX 6003, 10 LB/FT^3, 0.5 PSI

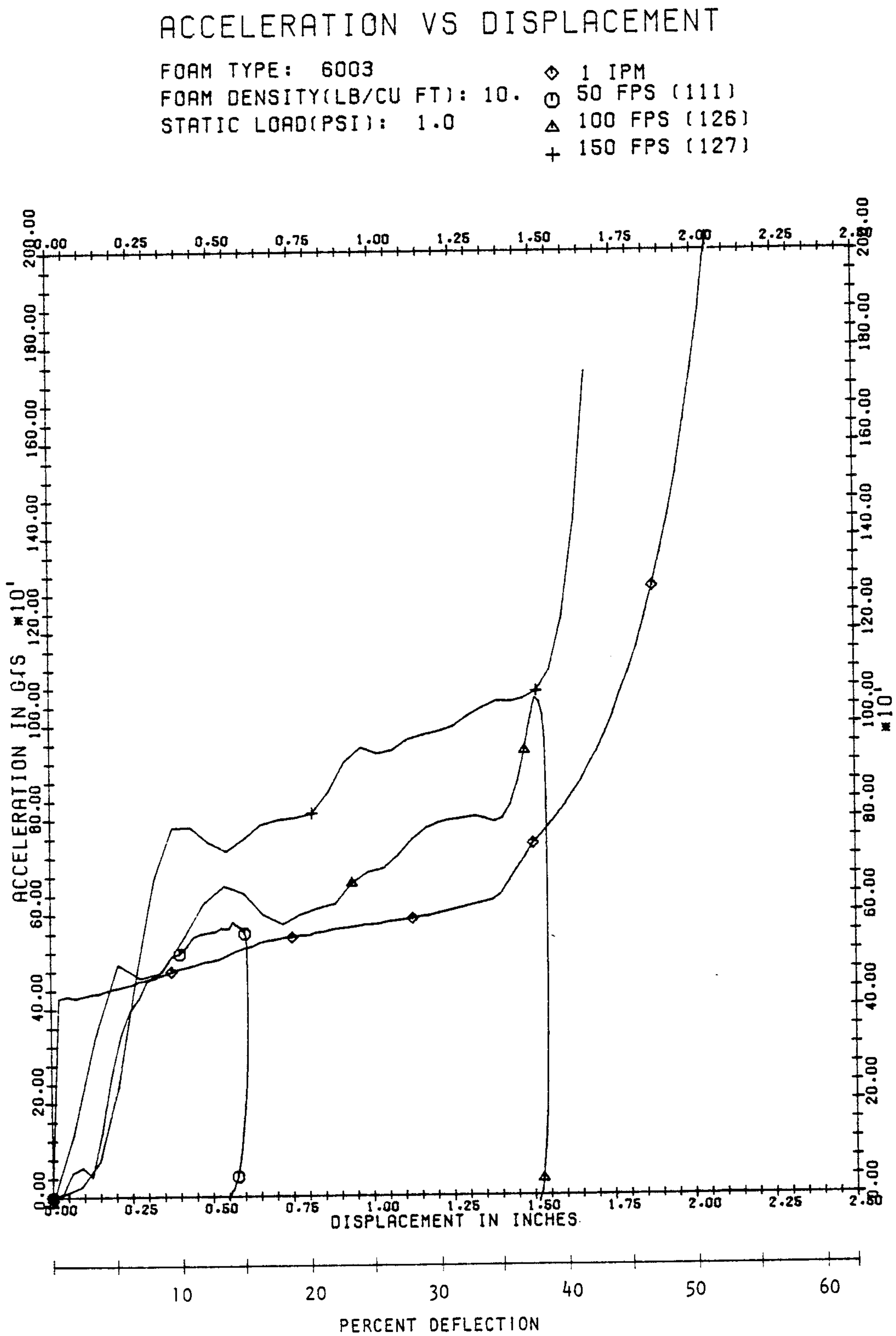

Figure B-32. BX 6003, 10 LB/FT^3, 1.0 PSI

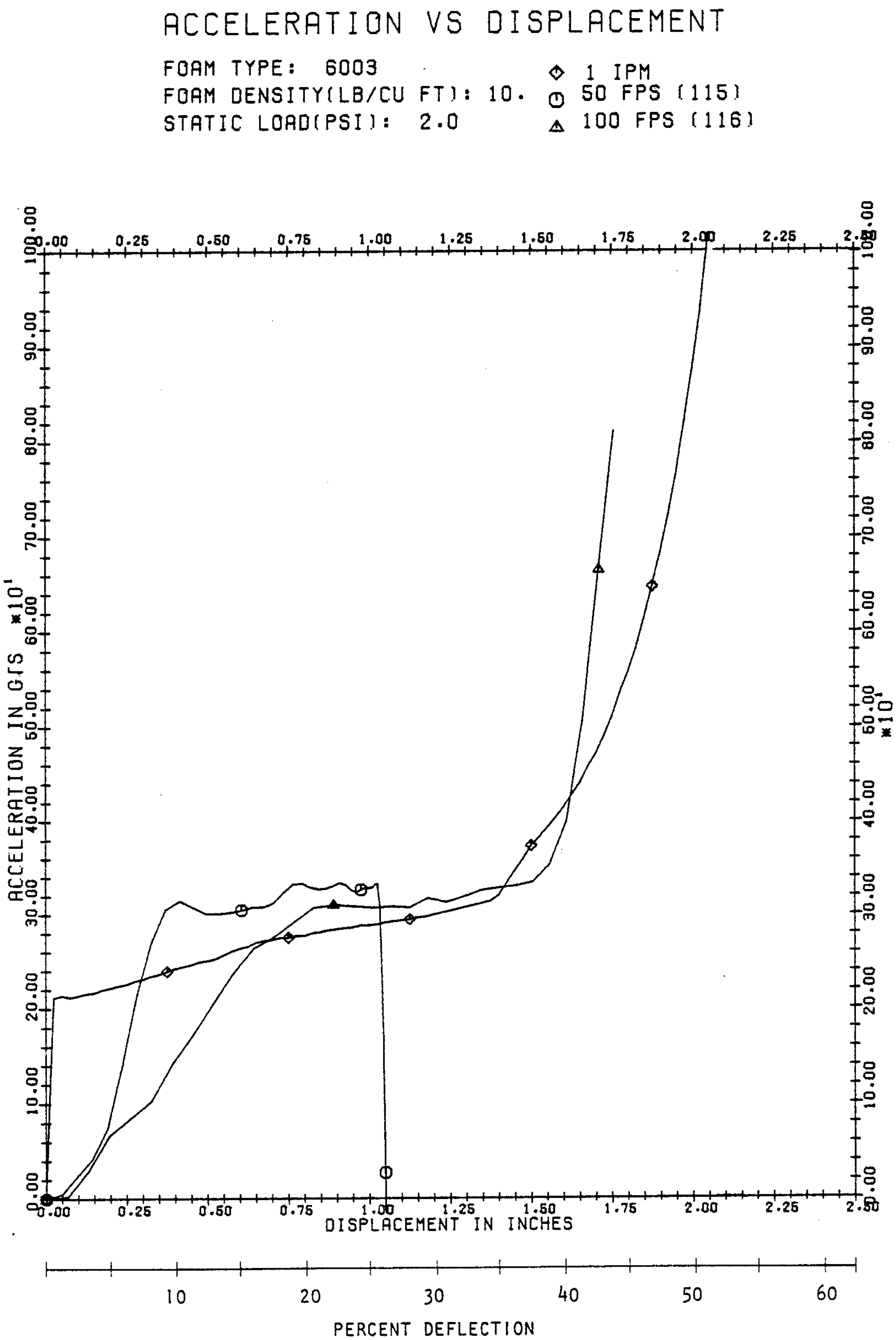

Figure B-33. BX 6003, 10 LB/FT^3, 2.0 PSI

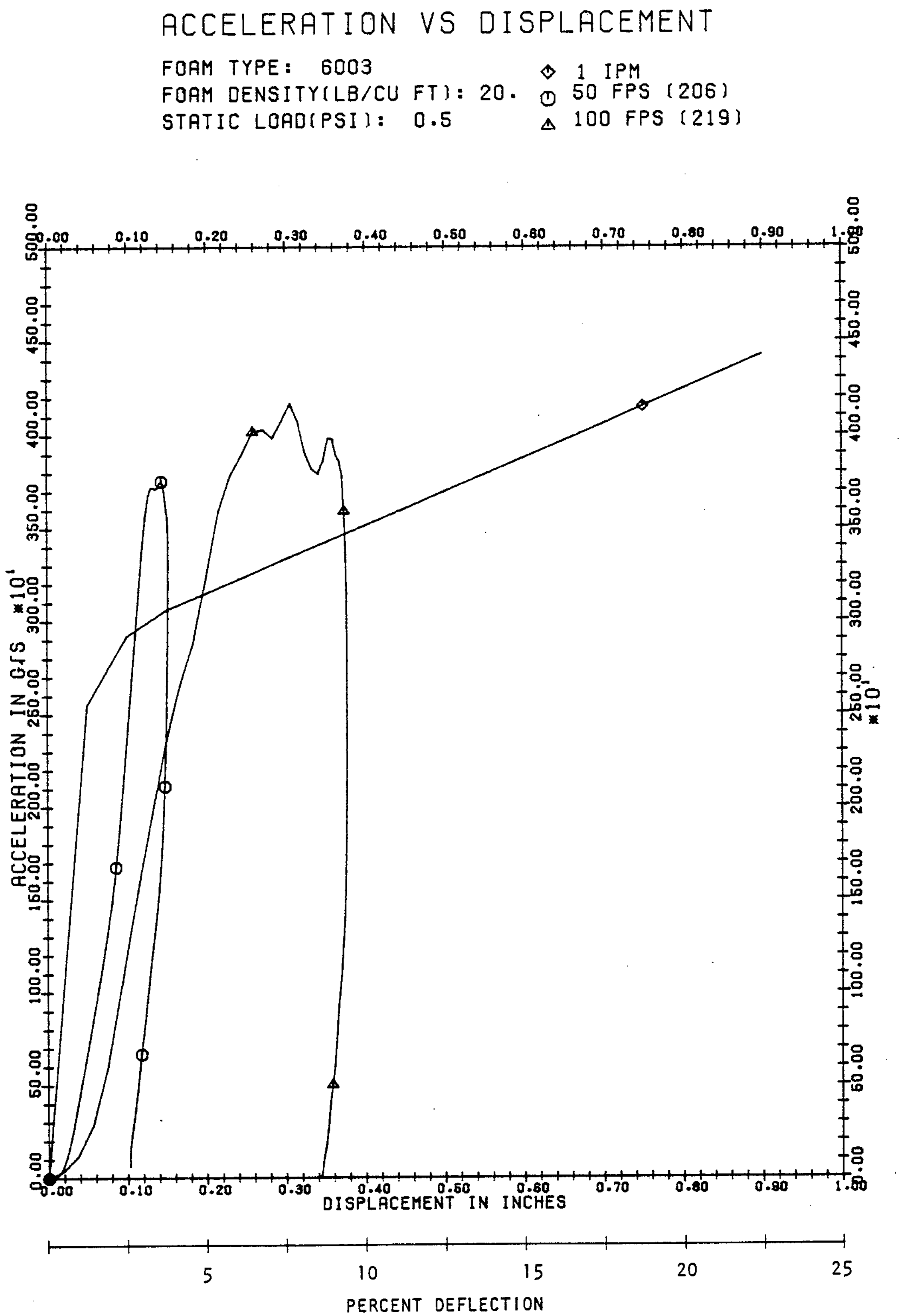

Figure B-34. BX 6003, 20 LB/FT^3, 0.5 PSI

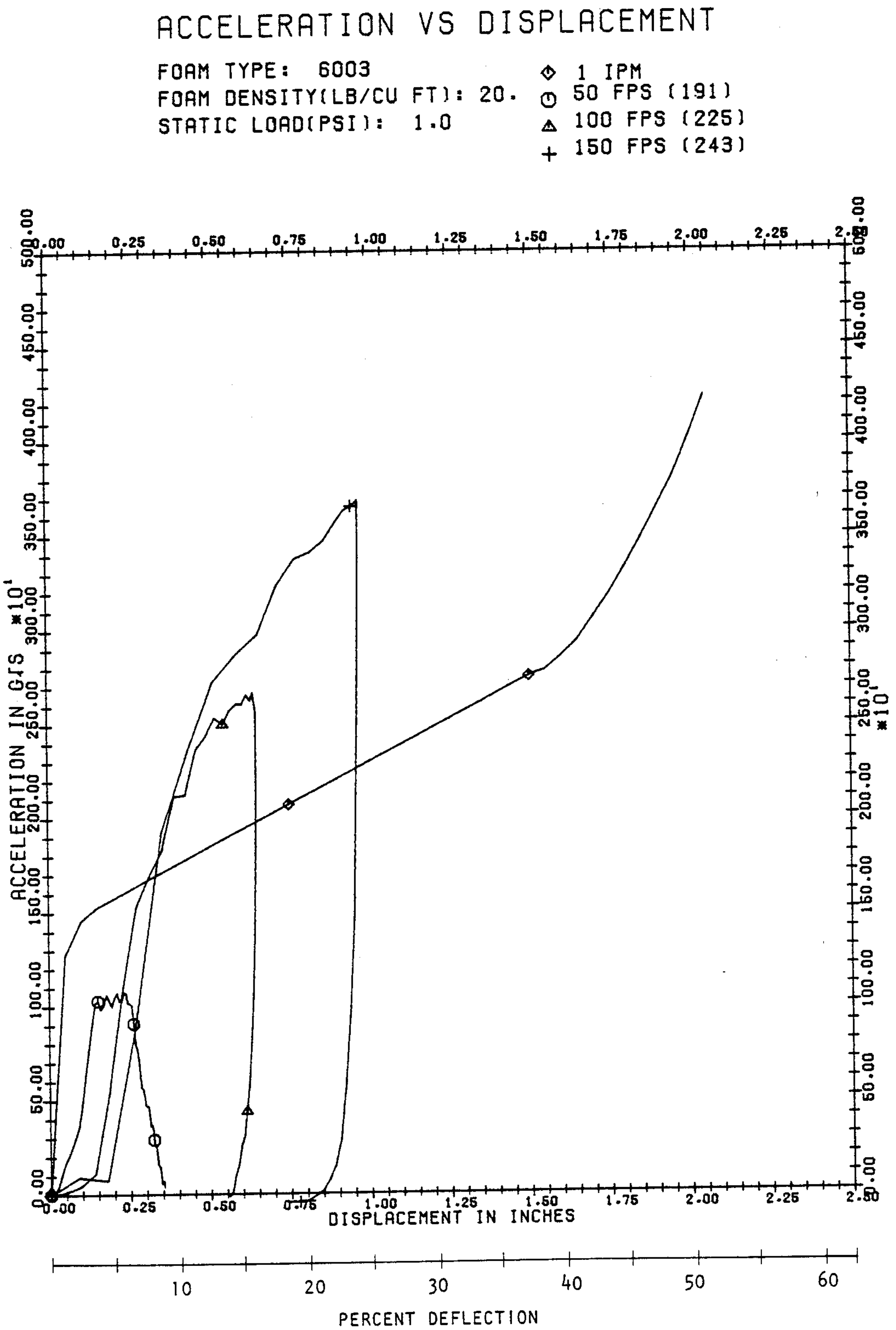

Figure B-35. BX 6003, 20 LB/FT^3, 1.0 PSI

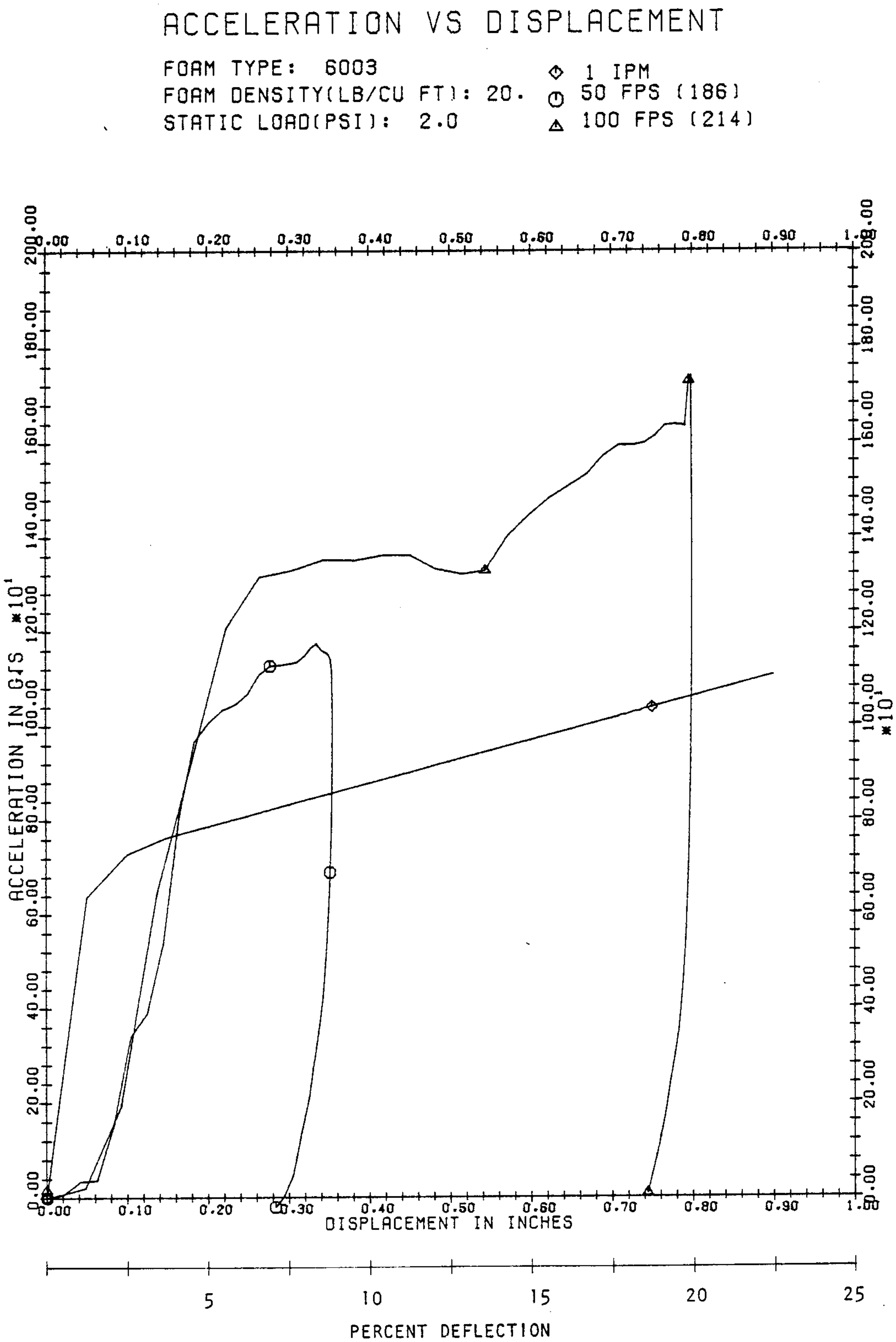

Figure B-36. BX 6003, 20 LB/FT^3, 2.0 PSI

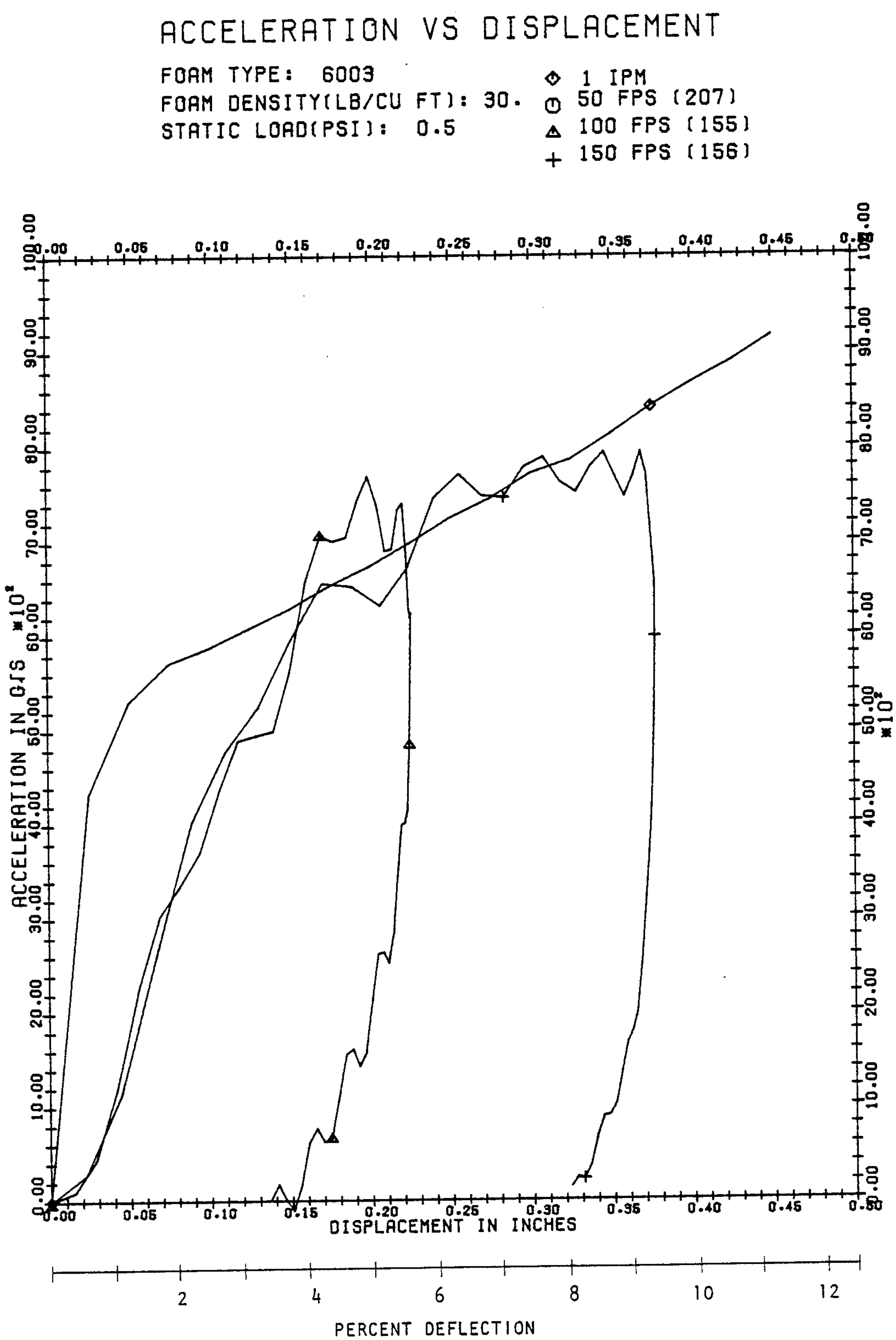

Figure B-37. BX 6003, 30 LB/FT^3, 0.5 PSI

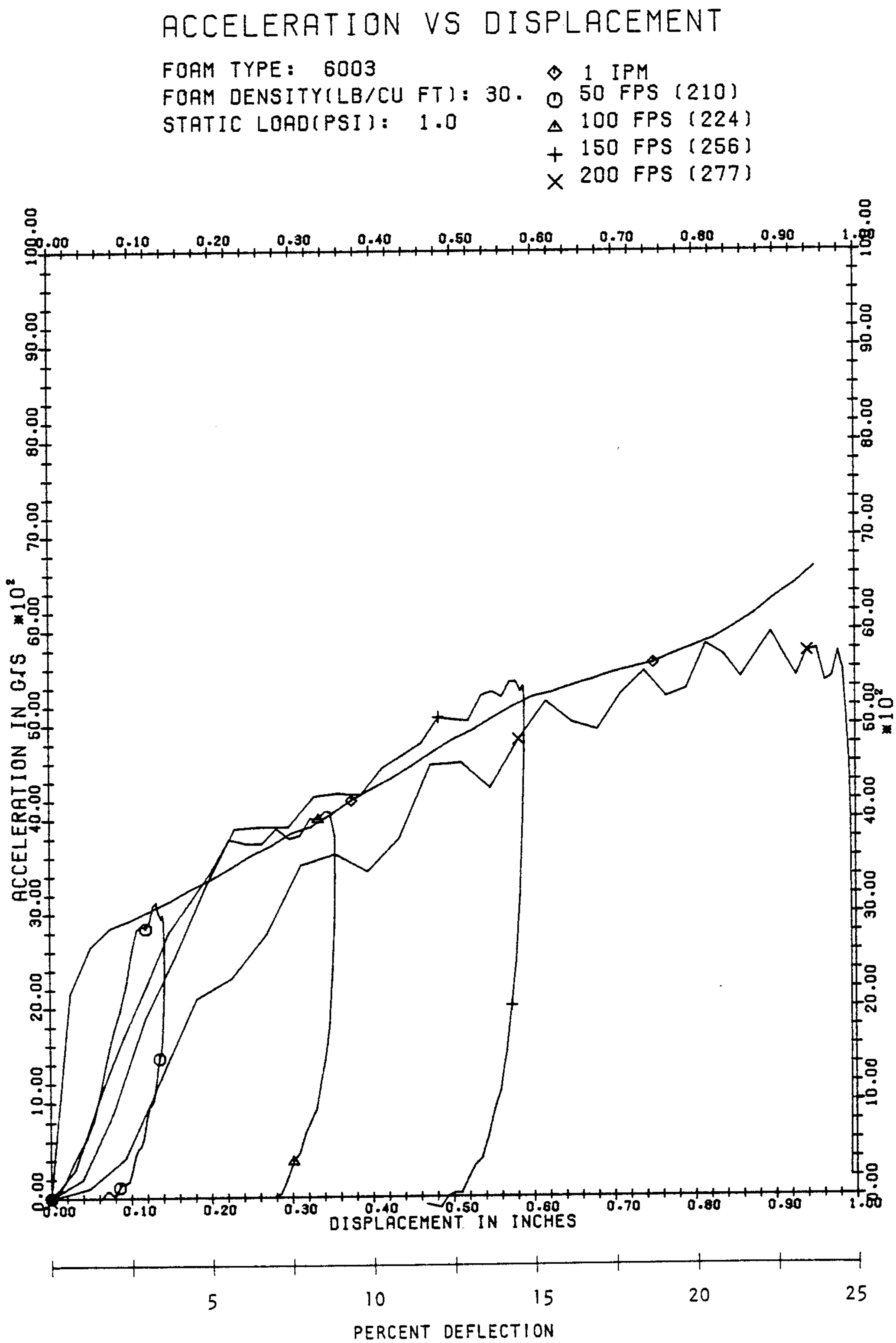

Figure B-38. BX 6003, 30 LB/FT^3, 1.0 PSI

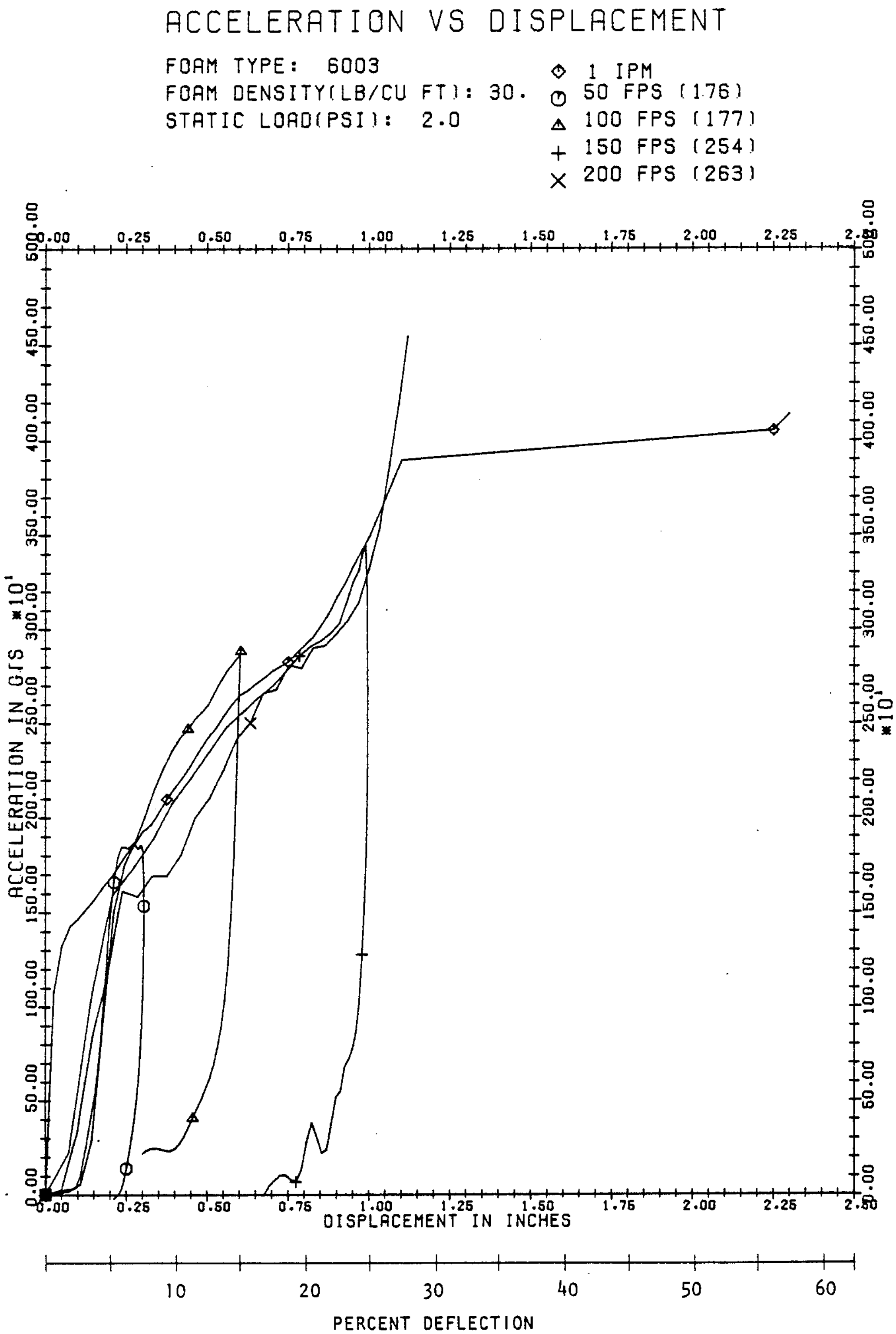

Figure B-39. BX 6003, 30 LB/FT^3, 2.0 PSI

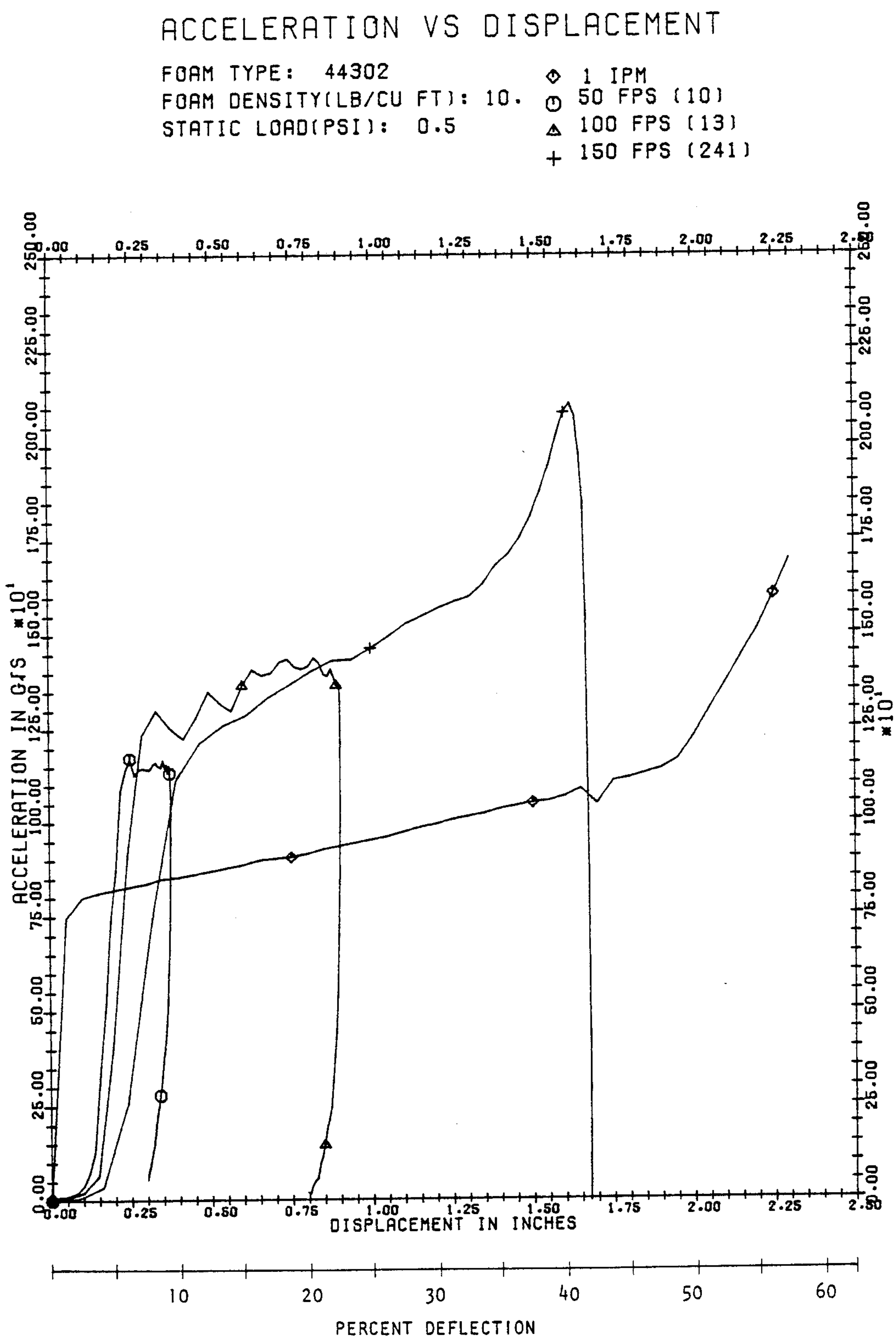

Figure B-40. BX 44302, 10 LB/FT^3, 0.5 PSI

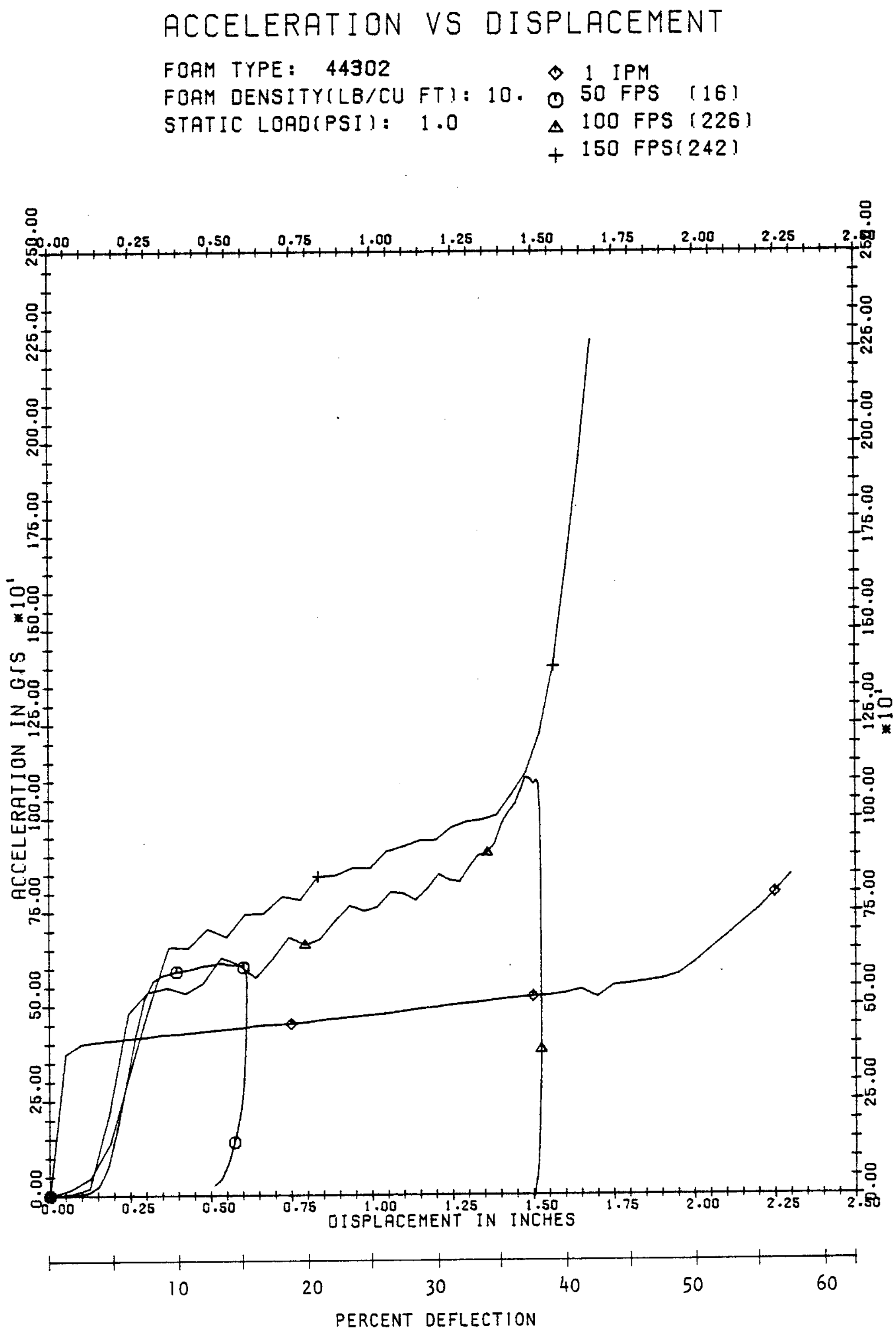

Figure B-41. BX 44302, 10 LB/FT^3, 1.0 PSI

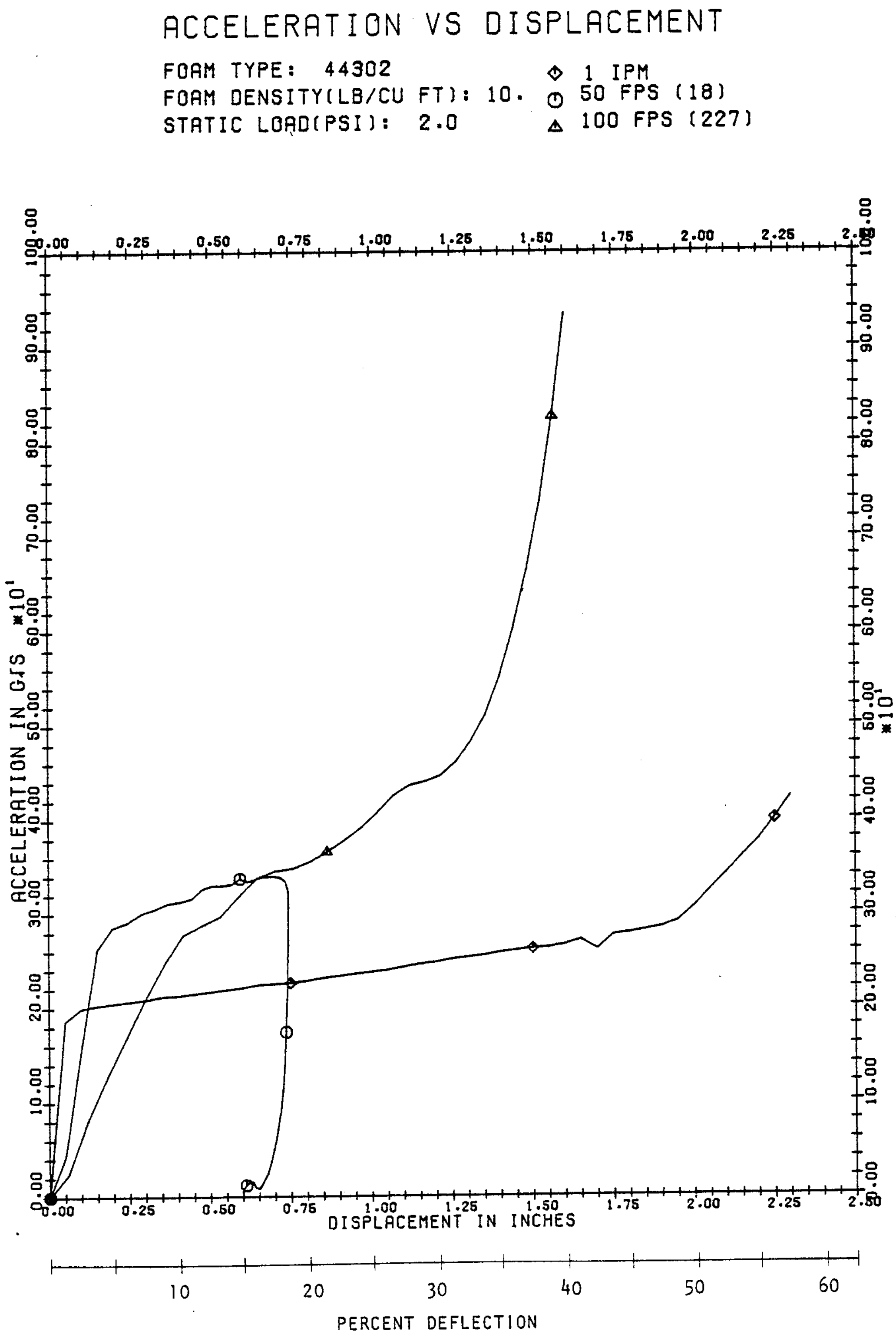

Figure B-42. BX 44302, 10 LB/FT^3, 2.0 PSI

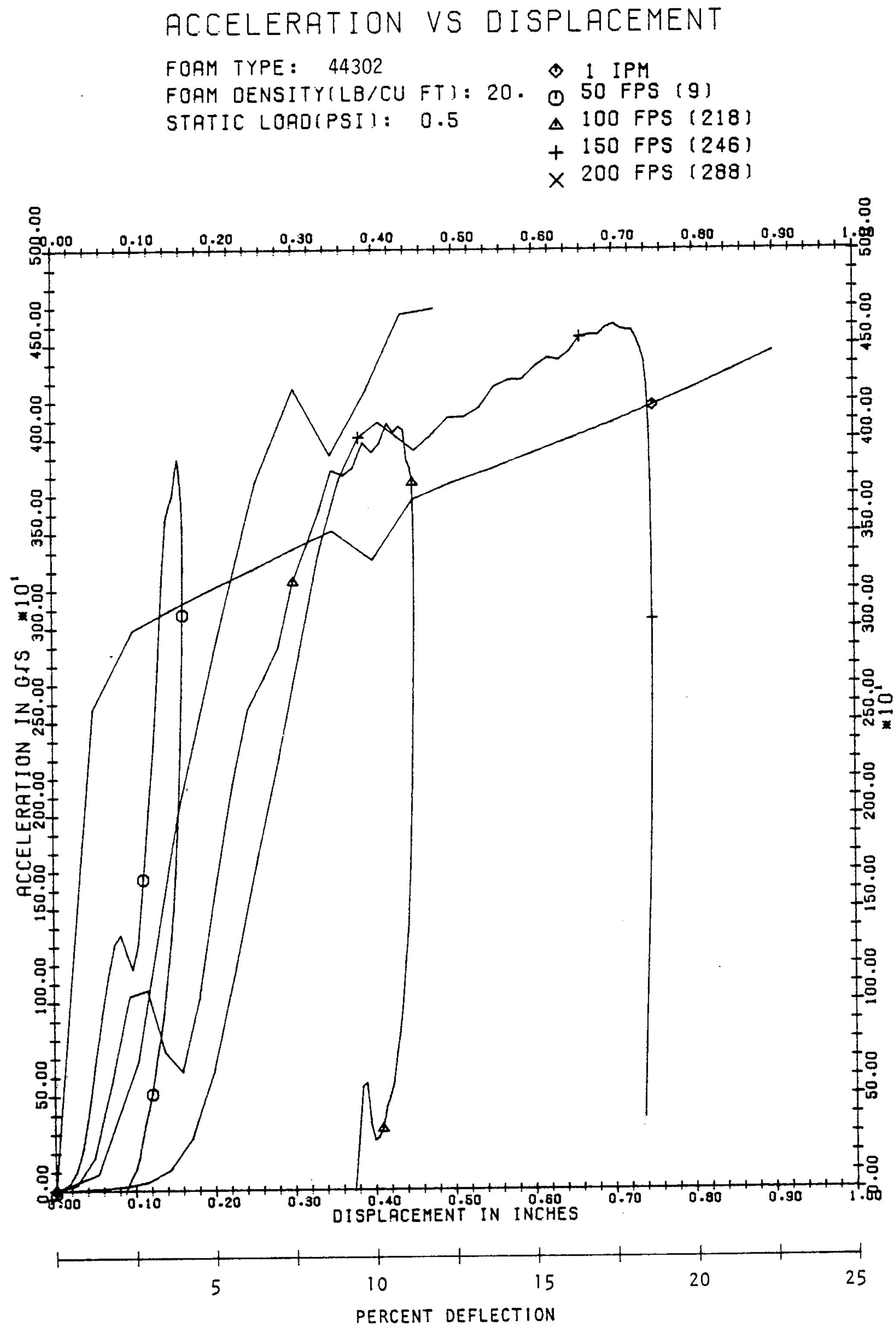

Figure B-43. BX 44302, 20 LB/FT^3, 0.5 PSI

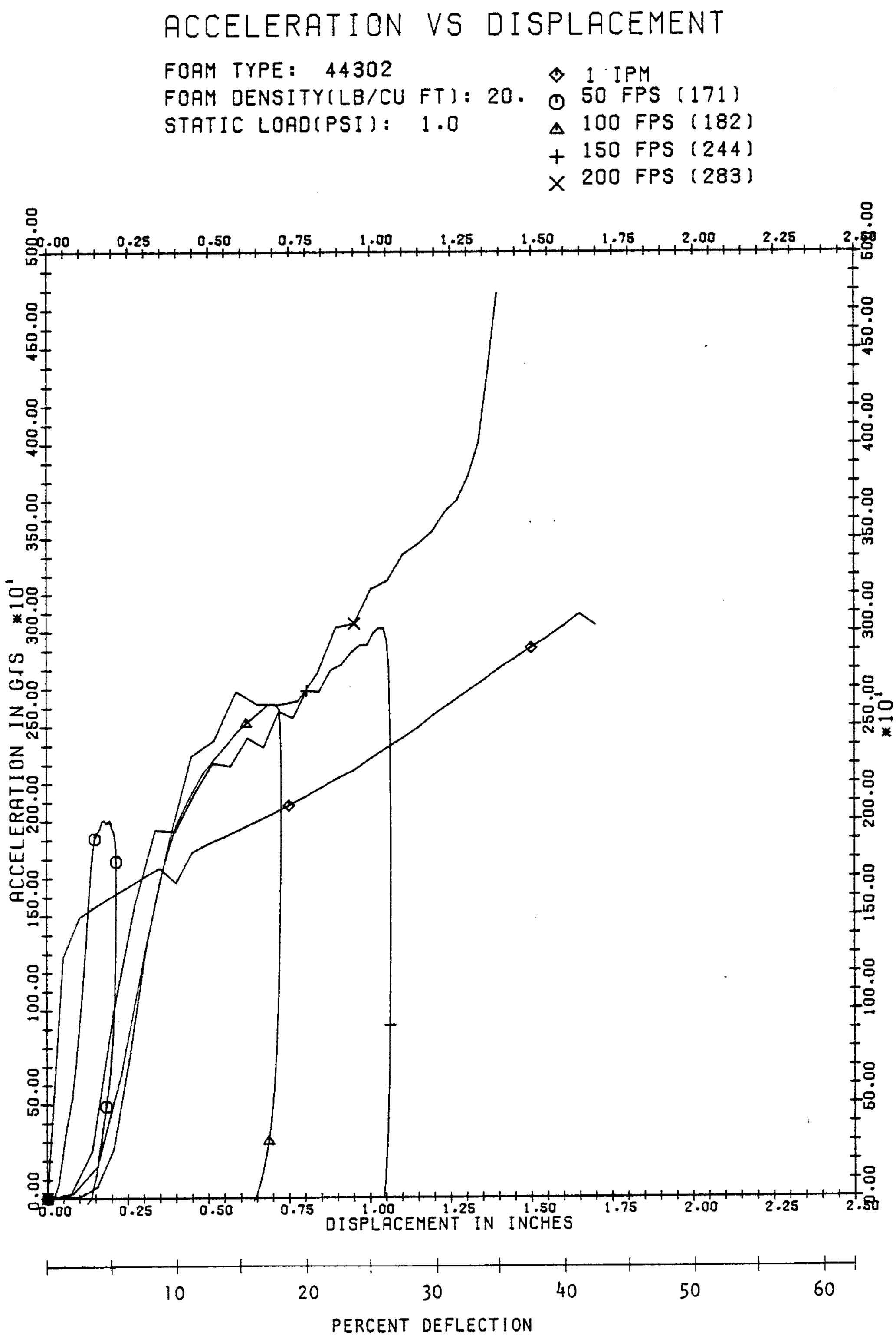

Figure B-44. BX 44302, 20 LB/FT^3, 1.0 PSI

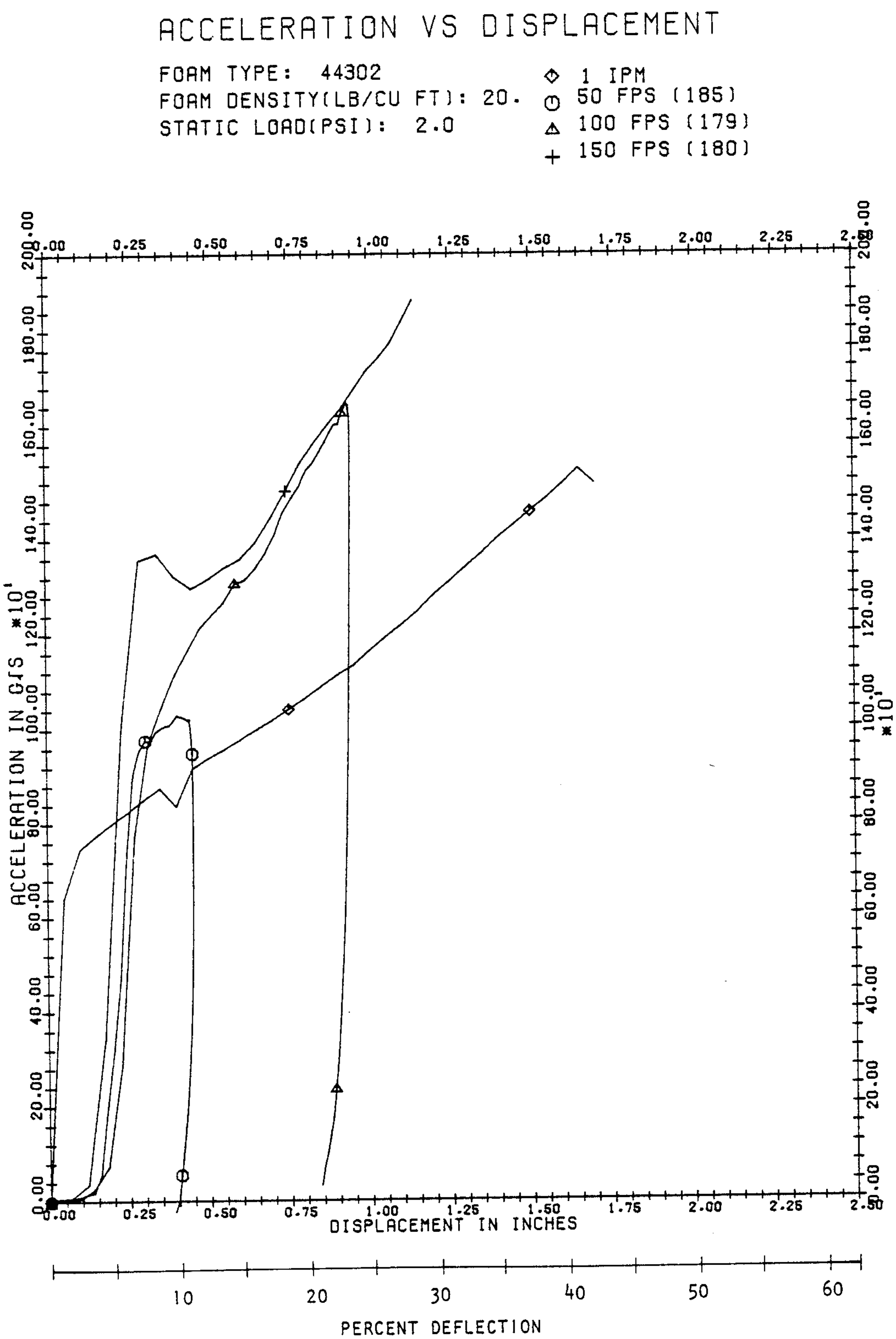

Figure B-45. BX 44302, 20 LB/FT^3, 2.0 PSI

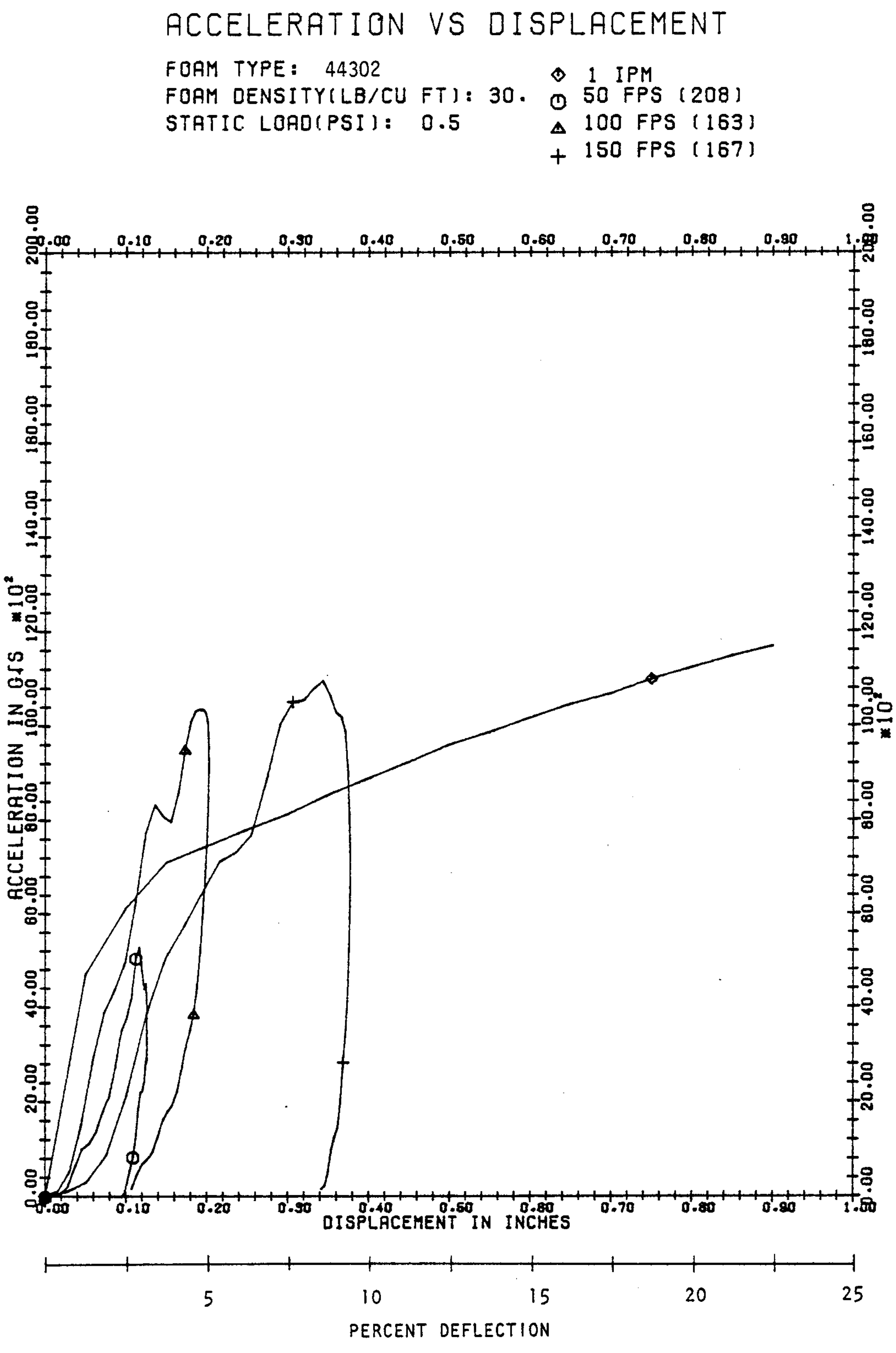

Figure B-46. BX 44302, 30 LB/FT^3, 0.5 PSI

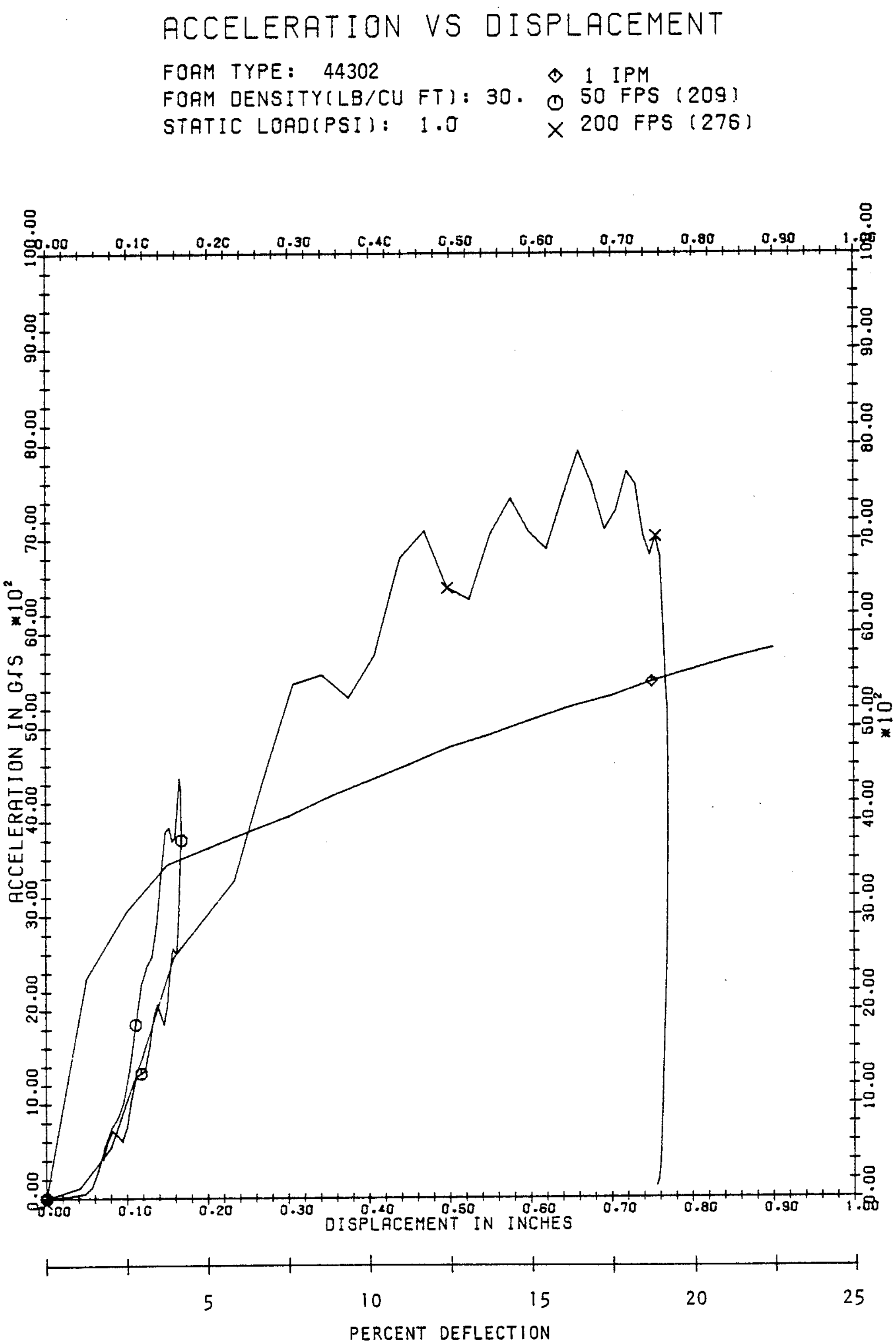

Figure B-47. BX 44302, 30 LB/FT^3, 1.0 PSI

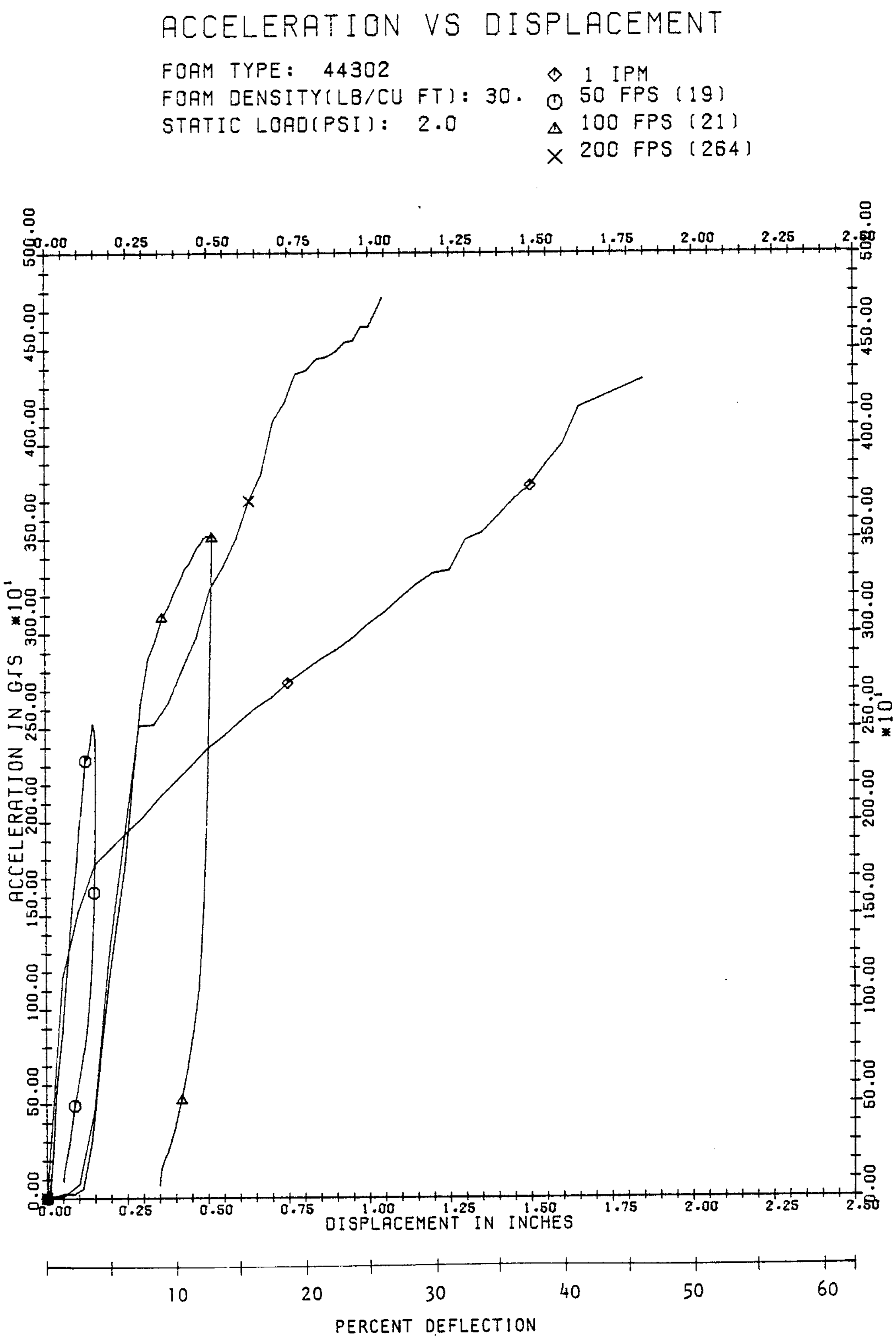

Figure B-48. BX 44302, 30 LB/FT^3, 2.0 PSI

DISTRIBUTION

	Copy
R. Bulcock, ERDA-KCAO	1
V. C. Vespe, ERDA-ALO	2
F. W. DuBois, LASL	3
J. A. Freed, LASL	4
S. J. Buginas, LLL	5
A. B. Copeland, LLL	6
H. M. Brinkmeier, Monsanto	7
D. R. Anderson, SLA	8
T. K. Hill/W. W. Joseph, SLA	9
H. M. Jones/R. Grover, SLA	10
P. B. Rand, SLA	11
C. B. Frost, SLL	12
L. F. Thorne/R. D. Jump, D/144, SA8	13
J. D. Corey, D/554, BD50	14-15
L. Stratton, D/554, 2C44	16-18
R. F. Pippert, D/700, 1A42	19
R. P. Frohmberg, D/800, 2A39	20
D. H. Hax, D/800, 2A41	21
C. H. Smith/S. L. DeGisi/T. E. Neet, D/814, 2C43	22
V. E. Alley/G. E. Martinette/J. R. Fender/ R. C. Swoboda, D/861, 2A31	23
R. A. Daniel, D/861, 2A31	24
R. H. Graham, D/861, 2A31	25
R. E. Kessler, D/865, 2C40	26